Lancaster University

An Investigation into the Molecular Targets Mediating Cannabidiol Action in the Free-living Ciliate *Tetrahymena pyriformis*

Nathan Tims

Student ID: 35358571

Under the Supervision of Dr. Jackie Parry & Dr. Karen Wright

A Thesis Submitted in Fulfilment of the Requirements for the Degree of
Master of Biomedical Science by Research

2021

Declaration

The Author would like to declare that this thesis has been composed solely by himself and that the work within was performed only by himself, without collaboration, unless specifically indicated. This thesis has not been submitted in fulfilment of any other degree scheme or qualification at this or any other institution. Many of the ideas providing the basis for this work were produced through discussion with supervisors Dr. Jackie Parry & Dr. Karen Wright.

Nathan Tims.

Table of Contents.

Glossary

2-AG	**2-arachidonoyl-glycerol**
2-OG	**2-Oleoylglycerol**
2-PG	**2-palmitoylglycerol**
5-HT	**5-hydroxytryptamine**
5-HTR	**5-hydroxytryptamine receptor**
AA	**Arachidonic acid**
AEA	**N-arachidonoyl ethanolamide**
AR	**Adenosine receptor**
Ar-DAG	**2-arachidonoyl diacylglycerols**
ARP	**Actin related protein**
BG 11	**Blue Green 11**
BPA	***Bauninia purpurea* agglutinin**
cAMP	**Cyclic adenosine monophosphate**
CB1/2	**Cannabinoid Receptor 1 / 2**
CBC	**Cannabichromene**
CBD	**Cannabidiol**
CBN	**Cannabinol**
CLR	**C-type lectin receptor**
CNS	**Central nervous system**
ConA	**ConcanavalinA**
COX	**Cyclooxygenase**
CS	**Chondroitin sulphate**
CTLD	**C-type lectin like domains**
DA	**Dopamine**
DAGL α/β	**Diacylglycerol lipase α/β**
DCAR	**Dendritic cell immune activating receptor**
DC-SIGN	**Dendritic cell-specific intercellular adhesion molecule-3-grabbing non-integrin**
DOR	**Delta opioid receptor**
DRP	**Dynamin related protein**
DS	**Dextran sulphate**
DTAF	**5-(4,6-dichlorotriazinyl) aminofluorescein**
ECS	**Endocannabinoid system**
EEA	***N*-eicosenoylethanolamine**
ERK 1/2	**Extracellular signal regulated kinase 1/2**
FAAH	**Fatty acid amide hydrolase**

FV	**Food vacuole**
GalLR	***N*- acetylgalactosamine lectin receptor**
GalNAc	***N*- acetylgalactosamine**
GlcLR	***N*-acetylglucosamine lectin receptor**
GlcNAc	***N*-acetylglucosamine**
GlyR	**Glycine Receptor**
GPCR	**G protein coupled receptor**
IR	**Ingestion Rate**
JNK	**c-Jun N-terminal kinase**
KOR	**Kappa opioid receptor**
LB	**Lysogeny broth**
LEA	***N*-linoleoylethanolamine**
LPS	**Lipopolysaccharides**
LTA	**Lipoteichoic acid**
LOX	**Lipoxygenase**
MAA	***Maakia amurensis* agglutinin**
MAG	**Monoacylglycerol**
MAGL	**Monoacylglycerol lipase**
MAPK	**Mitogen activated protein kinase**
MCL	**Macrophage C-type lectin**
MEK	**MAPK/extracellular regulated signal kinase kinase**
MIC	**Minimum inhibitory concentration**
MLR	**Mannose lectin receptor**
MOR	**Mu opioid receptor**
MPA	***Maclura pomifera* agglutinin**
MurNAc	**N-acetylmuramic acid**
NAE	***N*-acylethanolamine**
NADPH	**Nicotinamide adenine dinucleotide phosphate**
NAGly	***N*-arachidonylglycine**
NAPE	***N*-acylphosphatidylethanolamine**
NAPE-PLD	**NAPE specific Phospholipase D**
NArPE	***N*-arachidonyl-phosphatidylethanolamie**
NAT	***N*-acyltransferase**
OEA	**Oleoethanolamine**
OxLDL	**Oxidised low-density lipoproteins**
PAMP	**Pathogen associated molecular pattern**
PAP	**Phosphatidic acid phosphohydrolase**

PEA	***N*-palmitoylethanolamine**
PG-EA	**Prostaglandin glycerol ethanolamines**
PG-GE	**Prostaglandin glycerol esters**
PI3P	**Phosphatidylinositol 3-Phosphate**
PLC	**Phospholipase C**
PNA	**Peanut agglutinin**
PP	**Protease peptone**
PPAR	**Peroxisome proliferator activated receptor**
PPRE	**PPAR-responsive regulatory elements**
PRR	**Pattern recognition receptor**
PTM	**Post translation modification**
SBA	**Soy bean agglutinin**
SEA	***N*-stearoylethanolamine**
SR	**Scavenger receptor**
TRPA/M/V	**Transient receptor potential ankyrin/melastatin/vanilloid**
UM	**Undulating membrane**
VAMP	**Vesicle associated membrane protein**
V-ATPase	**ATP-dependent vacuolar protein pump**
VGCC	**Voltage gated calcium channel**
VFF	**Vacuole formation factor**
VFR	**Vacuole formation rate**
VPT	**Vacuole passage time**
WGA	**Wheat germ agglutinin**
Δ^9-THC	**Delta-9-Tetrahydrocannabinol**

Abstract

This study aimed to characterised the effect of cannabidiol (CBD) on the feeding behaviour of *Tetrahymena pyriformis* and to determine its molecular target(s). Experiments involved feeding *T. pyriformis* with a *Synechococcus* sp. prey (live or dead) or latex beads, in the presence/absence of CBD with/without the pre-blocking of specific receptors or components of the MAPK pathway. CBD caused a reduction in ingestion rate (IR) at *ca.* 2 μM until it was zero at ≥2.5 μM and this gave rise to a feeding lag. The lag was temporary, with its duration being positively correlated to CBD concentration. Post-lag, the ciliate began to feed again, and the resulting IR correlated positively with the duration of the lag; reflecting the satiation level of the ciliate, as food vacuoles continued to be defecated during this feeding lag. A feeding lag of >32 min, with the defecation of *ca*. 3 food vacuoles, induced 'starvation' in *T. pyriformis* and this resulted in the ciliate exhibiting hyperphagia.

The role of feeding receptors (C-type lectins [CLRs] and Scavenger Receptors [SRs]) in this CBD response was evaluated. *T. pyriformis* utilised SRs and CLRs for mannose, *N*-acetylglucosamine (GlcNAc), and *N*- acetylgalactosamine (GalNAc) for the ingestion of live *Synechococcus*, which were ingested at higher rates, and gave rise to more food vacuoles, than dead cells/beads. Heat-treatment destroyed the mannose, GlcNAc and SR ligands on *Synechococcus* cells, leaving only GalNAc residues to facilitate the uptake of dead cells. None of the receptors were involved in the uptake of beads. The blocking of these receptors, prior to adding CBD, did not abolish the CBD-induced feeding lag but post-lag IRs were not hyperphagic; being equivalent to that expected when blocking these receptors in the absence of CBD. This suggests that these receptors do not directly interact with CBD. The blocking of other receptors (GCPRs and TRPV, PPAR, Dopamine, Serotonin and Adenosine), which are known to interact with CBD in other eukaryotic cells, was also tested but none abolished the CBD-induced feeding lag, suggesting that *T. pyriformis* has few, if any, CBD-interacting receptors that are associated with its feeding mechanism. The ciliate also did not perceive CBD as an external stress as no evidence of activation of the MAPK pathway was recorded. It was therefore proposed that the target(s) of CBD, for reducing IR, might be vacuole formation/membrane recycling (which would prevent the development of nascent food vacuoles) and/or ciliary function (which would reduce swimming speed and the formation of feeding currents in the oral cavity); both of which involve actin, microtubules, and dynein.

The mechanism behind the action of CBD on *T. pyriformis* feeding is more complicated than first thought, but with its considerably reduced repertoire of potential targets, compared to human cells, elucidating its targets, and whether these are evolutionary conserved, might be achievable. It is hoped that the knowledge gleaned will aid in the future implementation of CBD as an effective therapeutic agent for a number of conditions.

Chapter 1. Introduction

1.1 The human endocannabinoid system (ECS)

The human endocannabinoid system (ECS) is responsible for mediating a broad range of neuromodulatory effects which include not only central-nervous-system (CNS) related processes such as memory, brain development, cognition and pain reception (Fernández-Ruiz et al., 2000; Alger, 2013; Pacher and Kunos, 2013) but also processes in more peripheral systems such as immunity, reproduction, digestion and inflammation (Maccarrone et al., 2015).

The ECS itself is a lipid based signalling system encompassing endogenous cannabinoid ligands (endocannabinoids) (see 1.1.1.1), cannabinoid receptor 1 and 2 (CB1 and CB2) (see 1.1.3.1 & 1.1.3.2) and the anabolic and catabolic enzymes involved in cannabinoid metabolism (see 1.1.2.1 & 1.1.2.2) (Lu and Mackie, 2016). Mediators of the ECS are extremely promiscuous and crosstalk between the ECS and other systems is common and forms what has been termed an 'endocannabinoidome' (Di Marzo and Piscitelli, 2015). As a result, the ECS is implicated in a range of diseases and its near ubiquity makes it an attractive therapeutic target in almost all diseases (Pacher et al., 2006; Pacher and Kunos, 2013).

1.1.1 Cannabinoids – ligands of the ECS

Cannabinoids are long chain, lipid based signaling molecules defined by their binding to cannabinoid receptors (Fonseca et al., 2013). Cannabinoids can either be produced endogenously (Endocannabinoids) or be plant derived (Phytocannabinoids).

1.1.1.1 Endogenous cannabinoids

The first endocannabinoid discovered in a mammalian brain was Anandamide/N-arachidonoyl ethanolamide (AEA) (Fig. 1.1.) (Devane et al., 1992). AEA is a member of the *N*-acylethanolamines (NAEs) and is a partial agonist of CB1 and CB2 (Gómez-Ruiz et al., 2007) with greater CB1 affinity than CB2 (Fonseca et al., 2013). The second endocannabinoid, 2-arachidonoyl-glycerol (2-AG) (Fig. 1.1.), belongs to the monoacyl glycerol (MAG) family and was first isolated from canine gut (Sugiura et al., 1995). 2-AG appears to have a much greater binding affinity for CB1 and CB2 than AEA and is present in higher concentrations. Furthermore, 2-AG is a full agonist of both CB1 and CB2, unlike AEA (Gómez-Ruiz et al., 2007). Both AEA and 2-AG are present in the CNS and periphery although 2-AG is found in higher concentrations in both (Fonseca et al., 2013).

There are also 'endocannabinoid like' compounds which are additional endogenous MAGs and NAEs. They share similar metabolizing enzymes to AEA and 2-AG and are able to modulate cannabinoid binding, but are not typically CB1/2 ligands (Fonseca et al., 2013; Kleberg et al., 2014). The two best understood examples are the NAEs *N*-oleoyethanolamine (OEA) and *N*-palmitoylethanolamine (PEA) (Fig. 1.1.) which share the same ethanolamine group as AEA. OEA and PEA bind less strongly to CB1 and CB2 and show binding preference for other targets (Iannotti et al., 2016).

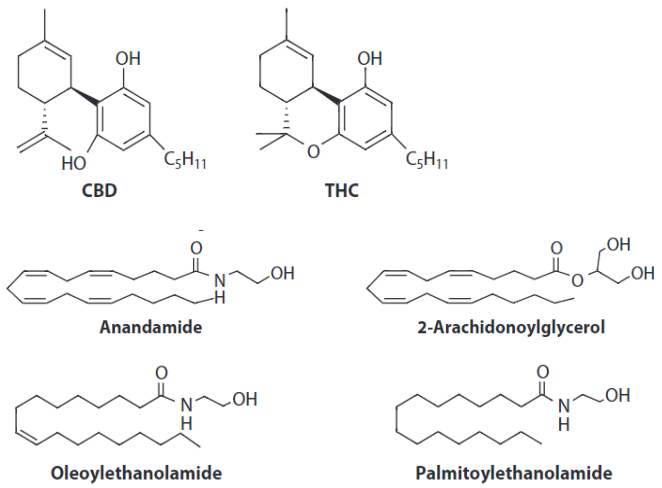

Figure 1.1.
Structures of the two primary phytocannabinoids cannabidiol (CBD) and Δ^9-Tetrahydrocannabinol (THC), the two primary endocannabinoids: anandamide and 2-Arachidonoylglycerol and the two primary endocannabinoid-like compounds: Oleoylethanolamide and Palmitoylethanolamide
Figure adapted from Pacher et al., 2020

1.1.1.2 Phytocannabinoids

Phytocannabinoids are derived from *Cannabis sativa* and over 140 have been isolated to date (Elsohly et al., 2017). Δ^9- tetrahydrocannabinol (Δ^9-THC) (Fig. 1.1.) is the main psychoactive component of *C. sativa* and was the first phytocannabinoid isolated and characterised (Gaoni and Mechoulam, 1964). THC is one of the few phytocannabinoids known to be a partial agonist for both CB1 and CB2 along with Δ^8-THC and cannabinol (CBN) (Di Marzo and Piscitelli, 2015; Aizpurua-Olaizola et al., 2017). THC and THC-derivatives have been investigated for their therapeutic potential and have shown promise in some areas such as in anti-convulsant, analgesic or anti-inflammatory effects (Lastres-Becker et al., 2005; Pacher et al., 2006; Mouhamed et al., 2018) although it's therapeutic use is limited by its psychoactive effects (Shevyrin and Morzherin, 2015).

Cannabidiol (CBD) (Fig. 1.1.) is the main non-psychoactive cannabinoid found in *C. sativa* and has been widely investigated for its therapeutic effects in a range of diseases (Devinsky et al., 2014; Chye et al., 2019). CBD has an impressive safety profile with minimal adverse effects and no psychoactive properties

(Iffland and Grotenhermen, 2017) making it an attractive therapy. Unlike THC, it only exhibits very low CB1/2 affinities with studies suggesting it can actually act as a negative allosteric regulator of CB1 (Laprairie et al., 2015; Tham et al., 2019). CBD is also known to have the ability to inhibit the activity of Fatty acid amide hydrolase (FAAH), a degradative enzyme of NAEs (see 1.1.2.2) and can somewhat inhibit the cellular uptake of AEA (Bisogno et al., 2001; De Filippis et al., 2008). CBD has been suggested to act upon over 65 molecular targets in humans (Bih et al., 2015). The amount of evidence for this activity differs between targets and, as a result, the clarity of CBD effects on many of these targets is poorly understood (Bih et al., 2015). Therefore, further research into these additional molecular targets is required to help elucidate the therapeutic potential of CBD.

1.1.2 Synthesis and degradation of endogenous cannabinoids

1.1.2.1. Anabolic enzymes

Synthesis of endocannabinoids occurs on demand which is unlike classic neurotransmitters which are stored and released when required (Lutz, 2004). AEA synthesis utilises the membrane bound phospholipid N-arachidonyl-phosphatidylethanolamie (NArPE), a type of N-acyl-phosphatidylethanolamine (NAPE) (Fig. 1.2, A). NArPE is synthesised using N-acyltransferase (NAT) via the transfer of arachidonic acid (AA) from phosphatidylcholine onto phosphatidylethanolamine (Cadas et al., 1996). In the primary route of AEA production, NArPE is hydrolysed via a NAPE specific Phospholipase D (NAPE-PLD) to release AEA (Schmid et al., 1983). Three alternative NAPE-PLD independent pathways have also been elucidated (Fig. 1.2, A) (Liu et al., 2006; Simon and Cravatt, 2006; 2008).

The synthesis of 2-AG involves a much simpler two step reaction beginning with the production of 2-arachidonoyl containing diacylglycerols (Ar-DAGs) from membrane bound glycerophospholipids by one of two reactions: 1) Hydrolysis of phosphoinositides, by a specific PLCβ or 2) The hydrolysis of phosphatidic acid via phosphatidic acid phosphohydrolase (PAP) (Fig. 1.2, B). The resulting Ar-DAG is hydrolysed by diacylglycerol lipase α or β (DAGL α/β) to produce 2-AG (Gómez-Ruiz et al., 2007; Muccioli, 2010). Two less characterised pathways have also been suggested for 2-AG synthesis although 2-AG seems to be produced chiefly via the DAGL mediated pathway (Fig 1.2, B) (Ueda et al., 2011; Yoshino et al., 2011)

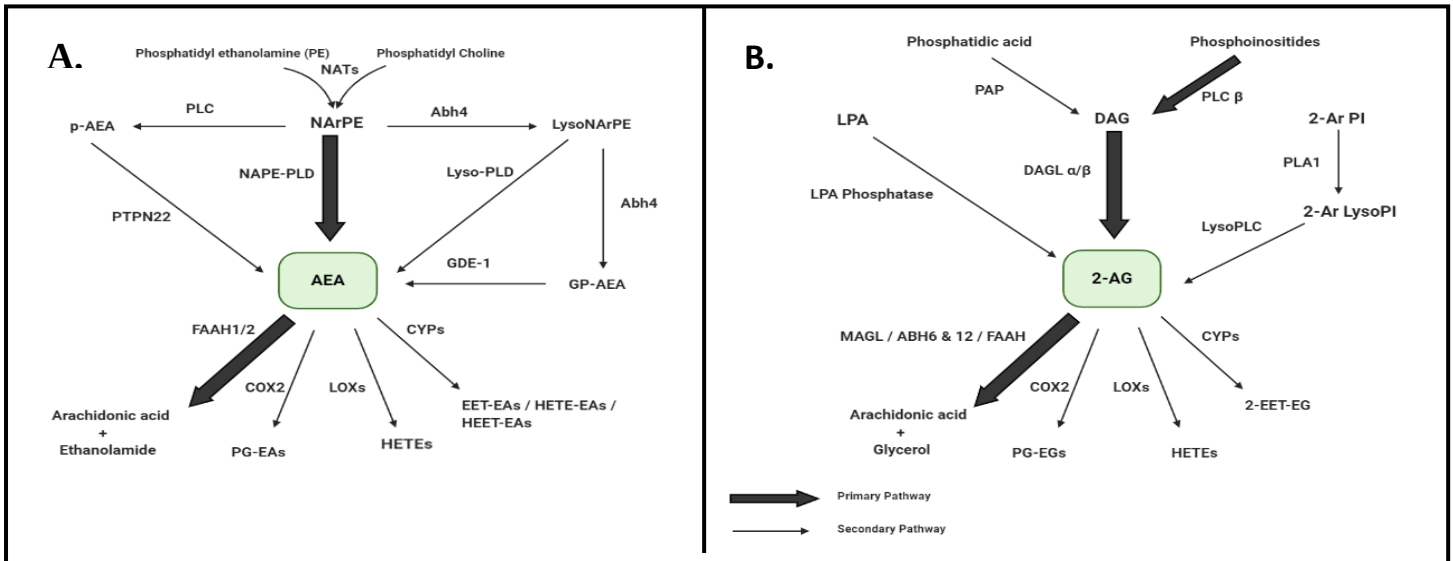

Figure 1.2. *Synthesis and inactivation of the primary endocannabinoids Anandamide and 2-arachidonyl-glycerol. Thicker black arrows denote the primary pathway of synthesis and degradation.*

Abbreviations*: Abh4, αβ hydrolase 4; ABH6 & 12, αβ hydrolase 6 & 12; AEA, Anandamide; COX2, Cyclooxygenase 2; CYPs, Cytochrome P450s; DAG, Diacylglycerol; DAGL, Diacylglycerol Lipase; EET-EA, epoxyeicosatrienoic acid ethanolamide; FAAH, Fatty acid amide hydrolase; GDE-1, Glycerophosphodiesterase 1; GP-AEA, Glycerophosphoanandamide; HETEs, hydroxy-eicosatetraenoic acids; HEET-EAs, hydroxylated epoxyeicosatrienoic acid ethanolamides*; *HETE-EAs, hydroxy eicosatetraenoic acid ethanolamides; LOXs, lipoxygenases; LPA, Lysophosphatidic acid; Lyso-PLC, lysoPI phospholipase C; Lyso-PLD, Lysophospholipase D; MAGL, Monoacylglycerol lipase; NAT, N-acyltransferase; NAPE-PLD, N-acyl phosphatidylethanolamine phospholipase D; N-ArPE, N-arachidonyl-phosphatidylethanolamine; p-AEA, Phosphoanandamide; PAP, Phosphatidic acid phosphohydrolase; PG-EA, Prostaglandin ethanolamine; PG-EG, prostaglandin glycerol ester; PLA1, Phospholipase A1; PLC, Phospholipase C; PTPN22, Protein tyrosine phosphatase, non-receptor type 22; 2-Ar PI, 2-arachidonoyl-lyso phosphatidylinositol; 2EET-EG, 2-epoxyeicosatrienoic acid glycerols.*

1.1.2.2. Catabolic enzymes

Hydrolysis is the primary route of degradation for all NAEs and MAGs including AEA and 2-AG (Fig 1.2). Hydrolysis of AEA cleaves the amide bond to release AA and ethanolamine. The primary enzyme involved in NAE hydrolysis is fatty acid amide hydrolase (FAAH) (Deutsch and Chin, 1993), a membrane bound serine hydrolase particularly active in brain tissue (Hillard et al., 1995) (Fig. 1.2, A). Mice deficient in FAAH showed drastically increased levels of AEA in the brain along with increase pain reduction (associated with CB1 stimulation) demonstrating the FAAH catabolic role (Cravatt et al., 2001). A second isomer of FAAH (FAAH-2) is also present in several other mammals including primates and humans. This isomer is localised to lipid droplets and shares 20% sequence identity with FAAH-1 (Wei et al., 2006). Substrate specificity between isomers is similar with both acting upon NAEs although FAAH-1 has a much greater specificity for AEA than FAAH-2 (Wei et al., 2006; Fonseca et al., 2013).

For 2-AG, hydrolysis of its ester bond releases AA and glycerol (Fig. 1.2, B). The primary enzyme involved is Monoacylglycerol Lipase (MAGL), a cytosolic serine hydrolase abundant in brain tissue coexpressed with CB1 receptors (Gómez-Ruiz et al., 2007; Fonseca et al., 2013). Two closely related isoforms have been identified in rats, 35 and 37kDa in size (Dinh et al., 2002). MAGL is the primary source of 2-AG degradation accounting for ~85% of 2-AG hydrolysis (Blankman et al., 2007). Two other membrane integral enzymes, ABH6 and 12, also contributed significant hydrolysis activity (~4% and 9% respectively) (Blankman et al., 2007). Together, MAGL, ABH6 and ABH12 account for ~98% of 2-AG hydrolysis in the brain (Blankman et al., 2007). The remaining activity is thought to be due to a range of serine hydrolases, including FAAH (Goparaju et al., 1998).

Enzymatic oxidation is a secondary method of degradation and mainly serves to create substrates for eicosanoid biosynthesis, mediated by Lipoxygenases (LOXs) (Fig. 1.2). Several types of LOX enzymes, such as 15-LOX, 12-LOX variants from both plants and mammals, have been shown to oxidise the AA unit of endocannabinoids (Rouzer and Marnett, 2011). Cyclooxygenases (COX) have 2 human isoforms and studies have shown that COX-2, but not COX-1, is able to oxidise 2-AG and AEA to prostaglandin glycerol esters (PG-GE) and prostaglandin glycerol ethanolamines (PG-EA) (Kozak et al., 2000; Kozak et al., 2002). Cytochrome P450 enzymes, of which there are 57 known human variants, have also demonstrated the ability to oxidise some endocannabinoids to epoxyeicosatrienoic acids (Zelasko et al., 2015). Although AEA is metabolized by a much wider range of P450 enzymes compared to 2-AG, both have demonstrated significant degradation via this mechanism (Zelasko et al., 2015).

1.1.3 Cannabinoid receptors and signaling

Endocannabinoid signalling occurs in a retrograde fashion (Fonseca et al., 2013; Di Marzo and Piscitelli, 2015). Endocannabinoids themselves are synthesised in post-synaptic terminals and released into the synaptic cleft where they bind presynaptic membrane bound cannabinoid receptors (Fonseca et al., 2013; Di Maezo and Piscitelli, 2015). There are two true classical cannabinoid receptors, CB1 and CB2, and two more recently accepted cannabinoid receptors (GPR55 and Transient Receptor Potential [TRP] channels) (Pacher et al., 2020). Typically, endocannabinoids induce a suppressive effect, with the endocannabinoid induced depolarization of the pre-synaptic terminal resulting in both transient and long-term synaptic plasticity (Kreitzer and Regehr, 2001; Gerdeman et al., 2002).

1.1.3.1. Cannabinoid receptor 1 - CB1

Early research revealed that cannabinoids acted via inhibiting cyclic adenosine monophosphate (cAMP) synthesis in a pertussis toxin sensitive manner (a bacterial toxin that inhibits Gi, Go and Gt receptor interactions) (Howlett et al., 1986; Howlett et al., 1988) suggesting a G protein-coupled receptor (GPCR)-mediated signalling event. CB1 was the first to be identified in humans and was characterised as a 472 amino acid GPCR coupled to an adenylate cyclase mechanism (Gérard et al., 1991). Distribution was mostly in the brain and it was also seen to share a 97.3% sequence identity with a previously identified murine receptor (Gérard et al., 1991).

CB1 brain distribution is conserved across mammals (Iannotti et al., 2016) and can be used to explain the effects of cannabinoids. For example, distribution in the forebrain and cerebellum may explain cannabinoid effect on cognition and movement and the lesser distributions of CB1 in medullary nuclei (which control respiratory and cardiovascular responses) could explain the relatively high safety profile of CBD (Herkenham et al., 1990; Iannotti et al., 2016). Conversely, CB1 peripheral expression is heterogenous and varies between excitatory (glutamatergic) and inhibitory (GABAergic) synapses, seeing more distribution in the latter (Kano, 2014). CB1 also exhibits expression beyond the brain being found in most peripheral tissues including smooth and skeletal muscle, adipose, heart, skin, GI tract and bone (Iannotti et al., 2016).

CB1 is chiefly expressed in the plasma membrane as is typical for GPCRs, although, a separate subpopulation has intracellular localisation in endosomes, lysosomes, and mitochondrial membranes (Zou and Kumar, 2018). CB1 is coupled primarily with Gi/o proteins and activation can have a variety of downstream effects: 1) Inhibition of adenylate cyclase (this being the primary pathway). 2) Activation of Mitogen activated protein kinases (MAPKs). 3) inhibition of voltage gated Calcium channels. 4) activation of inwardly rectifying K^+ currents (Fig 1.3.). Several other proteins beyond Gi/o have also demonstrated CB1 interaction, including the alternative G proteins Gs and Gq, although Gi/o still remains the primary protein (Howlett et al., 2010; Kano, 2014).

1.1.3.2. Cannabinoid receptor 2 – CB2

The second cannabinoid receptor, CB2, exhibits expression primarily in macrophages of the marginal zone of the spleen (Munro et al., 1993). It consists of a 360 amino acid protein and shares 44% sequence identity with CB1 (Zou and Kumar, 2018). CB2 seems to be less conserved between species with the human and rodent CB2 having only 80% sequence identity compared to the CB1's 97.3% (Zou and Kumar, 2018). CB2 binding specificities also differ from CB1 with CB2 demonstrating lower affinity for CBD but greater affinity for more biologically active cannabinoids like Δ^9-THC and cannabinol (Munro

et al., 1993; Zou and Kumar, 2018). CB2 also couples with Gi/o proteins but does not couple with Gs and Gq proteins unlike CB1, yet it still demonstrates very similar downstream effects (Fig 1.3.) (Kano, 2014; Iannotti et al., 2016).

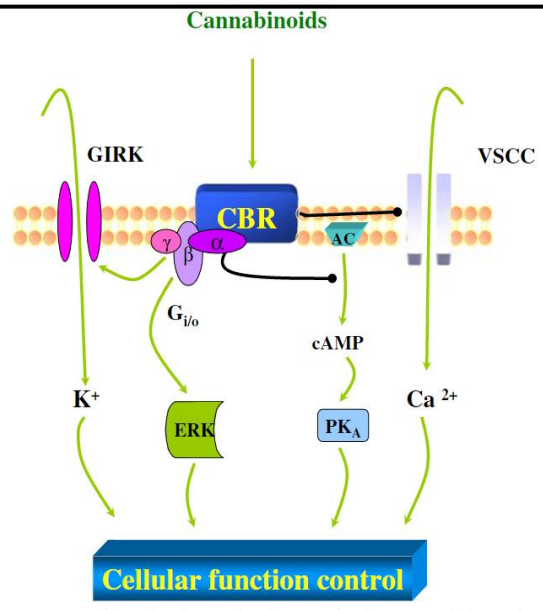

Figure 1.3.
The primary cannabinoid induced signal transduction mechanisms. Cannabinoid agonism of a cannabinoid receptor (CD1/2) causes activation of the heterodimeric Gi/o protein leading to dissociation of the alpha and beta/gamma subunits.
Green lines indicate activation whereas black lines indicate inhibition.
AC, Adenylate cyclase; cAMP, cyclic AMP; ERK, Extracellular signal related kinase AKA MAP kinase; GIRK, G protein coupled inwardly rectifying K^+; $PK_{a,}$, Protein Kinase A; VSCC, Voltage gated Ca^{2+} channel. (Gómez-Ruiz et al., 2007)

CB2 is primarily expressed in cells of the immune system (Graham et al., 2010; Zou and Kumar, 2018). Moderate/high levels are found in monocytes, NK cells, B-lymphocytes and low levels found in $CD4/8^+$ T lymphocytes cells suggesting that the ECS plays a large role in modulating the immune system (Graham et al., 2010). Expression is also seen in other organs of the immune system such as the spleen and tonsils but also in some other peripheral tissues including the heart, GI tract and reproductive system, albeit it in small quantities (Zou and Kumar, 2018). Very small quantities can also be found in the brain (Gong et al., 2006). With its presence in the immune system, CB2 is thought to play a role in immune system modulation with roles in regulation of inflammation, control of cytokine and lymphangiogenic factor release, and immune cell migration (Iannotti et al., 2016). Furthermore, despite its small quantity in the brain, CB2 is still thought to play a role in neuroinflammation due to its presence in activated astrocytes and microglial cells (Ashton and Glass, 2007; Benito et al., 2008).

1.1.3.3. GPR55

GPR55 is a 319 amino acid GPCR located in several tissues including the spleen, intestine, fetal and some regions of the brain (Sawzdargo et al., 1999). GPR55 exhibits coupling to Gq or G_{12} alpha subunits and triggers the release of Ca^{2+} from intracellular stores via a Gq, PLC (Phospholipase C) or G_{12}, RhoA

signaling pathway (Lauckner et al., 2008). It shares very little general amino acid sequence identity with CB1 (13.5%) and CB2 (14.4%) and binds most potently with an endogenous lysophospholipid (lysophosphatidylinositol) which is now thought to be its natural ligand (Oka et al., 2007). However, it can bind AEA, 2-AG, THC and CBD also (Ryberg et al., 2007; Lauckner et al., 2008). And, unlike CB1 and CB2 which exhibit highly conserved sequences in their ligand binding regions, this is not the case for GPR55 (Petitet et al., 2006).

1.1.3.4. TRP channels

Transient receptor potential (TRP) channels are a collection of trans-membrane, cation selective ion channels comprised of 4 subunits each containing 6 transmembrane helices (Caterina, 2014). Channels undergo homo or heterodimerization to form a functional pore (Caterina, 2014; Muller et al., 2019). Every cell expresses at least one subtype of TRP channel and so they are implicated in a diverse array of metabolic functions including sensation of pain, temperature and itching, cardiovascular function, neurotransmitter release and immune function (Caterina, 2014; Muller et al., 2019). There are 28 known TRP channels but cannabinoids are only known to modulate 6 members from 3 subfamilies: TRP vanilloid (TRPV 1-4), TRP ankyrin (TRPA 1), and TRP melastatin (TRPM 8) (Muller et al., 2019). The most well documented, with regards to interactions with cannabinoids, is TRPV1 which is a calcium channel whose natural ligand is capsaicin (Caterina, 2014). AEA, OEA, PEA, 2-AG, cannabichromene (CBC) and CBD have been shown to act as agonists for TRPV1

1.2. Evidence for an ECS in protists

1.2.1. General overview of protists

Protists are a heterogenous and ubiquitous collection of microbial eukaryotic organisms belonging to the domain Eukarya (Fenchel and Finlay, 2004; Foissner, 2008). Protist classification is difficult due to their immense diversity, but in brief, they encompass 3 broad groups: the protozoa (heterotrophic protists), algae and slime molds (Foissner, 2008). Protists are ubiquitous and are cosmopolitan in distribution, being able to grow wherever their habitat requirements are met (Fenchel and Finlay, 2004; Finlay and Fenchel, 2004; Foissner, 2008). In each environment, they play an important role as key producers and consumers in food chain (Pernthaler, 2005; Caron et al., 2012). For example, the ‘microbial loop’ describes how bacteria incorporate dissolved organic matter into their biomass which is then transferred to the next trophic level upon their consumption by protists (Azam et al., 1983). These protists also contribute significantly to nutrient regeneration through the release of dissolved nutrients, mainly

orthophosphate and ammonium (Sherr et al., 1983; Dolan, 1997), which can be used by their bacterial and algal prey (Caron et al., 1988; Kirchman, 1994). Their grazing pressure is also known to be a primary factor shaping the composition of bacterial and algal communities (Pernthaler et al., 1996; Macek et al., 1997).

Protists show diversity in metabolism, with heterotrophic, phototropic and mixotrophic protists all being common (Yaeger, 1996; Corliss, 2002). Within the heterotrophic protozoa, there are ciliates, amoeba and flagellates with the majority being ubiquitous, free-living organisms, although parasitic or endosymbiotic examples are present (Yaeger, 1996; Corliss, 2002). Their size generally ranges between 2 µm - 2000µm with most flagellates being < 2 µm, most amoebae < 20 µm and most ciliates < 200 µm (Finlay and Esteban, 1998). The three groups use different methods for locomotion and feeding (Yaeger, 1996; Corliss, 2002). Amoeba use their flexible cell shape to create cellular extensions called pseudopodia which are used for locomotion on surfaces and phagocytosis of prey in a similar fashion to macrophages (Geisen et al., 2018; Diaz and Laybourne-Parry 2019). Flagellates utilise flagella for motility and feeding, e.g. choanoflagellates use flagella to create a water current that pulls prey into a collar of prior to engulfment with pseudopodia (Caron et al 2012; Geisen et al., 2018; Diaz and Laybourne-Parry, 2019). The ciliates utilise cilia for feeding and locomotion with the majority being 'filter feeders', i.e., using cilia to pull water towards the cytostome (cell mouth) from which they can 'filter' out prey particles (Verni and Gualtieri, 1997; Caron et al., 2012; Geisen et al., 2018; Diaz and Laybourne-Parry, 2019). Their rate of bacterial consumption is extremely high, especially within the ciliates (Fenchel, 1982; Sherr and Sherr, 2007), and most information regarding the protozoan feeding mechanism has been gathered for this protozoan group.

There are a small number of studies which have examined either the behaviour of protists in the presence of cannabinoids or sought evidence for the presence of individual ECS components in their cells. To date, a complete picture of a protist ECS does not exist but the most comprehensive information has undoubtedly been gathered for the ciliate *Tetrahymena* (*T. thermophila* and *T. pyriformis*).

1.2.2. Effect of cannabinoids on *Tetrahymena* behaviour

Δ^9-THC has been shown to elicit a transient dose dependent response on *T. pyriformis* cell shape and motility, with cells becoming ovoid, sluggish and irregular in their movement (McClean and Zimmerman, 1976). The cells also showed delays in cell division and an overall reduction in the number of cells dividing, along with a decrease in nucleic acids synthesis (McClean and Zimmerman, 1976). A later study confirmed that the THC-induced delay in cell division occurred in the G2 phase of the cell cycle and was

attributed to a THC-mediated suppression of cyclic AMP and GMP production; levels of which normally fluctuate and control ciliate cell division (Zimmerman et al., 1981).
More recently, Wanlahbeh (2020) showed that CBD and AEA induced cell death in a *T. pyriformis* population (MICs of 3.16 and 1.17 µM, respectively), with the population recovering in ~90 minutes. Jaisswar (2020) also showed that CBD and AEA (at 4 µM) immediately halted feeding in *T. pyriformis* for 60 and 36 min, respectively, and when feeding resumed AEA-treated cells fed at the same rate as the Control cells whereas CBD-treated cells had elevated ingestion rates (hyperphagia). Further work revealed that neither CBD nor AEA halted food vacuole processing and defecation in *T. pyriformis* which led to the suggesting that the cannabinoid target was a factor involved in the initial recognition and uptake of prey by the ciliate (Jaisswar 2020).

1.2.3. Presence of FAAH and MAGL in *Tetrahymena*

T. pyriformis has been shown to possess two FAAH isoforms (tFAAH), i.e., a 66kDa membrane isoform and a 45kDa cytosolic form (Karava et al., 2005). These are of similar size to the 63-67kDa mammalian FAAH (Giang and Cravatt, 1997), and the 46kDa invertebrate FAAH (Matias et al., 2001). tFAAH is secreted from the ciliate cell and exhibits high activity particularly against AEA; 90% of AEA was hydrolysed to AA within 5 minutes of administration (Karava et al., 2001). The resulting AA was incorporated mostly into phospholipids and, to a lesser extent, into non-polar lipids (Karava et al., 2001). Although tFAAH is considered specific for AEA, under alkaline conditions the *T. pyriformis* supernatant could also hydrolyses OEA and PEA, suggesting this orthologue can have multiple NAE substrates, as has been recorded for the mammalian counterpart (Karava et al., 2001).

T. thermophila possesses two MAGL isoforms (tMAGL), i.e, a membrane active 45kDa protein and a cytosolic 40kDa protein (Evagorou et al., 2010). These are larger than the two isoforms identified mammals (35 and 37 kDa) (Dinh et al., 2002). Both ciliate isoforms are involved in the hydrolysis of 2-AG and 2-Oleoylglycerol (2-OG) and they have similar optimum conditions to the MAGL in mammals, i.e., optimum pH of 8-9 and temperature of 37-40^{o}C (Evagorou et al., 2010).

1.2.4. Presence of endocannabinoids in *Tetrahymena*

To date, no endocannabinoid synthesizing enzymes have been identified in *Tetrahymena* and yet, Anagnostopoulos et al., (2010) discovered a suite of endocannabinoids in *T. thermophila* which included NAEs, 2-AcGs and free fatty acids.

With regards to the NAEs, the 6 most common were *N*-γ-linolenoylethanolamine (GLEA), *N*-eicosenoylethanolamine (EEA), *N*-linoleoylethanolamine (LEA), *N*-palmitoylethanolamine (PEA), *N*-

oleoylethanolamine (OEA) and *N*-stearoylethanolamine (SEA). AEA was identified but at low concentrations (Anagnostopoulos et al., 2010). Although common within the *T. thermophila* cell, GLEA, SEA and EEA are very rare in nature (Anagnostopoulos et al., 2010; Kleberg at al., 2014; Gaitán et al., 2018), while LEA, PEA and OEA are more common and are found primarily in the GI tract (Artmann et al., 2008). All NAEs were hydrolyzed by FAAH, with the highest enzyme activity being evident with AEA, followed by LEA and GLEA (Anagnostopoulos et al., 2010).

1.2.5. Cannabinoid receptors in *Tetrahymena*

Although *Tetrahymena* possesses endocannabinoids, and the enzymes that metabolise them, a cannabinoid receptor has yet to be identified. A *de novo* phylogenetic analysis of functional orthologues of some known receptors strongly suggested that *Tetrahymena* does not possess CB1, CB2 TRPV1 and GPR55 (McPartland et al., 2006), however, there are other lesser known receptors which have been shown to interact with endocannabinoids, phytocannabinoids and/or synthetic cannabinoids, and which are putatively present in *Tetrahymena* (Table 1.1). Thus, one or more of these might be acting as the cannabinoid receptor in *Tetrahymena*.

1.2.5.1. G protein-coupled receptors (GPCRs)

Considering the classical endocannabinoid receptors, CB1 and 2, are both GPCRs it is considered likely that cannabinoids interact with a GPCR in *Tetrahymena*. Indeed, a variety of GPCRs are now considered as putative endocannabinoid receptors (see 1.1.3.3).

1.2.5.1.1. Opioid receptor

Tetrahymena possess the ability to produce and respond to a range of hormones which can influence cellular function, particularly phagocytosis (Csaba, 2012; 2017). For example, the opioid β-endorphin, when applied exogenously, can stimulate a chemotactic effect in *Tetrahymena* (O'Neill et al., 1988*)* and inhibit phagocytosis (Salaman et al., 1990; Chiesa et al., 1993). *Tetrahymena* spp. can produce β-endorphin-like peptides which also antagonise phagocytosis (Renaud et al., 1995; Rodriguez et al., 2004). This inhibitory effect appears to be mediated by an opioid receptor homologue (O'Neill et al., 1988), which is a GPCR exhibiting $G_{i/o}$ linkage (Benarroch, 2012), and which appears to be most similar to the μ (MOR) class of opioid receptors (Chiesa et al., 1993).

Although no endogenous cannabinoid has yet been shown to interact with opioid receptors, work on murine models revealed that the phytocannabinoids CBD and THC exhibit allosteric modulation of MORs with both exhibiting negative regulation (Vaysse et al., 1987; Kathmann et al., 2006). The

synthetic cannabinoid receptor agonist 'rimonabant' also exhibits allosteric modulation of MORs despite being structurally unrelated to CBD or THC (Cinar and Szücs, 2009).

Table 1.1. *Some known receptors and the traditional cannabinoids and cannabinoid like compounds that interact with them. a, McPartland (2006b); b, Pertwee et al (2010); c, Turner et al (2017); d, Muller et al (2019); e, Zygmunt et al, (2013); f, O'Sullivan (2016); g, De Duve and Baudhuin (1996); h, Bih et al (2015); i, Ciliate.org; j, Laun et al (2019); k, Kohno et al (2006), L, Chiesa et al (1993), m, Ud-daula (2012), n, Csaba (2012), o, Baig and Ahmad (2016)*

Receptor	**Classic cannabinoid and cannabinoid-like ligands**	**Evidence for their presence in *Tetrahymena* sp.**
Cannabinoid receptor 1 & 2. (CB1 & 2)	AEA [b], 2-AG [b], THC [b]	No [a]
TRPV1	AEA [b,d], PEA [b,d], OEA [b,d], 2-AG [e], CBD [b,d]	No [a]
PPAR	AEA, PEA, OEA, 2-AG, CBD, THC [h f]	None identified currently but peroxisomes are present [g]
Adenosine receptors	AEA [b], 2-AG [b], CBD [c,h]	No
Serotonin (5-HT)	AEA [b], THC [b], CBD [c,h]	*Tetrahymena* are able to produce and respond to serotonin [n] but receptor not yet characterised.
Nicotinic/muscarinic acetylcholine	AEA & 2-AG to Nicotinic, only AEA to muscarinic [b], CBD to Nicotinic [h]	No, but muscarinic receptors are present in some protists [o]
Opioid	THC [b], CBD [h]	Yes, μ (MOR)-like receptor. Interactions with a variety of opioids is also possible [L]
Dopamine	No classical cannabinoids exhibit binding yet but some synthetic cannabinoids have[b]	Yes. D1 like-receptor[m]
GPR55	AEA [b], 2-AG [b], THC [b,c], CBD [c,h]	No [a]
GPR 3, 6, 12	CBD [j]	GPR6 only [i]
GPR18	AEA [k], 2-AG [k], THC [c], CBD [h]	No

1.2.5.1.2. Dopamine receptors

Tetrahymena can synthesize and react to catecholamines, with dopamine being considered the primary catecholamine present in its cells (Csaba, 2012; 2015). Endogenous dopamine effects have been suggested to differ from those in higher eukaryotes (Gundersen and Thompson, 1985) but the actual effect is still unknown. However, levels are known to fluctuate between stationary and logarithmic growth stages suggesting a potential role in cell growth (Goldman et al., 1981)

In humans, dopamine acts upon two families of GPCR dopaminergic receptors, i.e., D1-like receptors (encompassing D1 and D5), and D2-like receptors (encompassing D2, D3 and D4) (Mishra et al., 2018). D1-like receptors couple primarily to the Gs family of G proteins (G_s and G_{olf}), whereas D2-like receptors couple primarily to the $G_{i/o}$ family (Mishra et al., 2018). Previous work has shown that Δ^9-THC can bind directly to D1 receptors (Miyamoto et al., 1996) while CBD binds to, and acts as a partial agonist of D2 receptors (Seeman, 2016). AEA can also be an antagonist of D2 receptors which is thought to play regulatory roles in dopamine-induced behaviours (Beltramo et al., 2000).

A D1-like receptor has been identified in *T. thermophila* although the authors did not rule out the possible presence of a D2-like receptor as well (Ud-Daula et al., 2012).

1.2.5.1.3. Serotonin (5-HT) receptors

Tetrahymena is known to synthesize and respond to serotonin (Csaba, 2015) with the main response being a stimulation of phagocytosis (Quiñones-Maldonado and Renaud, 1987). In humans, serotonin mediates its effects via diverse families of 5-HT receptors (5-HTRs) of which there are seven subclasses (5-HT 1-7) (Bockaert et al., 2010). 5-HTRs are GPCRs that are linked with $G_{i/o}$, $G_{q/11}$ and G_s alpha subunits (Bockaert et al., 2010; Masson et al., 2012). 5-$HT1_A$ is the receptor that has been shown to mediate serotonin-induced stimulation of phagocytosis in macrophages (Freire-Garabal et al., 2003) and it has also been shown to interact directly with CBD (Rock et al., 2012; Pazos et al., 2013; Fogaça et al., 2014; Sonego et al., 2016; De Gregorio et al., 2019). 5-$HT1_{A,B,D,E}$ and 5-$HT2_C$ receptors can also interact directly with AEA, which inhibits binding to 5-HT to these receptors (Pertwee et al., 2010).

No 5-HT analogue has been found in *Tetrahymena* or other protists to date. However, Al-Hammadi (2020) found that the negative action of CBD on phagocytosis in the amoeba *Naegleria gruberi* was abolished in the presence of (S)-WAY 100135, which is a specific 5-$HT1_A$ blocker, suggesting the presence of an orthologue of some kind.

1.2.5.1.4. Adenosine receptors

Adenosine is present in *Tetrahymena* and used for metabolism of its phosphate linked derivatives (Voichick et al., 1973), but little work has been done on the physiological effects of adenosine itself.

Adenosine receptors (ARs) belong to the GPCR family and are divided into 4 subtypes: A_1, A_{2A}, (both of which display high adenosine affinity) A_{2B}, and A_{3A} (displaying low adenosine affinity) with A1 and A_{3A} exhibiting $G_{i/o}$ coupling while A_{2A} and A_{2B} exhibit $G_{s/olf}$ coupling (Sheth et al., 2014). Human macrophages and monocytes both possess A_1 or A_2 receptors, with stimulation either increasing or inhibiting phagocytosis depending on temporal factors relating to the timeline of monocyte differentiation into macrophages (Haskó et al., 2007). ARs have demonstrated some limited interactions with CBD in mammalian models (Castillo et al., 2010; Mecha et al., 2013). The antiarrhythmic properties of CBD were shown to be abolished through the use of an A_1 antagonist (Gonca and Darıcı, 2015) and evidence also showed that CBD anti-inflammatory effects may partially be mediated through A_{2A} (Castillo et al., 2010; Mecha et al., 2013). Furthermore, AEA and 2-AG have both been shown to be negative allosteric inhibitors of human A_3 receptors but not A_1 receptors (Lane et al., 2010).

No AR analogue has been found in *Tetrahymena* or other protists to date.

1.2.5.1.5. Orphan GPCRs

Orphan GPR3, 6 and 12 belong to a family of GPCRs that bind Sphingosine-1 phosphate (Uhlenbrock et al., 2002). They exhibit 60% sequence similarity with each other and 40% similarity with CB1/2 (Morales et al., 2018). They exhibit coupling to either $G_{i/o}$ or G_s which inhibit and activate adenylate cyclase, respectively (Uhlenbrock et al., 2002; Pertwee et al., 2010). Endogenous agonists for all 3 are yet to be confirmed and hence why they are termed ‘orphan’ (Morales et al., 2018). Neither AEA nor 2-AG demonstrate significant activity at any of the three GPRs (Yin et al., 2009; Laun et al., 2019), whereas CBD has been shown to demonstrate significant agonism for the trio (Laun et al., 2019).

GPR18 is an 331 amino acid orphan GPCR and studies suggest that *N*-arachidonylglycine (NAGly), a carboxylic metabolite of AEA, is its endogenous ligand which, upon binding, activates coupled $G_{i/o}$ proteins (Gantz et al., 1997). In addition, some evidence is present suggesting AEA, 2-AG and synthetic CBD analogues can activate GPR18 (Kohno et al., 2006; McHugh et al., 2010).

GPR119 is another orphan GPR which is 335 amino acids in length and shares little sequence identity with other known GPRs (Fredriksson et al., 2003). The receptor exhibits coupling to a G_s protein-adenylate cyclase based mechanism (Ritter et al., 2016). Ligands with the highest affinity for GPR119 are fatty acid amides, particularly OEA (present in *Tetrahymena*), which has been proposed as the primary

orthosteric ligand of GRP119 (Overton et al., 2006). AEA, PEA and SEA (present in *Tetrahymena*) can also act as slight agonists although not to the same degree as OEA (Overton et al., 2006).

Only relatively recently has a GPR6 homologue been found in *T. thermophila* via a study utilising the *Tetrahymena* genome database (Lampert et al., 2011). This *Tetrahymena* GPR6 possessed the closest sequence similarity with a GPCR from several plants and the ciliate *Paramecium* and seems to be involved with *Tetrahymena* chemotaxis (Lampert et al., 2011). A second orphan GPCR was identified in *T. thermophila* by (Lampert et al.,2011b), i.e., GPR37 which shared the greatest sequence similarities with a known GPCR from *Dictyostelium* and with the *T. thermophila* GPR6 (Zou and Hennessey, 2017). Current understanding of GPR37 identifies it as a chemorepellent receptor for a currently unknown factor produced directly by *T. thermophila* cells (Zou and Hennessey, 2017). No homologues of GPRs 3, 12 and 18 have been identified in *T. thermophila* to date, but they might be one of the seven remaining candidates that have been suggested to exist via the *T. thermophila* genome analysis (Lampert et al., 2011), and which are currently being investigated.

1.2.5.2. Peroxisome proliferator-activated receptors (PPARs)

Peroxisome proliferator activated receptors (PPARs) are a subfamily of ligand activated receptors belonging to a superfamily of nuclear receptors (Tyagi et al., 2011). They are key regulators of lipid and glucose metabolism (Wahli et al., 1995; Varga et al., 2011). Mammalian PPARs exist in 3 isoforms: α, β/δ, and γ (Kliewer et al., 1994). Ligands include small lipophilic molecules such as fatty acids and their derivates so, due to their lipid nature, cannabinoids and their derivates exhibit PPAR α and/or γ binding activity; there is little evidence for the activation of PPAR β/δ (O'Sullivan and Kendall, 2010). In mammalian cells, AEA and 2-AG can activate both PPAR α and γ (Sun and Bennett, 2007; O'Sullivan, 2016), OEA and PEA bind to PPAR α (Fu et al., 2003; Guzmán et al., 2004; Sun and Bennett, 2007) while THC and CBD (and other phytocannabinoids) bind to PPAR γ (O'Sullivan et al., 2005; O'Sullivan et al., 2009).

Although no PPARs have been identified in *Tetrahymena* to date, they do possess peroxisomes (De Duve and Baudhuin, 1966; Fok and Allen, 1975) which are organelles that display PPAR mediated proliferation (Issemann and Green, 1990). Peroxisomes are single membrane, spherical organelles containing various oxidative enzymes that are mediators of oxidative reactions within eukaryotes (Smith and Aitchison, 2013). Peroxisomes are therefore utilised in many biochemical pathways with the most notable function in higher eukaryotes being in β-oxidation of fatty acids (Smith and Aitchison, 2013). β-oxidation still appears to be the primary function of peroxisomes in *Tetrahymena* as the enzymatic profile suggests a primary role in gluconeogenesis, which requires prior oxidation of fatty acids (Takei et al., 1982).

Wanlahbeh (2020) showed that a range of PPAR agonists (OEA, PEA, GW0742 and Rosigitazone), together with CBD and AEA, induced cell death in a *T. pyriformis* population. The negative effect of the PPAR agonists was blocked with their respective isoform antagonist (OEA/PEA, PPAR α; GW0742, PPAR β/δ; Rosigitazone, PPAR γ). AEA-induced death was blocked by all three isoform antagonists (α, β/δ and γ) while CBD-induced death was only blocked by the PPAR α antagonist. Since only vertebrates are known to possess the three distinct PPAR isoforms (Kliewer et al., 1994), Wanlahbeh (2020) suggested that *T. pyriformis* might possess one promiscuous PPAR-like receptor that can interact with agonists/antagonists for the three isoforms at different sites in the molecule.

Jaisswar (2020) investigated the effects of OEA, CBD and AEA (at 4 µM) on *T. pyriformis* feeding behaviour and found that OEA (PPAR α agonist) had no effect, while CBD and AEA immediately halted feeding. When feeding resumed, AEA-treated cells fed at the same rate as the Control cells whereas CBD-treated cells exhibited hyperphagia. Since a good proportion of *T. pyriformis* cells would have been dying at a concentration of 4 µM (Wanlahbeh, 2020), the cannabinoid-induced feeding response was monitored in the presence of a PPAR α antagonist. However, even though this antagonist alleviates cell death (Wanlahbeh, 2020) it was not able to alleviate the cessation of feeding (Jaisswar, 2020), suggesting that cannabinoids act on ciliate cells in at least two ways, (i) they cause cell death (which involves PPAR) and, 2) they affect feeding (which does not involve PPAR). This latter response differed from that of the amoeba *Vermamoeba vermiformis* which showed a similar cessation in feeding to *T. pyriformis* in the presence of CBD (but not AEA) (Al-Hammadi, 2020). In this case however, the CBD-induced feeding lag was blocked with the PPAR α antagonist. So, both protists respond to the PPAR α antagonist, but it stops cell death in *T. pyriformis* (with no effect on feeding) and stops the cessation of feeding in *V. vermiformis*; cell death was not monitored by Al-Hammadi (2020).

1.2.6 Summary

Tetrahymena clearly contains a rudimentary endocannabinoid system, equipped with a suite of endogenous cannabinoids including NAEs, 2-AcGs and free fatty acids. Catabolic enzymes for these endocannabinoids have also been identified although the anabolic enzymes have yet been elucidated. Furthermore, *Tetrahymena* can directly respond to exogenously administered cannabinoids, including the classical phytocannabinoids THC and CBD. Of particular interest is CBD due to its therapeutic potential.

Previous work has identified that CBD directly affects the phagocytic feeding behaviour of *Tetrahymena* cells through a yet unidentified mechanism. However, given the wide array of potential cannabinoid receptors, and the paucity in the knowledge of CBD mechanisms, identifying a particular target is

difficult. However, in order to begin unravelling this, a good understanding of the *Tetrahymena* phagocytic mechanism is needed.

1.3 The ciliate feeding mechanism

Ciliate feeding involves several distinct steps and each is described below with special emphasis on the model ciliate used in the current study (*Tetrahymena pyriformis*) and whether evidence exists for an interaction with cannabinoids.

1.3.1. Prey capture

T. pyriformis is a classic filter feeder and as such, uses its cilia to direct prey into its oral cavity (mouth organelle) (Fig. 1.4). This cavity comprises 3 sections: an undulating membrane, oral ribs and 3 oral membranelles (M1-3) surrounding the cavity (Smith, 1982) (Fig. 1.4). The undulating membrane (UM) is formed from a line of kinetosomes (ciliary basal bodies) that ridge the top of the right side of the oral cavity and below this lie the oral ribs, a series of ridges formed from microtubules that line the right cavity wall (Smith, 1982) (Fig. 1.4). Opposite this, M1, 2 and 3 sit on the left wall and are covered in 3 rows of cilia (typically longer than those found on the rest of the ciliate) (Smith, 1982) (Fig. 1.4).

Beating of these membranelles, plus the cilia on the UM, creates currents in the extracellular fluid bringing prey into the cavity (Rasmussen, 1976; Smith, 1982) where they are then pushed down a ciliated channel (cytopharynx) and into the cytostome where they are packaged into a food vacuoles (FVs) (Elliott and Clemmons, 1966; Smith, 1982; Verni and Gualtieri, 1997).

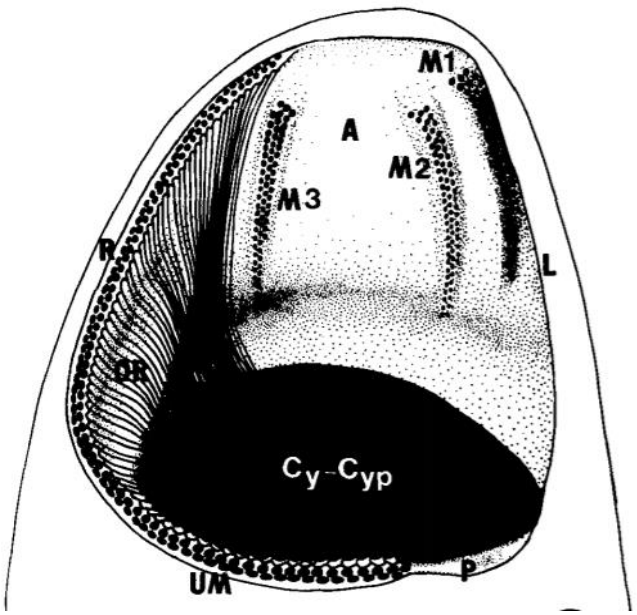

Figure 1.4.
Three-dimensional illustration depicting the basic structure of the oral cavity in the ciliate Tetrahymena. The cytostome-cytopharyngeal complex (Cy-Cyp) sits at the base of the oral cavity with the right wall (R) being lined by the oral ribs (OR) which curve down into Cy. The undulating membrane (UM) lines the right and part of the posterior margin (P) of the oral cavity. Several membranelles are located on the anterior wall (A) of the cavity. Membranelle 1 (M1) is located next to the left wall (L) of the cavity, membranelle 2 (M2) sits adjacent to M1 while membranelle 3 (M3) sits adjacent to R. Cilia protrude from the UM and M1,2 and 3 but have been omitted from the illustration.

(Smith 1982)

Prior to the mechanical action of packaging vacuole, ciliates must recognise their prey through a combination of mechanical (Fenchel, 1980; Montagnes et al., 2008) and chemosensory factors (Verity, 1991). While ingestion of particles can seem to be unspecific because ciliates can ingest abiotic particles such as latex beads or indian ink (Weidenbach and Thompson, 1974; Batz and Wunderlich, 1976), selectivity of prey is still seen, suggesting receptor-based prey recognition is important (Ricketts, 1971; Montagnes et al., 2008).

1.3.2 Prey recognition (Fig 1.5, Stage 1-2)

Phagocytes utilise Pattern Recognition Receptors (PRRs) to identify structural motifs on bacterial cell surfaces; collectively known as Pathogen Associated Molecular Patterns (PAMPs) (Dambuza and Brown, 2015; Rosales and Uribe-Querol, 2017). The two major classes of PRRs are C-type lectins (CLRs) and Scavenger receptors (SRs); both of which bind to specific carbohydrates moieties such as those found in bacterial cell walls (Dambuza and Brown, 2015; Rosales and Uribe-Querol, 2017).

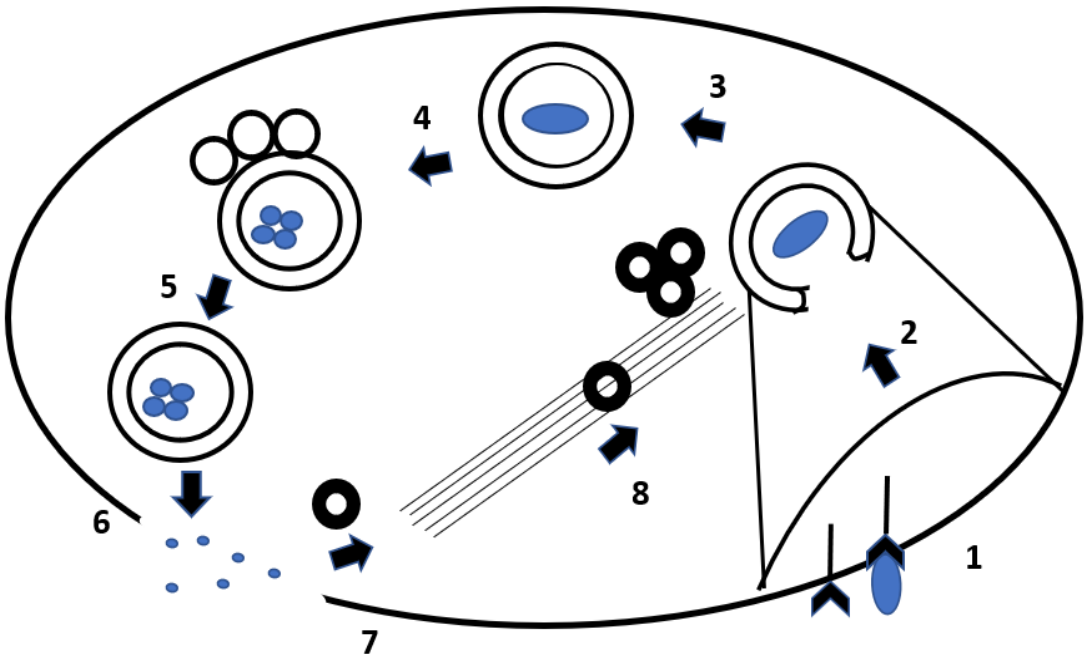

Figure 1.5. *Simplified diagram representing the overall process of the ciliate phagocytic cycle. 1. Receptors available at the oral cavity (precise receptor location unknown) bind available prey filtered into the oral apparatus via ciliary beating. 2. Prey is swept down the cytopharynx into the cytostome where recycled membrane is used to form a food vacuole (FV) around the prey via the polymerisation of F-actin. 3. Myosin activation and actin depolymerisation begins FV closure and dynactin activation facilitates scission of the FV from the cytostome. The Nascent FV then travels into the cytoplasm. 4. Nascent FV binds endosomes and lysosomes for FV maturation and digestion of prey 5. Mature FV is transported to cytoproct. 6. Indigestible particles are exocytosed via binding of FV membrane with membrane of cytoproct. 7. FV membrane is endocytosed from the cytoproct membrane and forms small disc-shaped vesicles. 8. Discoid vesicles are transported back to oral cytostome via a microtubule network and recycled for use in additional nascent FV synthesis. (Figure adapted from Al-Hammadi, 2020).*

1.3.2.1. C-type lectin receptors (CLRs)

CLRs encompass a superfamily of over 1000 functionally diverse proteins characterised by the possession of C-type lectin-like domains (CTLDs) (Dambuza and Brown, 2015; Rosales and Uribe-Querol, 2017). CLRs derive their name from their Ca^{2+} dependent binding of carbohydrates afforded by a conserved carbohydrate binding motif present within their CTLD (Dambuza and Brown, 2015). The two most prominent motifs are EPN (Glu-Pro-Asn) which binds to mannose, *N*-acetylglucosamine (GlcNAc), *L*-fructose and glucose, and QPD (Gln-Pro-Asp) which binds to galactose and *N*- acetylgalactosamine (GalNAc) (Dambuza and Brown, 2015). Studies have revealed that protists utilise CLRs as PRRs for prey recognition, with CLRs that bind mannose, GalNAc and/or GlcNAc receiving the most attention.

A receptor that binds mannose has been identified in the filter feeding ciliate *Eupoltes mutabilis* using Concanavalin A (ConA); a fluorescent lectin which binds to mannose residues (Wilks and Sleigh, 2004). Over a period of 10s – 30 mins, ConA bound to the cytostome first, then at the cytostome and the FVs, then only the FVs and then no binding was seen; labeling of the whole FV membrane was observed (Wilks and Sleigh, 2004). *T. pyriformis* also possesses such a receptor but ConA labelling only revealed its presence on the FVs (Dürichen et al., 2016). More recently, pre-treatment of *T. pyriformis* with 100mM mannose (to block the receptor) has been shown to significantly decreases the ingestion of live *Salmonella enterica* cells by the ciliate (Boboc, 2020).

A receptor that recognises GalNAc has been identified in *Euplotes* spp. using the fluorescent plant lectins *Glycine max* (soy bean) (SBA), *Maclura pomifera* (MPA), peanut agglutinin (PNA) and *Maakia amurensis* agglutinin (MAA), all of which bind GalNAc residues (Wilks and Sleigh, 2004). Specifically, lectins bound to the *E. mutabilis* cytostome and FVs in the first 5 minutes of feeding (Wilks and Sleigh, 2004). More recently, pre-treatment of *T. pyriformis* with 100mM GalNAc (to block the receptor) has been shown to significantly decreases the ingestion of live *Salmonella enterica* cells by the ciliate (Boboc, 2020).

A receptor that recognises GlcNAc has been identified in *Euplotes* spp. using wheat germ aggultinin (WGA) lectins. WGA bound to the oral membranelles in *Euplotes* with the degree of binding being dependent on the species (Wilks and Sleigh, 2004). Again, in *E. mutabilis* lectin binding was sequential, as seen with ConA, and no fluorescence was observed after 60 minutes (Wilks and Sleigh, 2004). Conversely, WGA binding differed in *T. pyriformis* whereby only nascent FVs bound WGA, not older ones, suggesting this receptor only plays a role in the very early stages of FV formation but is excised or masked in the later stages (Dürichen et al., 2016). In addition, WGA binding to FVs was patchy, unlike

complete binding observed with ConA (Dürichen et al., 2016). More recently, pre-treatment of *T. pyriformis* with 100mM GlcNAc (to block the receptor) has been shown to significantly decreases the ingestion of live *Salmonella enterica* cells by the ciliate (Boboc, 2020).

Receptors that recognise all three sugars (mannose, GalNac and GlcNac) have therefore been demonstrated to exist in *T. pyriformis* (Dürichen et al., 2016) but whether they are targeted by cannabinoids, to induce the negative effect on feeding observed by Jaisswar (2020), is currently unknown. Indeed, there is no evidence to date that C-type lectins can actually bind cannabinoids, although there is some evidence that C-type lectins can bind lipids (Cummings and McEver, 2009). Despite this, not all CLRs are carbohydrate-specific receptors with some lacking a carbohydrate binding domain and Ca^{2+} interaction, and instead binding proteins, lipids and even inorganic molecules (Dambuza and Brown, 2015; Brown et al., 2018).

The only study to date that has examined the interaction between cannabinoids and C-type lectins, and their effect on feeding, was carried out by Al-Hammadi (2020) on the amoeba *Vermamoeba vermiformis*. Here, the blocking of the three CLRs with 100mM of their respective sugar did not induce a feeding lag, whereas the presence of CBD did. Pre-blocking cells with mannose or GalNAc prior to adding CBD did not affect the CBD-induced lag (suggesting no interaction) but pre-blocking with GlcNAc doubled the length of the CBD-induced lag (suggesting an interaction) (Al-Hammadi, 2020). The exact nature of this interaction is currently unknown but similar experiments with *T. pyriformis* and CBD were carried out in the current study.

1.3.2.2. Scavenger receptors (SRs)

Scavenger receptors (SRs) are a family of receptors able to act as PRRs in macrophages (Brown and Goldstein, 1979). Mammalian SRs have a variety of ligands including both modified and unmodified endogenous lipoproteins and proteins (Canton et al., 2013) and glycans/glycosylated structures (Taylor and Drickamer, 2019) including some microbial structures such as lipoteichoic acid (LTA), lipopolysaccharides (LPS) and unmethylated bacteria DNA (Plüddemann et al., 2006; Plüddemann et al., 2011). The grouping of SRs into classes (A-J) is based solely on their function as there is little similarity between the 10 classes (Zani et al., 2015). Class A and B are the most prominent SRs (Zani et al., 2015) with class A (SR-A) being the primary SR in macrophages and Class B primarily binding oxidised low density lipoproteins (OxLDL) (Zani et al., 2015).

Despite widespread distribution in mammalian phagocytes only one paper has suggested the presence of SRs in protists. The slime mold *Dictyostelium discoideum* was shown to possess homologues of the class

B SRs, LIMP-2 and CD36 (Lmp A and Lmp B respectively). Lmp A was found to be associated with endosome transport, phagolysosome acidification/formation, and phagocytosis of mainly Gram-positive bacteria while LmpB was localized to the plasma membrane and early phagosomes and was exclusively involved in the uptake of Gram-positive bacteria (Sattler et al. 2018). To date, there are no reports of SRs existing in ciliates, or their involvement in phagocytosis, although a putative homologue of LmpB does exists in *T. thermophila* (Ciliate.org). The presence of SRs in *T. pyriformis*, and potential interaction with CBD, was investigated in the current study.

1.3.3 Food vacuole formation (Fig 1.5, Stage 3)

The exact mechanism of FV formation in *Tetrahymena* is not fully understood, but it is considered to be similar to that occurring in other phagocytes, as protists share many of the proteins known to be involved in phagocytosis and vacuole maturation in mammalian phagocytes (Jacobs et al., 2006). In these phagocytes, PRR-ligand interaction triggers intracellular signalling pathways resulting in actin rearrangement for pseudopodia extension and phagocytic cup formation (Rosales and Uribe-Querol, 2017; Lee et al., 2020). Activation of actin related protein 2/3 complex (ARP2/3) via the same signaling pathway seeds *de novo* polymerisation of filamentous actin (F-actin) (Ma et al., 1998; Babuta et al., 2015; Lee et al., 2020).

While filter feeding ciliates do not utilise pseudopodia, the remodeling of the actin cytoskeleton is still known to be involved in ciliate FV formation (Nilsson et al., 1973; Elde et al., 2005; Williams et al., 2006). Successful FV formation in *Tetrahymena* requires a function ACT1 gene (actin coding gene) (Williams et al., 2006) and the primary actin modulating protein ADF/Cofilin (Shiozaki et al., 2013). *Tetrahymena* possesses ARP homologues including ARP 2 and 3 which are believed to also facilitate F-actin formation (Kuribara et al., 2006), suggesting a similar ARP2/3 based mechanism to that of other phagocytes. However, actin is also known to play a role in FV trafficking (Méténier, 1984; Hosein et al., 2005; Sehring et al., 2007b) and considering CBD does not affect FV trafficking in *T. pyriformis* (Jaisswar., 2020), it seems unlikely that CBD acts negatively on actin at the FV formation stage, unless completely different actin isoforms are employed in the two processes.

The sealing and detachment of phagosomes is initiated by phosphoinositide signalling which triggers actin depolymerisation from the base of the cup (Rosales and Uribe-Querol, 2017). Signalling also activates myosin motor proteins to generate localised contractile forces which facilitate the closing of the cup (Swanson et al., 1999; Dart et al., 2012). Detachment of the phagosome membrane utilises Dynamin-2, which carries out scission of endocytic vesicles, to excise the phagosome from the plasma membrane

(Marie-Anaïs et al., 2016). Dynamin is recruited to the closing phagosome via actin interactions, and depolymerization of actin is the trigger for dynamin activity, resulting in scission (Marie-Anaïs et al., 2016). *Tetrahymena* is known to utilise dynamin for vesicle scission, with *T. thermophila* possessing 8 families of dynamin related proteins (DRP 1-8) (Elde et al., 2005). There is one study that has reported that CBD can modulate a hippocampal dynamin-1-like protein (DNM1L) in the brain (Da Silva et al., 2014) but nothing can be found on its modulation of FV closure, so FV sealing is a candidate target for CBD in *T. pyriformis*.

In *Tetrahymena,* FV formation involves calcium signalling and depletion of intracellular calcium stores and blocking this Ca^{2+}/CaM signalling can inhibit phagocytosis (Gonda et al., 2000; Moya and Jacobs, 2006). In ciliates, two Ca^{2+}/CaM interacting proteins, p85 and EF-1α, are localised to the cytostome, cytopharynx, and an actin based 'deep fiber' that connects the oral apparatus to the cytoplasm (Gonda et al., 2000). This deep fiber is thought to be responsible for trafficking nascent FVs from the oral apparatus into the cytoplasm (Gonda et al., 2000). This demonstrates Ca^{2+}/CaM signalling involvement in both FV formation and trafficking, which once again makes it an unlikely target for CBD, unless CBD only specifically acts upon the FV formation Ca^{2+}/CaM signal.

1.3.4. Food vacuole maturation/digestion (Fig 1.5. Stages 4-5)

FV maturation/trafficking in *T. pyriformis* has been shown to be unaffected by CBD treatment (Jaisswar, 2020) but it is still worth noting the overall process for completeness. FV maturation entails fusion events, modification of the phagosome proteome, and a decrease in phagosome pH (Pauwels et al., 2017; Rosales and Uribe-Querol, 2017). Digestion can be broadly grouped into 4 stages: Stage 1. FV formation, Stage 2. rapid FV condensation and acidification, Stage 3. FV-lysosome fusion and digestion of FV contents, Stage 4. Completion of digestion and awaiting defecation (Fok et al., 1982). Maturation encompasses stages 2 and 3 (Fig 1.6.).

The exact molecular mechanisms are largely unknown in ciliates, but there is a better understanding of the mechanisms in mammalian phagocytes. Nascent phagosomes begin by binding acidosomes which endower them with ATP-dependent vacuolar protein pumps (V-ATPase); used for acidification of the phagosome lumen (Allen et al., 1993; Yates et al., 2005). The *Tetrahymena* phagosome proteome contains 3 of these V-ATPases (Jacobs et al., 2006). Maturation then occurs via the sequential binding of endosomes and lysosomes which provide the necessary proteins required to generate a 'phagolysosome' (Fig 1.6.). GTPases, termed 'Rabs' (donated by endosomes), define the 'early' and 'late' stages of maturation and interact with stage-specific effectors (Meyer et al., 1998; Guerrier et al., 2017). At least 56

Rab proteins have been identified in *T. thermophila*, 11 of which are associated to the FV proteome (Bright et al., 2010). In *T. pyriformis*, lysosomes donate at least 5 hydrolases for digestion: acid phosphatase, ribonuclease, deoxyribonuclease, amylase and protease (Rasmussen, 1976). NADPH oxidases also generates reactive oxidative species for additional digestive properties (Minakami and Sumimotoa, 2006; Nunes et al., 2013). Components of the degraded cargo are transported across the membrane for use in cellular processes, whilst indigestible products are defecated (Levin et al., 2016).

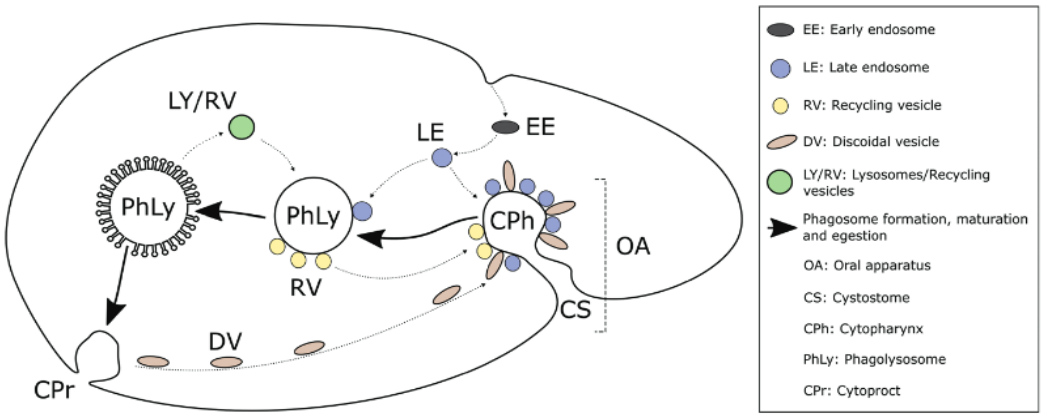

Figure 1.6. *Food vacuole maturation during phagocytosis in ciliates:. A nascent phagosome is formed in the cytopharynx (CPh) using discoidal vesicles (DVs) recycled from the cytoproct (CPr) and recycling vacuoles (RVs) from maturing phagolysosomes (PhLy). Acidosomes/late endosomes (LE) fuse with nascent phagosomes and endow them with V-ATPases allowing acidification of the lumen. Fusion with lysosomes (LY) recycled from spent phagolysosomes, provides digestive enzymes required to form a mature phagolysosome. The nascent phagolysosome, in turn, can then donate recycling vesicles to nascent phagosomes at the cytopharynx. Once contents are digested a spent phagolysosome (far left phagolysosome) will donate lysosomes/recycling vesicles (LY/RV) to subsequent phagosomes. Any waste contents are exocytosed at the cytoproct and spent vesicle membrane is sent back to the cytopharynx as discoidal vesicles for nascent vacuole synthesis.*
(Figure obtained from Guerrier et al., 2017)

The time taken for the FV trafficking phase to be complete is indicated by the Vacuole Passage Time (VPT) (i.e. the total lifespan of one FV/phagosome). Thurman et al (2010) reported a VPT of ~30 minutes in *T. pyriformis* but also noted that this was somewhat dependent on feeding history and prey species (Thurman et al., 2010). Indeed, ciliates appear to possess a secondary level of prey recognition (within the FV) which differentiates between digestible and non-digestible particles (Ricketts, 1971; Boenigk et al., 2001). For example, FVs of *T. pyriformis* which contain indigestible material do not show an increase in acid phosphatase activity (a biomarker for digestion) whereas vacuoles containing digestible prey do (Ricketts, 1971). Heterotrophic nanoflagellates also egest indigestible particles 1-2 minutes post ingestion whereas digestible particles are retained (Boenigk et al., 2001a).

1.3.5. Defecation and food vacuole membrane recycling (Fig 1.5, Stage 6-8)

Defecation of indigestible FV cargo in ciliates occurs at a precise location called the cytoproct (Blum and Greenside, 1976). Egestion of also appears to occur in order, i.e., cargo of the first vacuole formed is the first to be defecated, and can therefore alter VPT through a backlog of vacuoles awaiting defecation which will affect their VPTs (Ricketts and Rappitt, 1976; Thurman et al., 2010). CBD has already been shown not to affect the rate of defecation in *T. pyriformis* (Jaisswar, 2020).

Because there is a limited volume of membrane available in the ciliate cell for FV formation (Allen, 1974; Allen and Fok, 1980), old FV membrane must be recycled to the cytostome, for the formation of new FVs. In *Paramecium* and *Tetrahymena* it was shown that membrane from spent FVs fuses with the plasma membrane at the cytoproct and is then removed back into the cytoplasm, where it forms small disk-shaped vesicles (discoidal vesicles) (Allen and Fok, 1980). Within 3 minutes, these vesicles are coated with F-actin (Sugita et al., 2009) and become aligned to a bundle of microtubule ribbons, where they are then transported from the cytoproct to the cytostome in *ca*. 4 minutes (Allen and Fok, 1980). Considering microtubules and microfilaments in mammalian cells have been shown to be disrupted in a dose-dependent manner following treatment with CBD, THC and CBN (Tahir et al., 1992), this recycling stage remains a potential target for the action of CBD on *T. pyriformis*.

1.4. Conclusion and aims

The human endocannabinoid system is responsible for mediating a broad range of neuromodulatory effects and has been shown to be implicated in a number of diseases and disorders. This has made the ECS an attractive therapeutic target through the use of cannabinoids. Of great recent interest has been the phytocannabinoid cannabidiol (CBD), which targets a wide variety of molecular targets beyond the classical ECS receptors CB1 and 2. However, details on the relative importance of each of these other targets on CBD functioning is patchy. The ciliate *Tetrahymena* is the most well studied protist with regards to cannabinoid interactions, and feeding, and also lacks the classical CB1/2 receptors. This makes it an excellent model to study the potential importance, and evolution, of these alternative CBD targets in eukaryotic cells.

The aims of this study were:

i) To determine the effect of CBD concentration on *T. pyriformis* feeding behaviour (ingestion rate and feeding lag duration).
ii) To screen a wide variety of potential CBD receptors (based on previous literature) in an attempt to identify a molecular target responsible for mediating the CBD feeding effect.
iii) Investigate the involvement of C-type lectins and scavenger receptors in *T. pyriformis* feeding and evaluate whether they interact with CBD.

Chapter 2. Materials and Methods

2.1. Cell/microsphere maintenance and preparation

2.1.1. *Tetrahymena pyriformis*

The ciliate *T. pyriformis* (Culture Collection of Algae and Protozoa [CCAP] 1630/1W) was cultured in 500 ml Chalkley's medium (Appendix 1) with 3 ml of live *Klebsiella aerogenes* suspension (see 2.1.2). and incubated at room temperature (23 ^{o}C) 3 days prior to experiments.

On the day of an experiment, the *T. pyriformis* culture was concentrated by centrifuging multiple tubes (of 15 ml culture) at 2000 rpm for 20 mins at room temperature. The top 14 ml was removed, and the remaining 1 ml suspensions were pooled and briefly vortexed. The resulting *T. pyriformis* concentration, as determined through cell counts (see 2.2.1), varied between 5.3×10^4 - 7.5×10^5 cells/ml.

2.1.2. *Klebsiella aerogenes*

The heterotrophic bacterium *K. aerogenes* (National Collection of Type Cultures [NCTC] 9528) was used as the prey for *T. pyriformis* during routine culturing (see 2.1.1). The bacterium was streaked onto Lysogeny Broth (LB) agar plates (Appendix 1) and incubated at 25 ^{o}C for 2 days. The cells from two *K. aerogenes* plates were then suspended by pouring *ca.*7 ml sterile water onto each plate and dislodging the cells with a sterile spreader, before pooling the two suspensions. The resulting suspension was vortexed and stored at 4 ^{o}C.

2.1.3. Live *Synechococcus* sp.

The autotrophic bacterium *Synechococcus* strain S-KH3 (Dillon and Parry, 2009) was the experimental prey used in feeding experiments due to it being indigestible to *T. pyriformis* and displaying innate Chlorophyll a autofluorescence (red fluorescence under green excitation). The bacterium was cultured in Blue Green 11 (BG 11) broth (Appendix 1) at room temperature on a rotary shaker (0.00118 *g*) in a 16:8 natural light:dark cycle, 5 days prior to experiments.

On the day of an experiment, the culture was concentrated by centrifuging one tube (of 15 ml culture) at 2000 rpm for 20 mins at room temperature. The top 13 ml was discarded, and the remaining 2 ml of suspension was vortexed before determining cell concentration (see 2.2.2.).

2.1.4. Heat killed (dead) DTAF-stained *Synechococcus* sp.

Live *Synechococcus* cells were heat-killed and stained following the method of Sherr and Sherr (1987). A 15 ml sample of cells was heated in a 60 ºC water bath for 2 hours with 5 mg of 5-(4,6-dichlorotriazinyl) aminofluorescein (DTAF) (Sigma). The cells were washed via centrifugation at 3500 rpm for 10 minutes, removing the supernatant and resuspending the pellet in 10 ml of solution 1 (Appendix 1) followed by vortexing and sonication for 10 minutes. This washing procedure was performed 4 times, but the final pellet was resuspended in 10 ml of solution 2 (Appendix 1) and left overnight at 4 ºC. The suspension was then washed 3 more times using Chalkley's medium.

Cell concentration was determined (see 2.2.2) before samples were aliquoted into 300 µl samples and frozen at -20 ºC. On the day of an experiment, an aliquot was thawed at room temperature and then vortexed and sonicated for 10 minutes.

2.1.5. Fluorescently Labelled Microspheres

Yellow/green inert fluorescently labelled microspheres ('Beads') (Fluoresbrite, Polyscience Inc.) of 0.49 µm diameter were suspended in sterile water (Milli-Q) and their concentration determined (see 2.2.2) before storing at 4 ºC. Prior to experiments, suspensions were vortexed and sonicated for 10 minutes.

2.2. Cell/Bead counts

2.2.1. Determining *T. pyriformis* concentration

An aliquot of *T. pyriformis* suspension was fixed with glutaraldehyde (0.5% v/v final concentration) and loaded into two haemocytometers. Cells were counted in 9 medium-sized squares (x4 grids) with a light microscope (x40 magnification) and equation 1 was used to determine cell concentration (cells/ml).

Equation 1:

$$\frac{Total\ number\ of\ cells\ in\ 36\ medium\ squares\ (4\ grids)}{36} \times 10^4 = Concentrations\ \ (Cells/ml)$$

2.2.2. Determining *Synechococcus sp.*/bead concentration

Serial dilutions of live and dead *Synechococcus*, or beads, were prepared down to 10^{-3}. An aliquot was removed (usually 200 µl) from the 10^{-2} or 10^{-3} dilution and filtered, using a vacuum pump, onto a black membrane filter with a pore size of 0.2 µm (MF-Millipore, Whatman). A drop of immersion oil was placed onto a microscope slide onto which the membrane filter (cell/bead side up) was loaded; ensuring

no creases in the filter. Another drop of immersion oil was placed on top of the filter followed by a cover slip and another drop of oil.

Cells/beads were viewed with an epifluorescence microscope (x1600 final magnification) using green excitation for live *Synechococcus* (cells fluoresce red) and blue excitation for dead *Synechococcus* and beads (cells/beads fluoresce yellow). The number of prey within randomly selected whipple grids (contained within the eyepiece) was counted until at least 400 cells/beads had been counted in total. The concentration (cells/ml or beads/ml) of the undiluted suspension (10^0) was calculated using equation 2.

Equation 2:

$$\frac{Average\ cells/beads\ per\ Whipple\ Grid}{Volume\ of\ suspension\ added\ to\ filter\ (ml)} \times 23068 \times Dilution\ factor\ (i.e.\ 10^3)$$

$$= Concentration\ (Prey/ml)$$

2.2.3. Counting prey inside *T. pyriformis* cells

Feeding experiments generated fixed samples of *T. pyriformis* from which 8µl was placed onto a microscope slide and covered with a coverslip, then a drop of immersion oil. Cells were viewed with an epifluorescence microscope (x1600 final magnification) using bright light (to locate ciliate cells) and then either green or blue excitation (to view the prey inside). The number of prey/cell (P/C) and food vacuoles/cell (V/C) for 10 ciliate cells were determined per sample, for triplicate samples, and the average taken.

2.3. Experimental compounds

2.3.1. Cannabidiol (CBD)

A 10 mM stock solution of Cannabidiol (CBD) (TOCRIS) was prepared in ethanol and stored at -20 ^{o}C. On the day of an experiment, 10^{-1} and/or 10^{-2} dilutions were prepared in Chalkley's medium depending on experimental requirements, e.g., for 4 µM CBD, 4 µl of 10^{-1} CBD dilution was added to 1 ml *T. pyriformis* suspension for 5 minutes, prior to addition of any prey.

2.3.2. C-type lectin receptor (CLR) and scavenger receptor (SR) blockers

One mol/L stocks of D (+)-Mannose (M6020), N-Acetyl-α-D-glucosamine (GlcNAc) (A3286) and N-Acetyl-D-galactosamine (GalNAc) (A2795) (Sigma), and 400 mg/ml stocks of Dextran Sulphate (DS) (D8906) and Chondroitin Sulfate A bovine (CS) (C9819) (Sigma), were prepared in water on the day of an experiment. Incubation of *T. pyriformis* for 30 min with Mannose, GlcNAc and GalNAc (at 100 mM) blocks their respective C-type lectin receptor (CLR) whilst a 30 min incubation with DS (at 400 µg/ml)

blocks scavenger receptors A and B (SRs) - CS is structurally related to DS but does not bind SRs and is used as an additional control.

2.3.3. Other antagonists/receptor blockers

A number of antagonists (Table 2.1) were used to block presumptive CBD-interacting receptors in *T. pyriformis* (Table 1.1.), and components of the MAPK pathway, prior to the addition of CBD. The working concentration of all blockers was 10 µM except for PTX and Melittin which were 100 ng/ml and 0.3 µM respectively (Appendix 2). The ciliate was pre-incubated with the blocker for 30 mins (PTX, 5 hours) prior to the addition of CBD.

Table 2.1. *Summary of receptor antagonists (TOCRIS), their solvent and molecular target. All stocks were prepared at 10 mM and stored at -20 °C apart from PTX (0.1 µg/µL, 4 °C) and Melittin (0.3 mM, 4 °C).*

Antagonist (TOCRIS Cat No.)	Solvent	Molecular target
PPARs		
GW9662 (1508)	Ethanol	General PPAR antagonist for all isoforms
TRPV		
Capsazepine (0464)	Ethanol	General Vanilloid receptor antagonist
GPCRs		
Gallein (3090)	DMSO	All GPCRs - βγ complex inhibitor
Pertussis Toxin (PTX) (3097)	Distilled Water	Gi/o and Gt inhibitor (includes CB1, CB2, Dopamine D2, Adenosine A1, Serotonin 5-HT1_A and Opioid [all forms])
Melittin (1193)	Distilled Water	Gs inhibitor (includes GPR55, GPR119 and the two GPRs in *T. pyriformis* [6 and 37])
Dopamine D1		
LE300 (1674)	DMSO	Selective D1 receptor antagonist (D2 blocked by PTX)
Serotonin 5-HT2A		
EMD281014 (4470)	Ethanol	Selective 5-HT2A antagonist (5-HT1_A blocked by PTX)
Adenosine A2		
ZM241385 (1036)	DMSO	Selective A2 antagonist (A1 blocked by PTX)
Components of MAPK pathway		
PD98059 (1213)	DMSO	MEK inhibitor
U0126 (1144)	DMSO	Selective MEK1/2 inhibitor
SB 203580 (1202)	DMSO	P38 MAPK inhibitor
ZM336372 (1321)	DMSO	Selective c-Raf inhibitor

2.4. Effect of CBD concentration on *T. pyriformis* feeding

These experiments were not all performed at the same time, due to the numerous CBD concentrations being tested (0 µM, 0.5 µM, 1 µM, 1.5 µM, 1.75 µM, 2 µM, 2.25 µM, 2.5 µM, 2.75 µM, 3 µM, 3.25 µM, 3.5 µM, 4 µM, 4.5 µM and 6 µM). Experiments were performed at room temperature and there now follows an example of how each CBD concentration was tested.

Concentrated ciliate and prey suspensions were prepared (see 2.1.1., 2.1.3.– 2.1.5.) and concentrations determined (see 2.2.1. and 2.2.2.). Six 500 µl *T. pyriformis* aliquots were prepared and the desired volume and dilution of CBD (see 2.3.1) was added to three tubes (Tests) for 5 minutes (Control tubes received an equivalent volume of Chalkley's medium). Then, live *Synechococcus* was added to all 6 tubes to give a starting concentration of 1 x 10^7 cells/ml (this was time zero). Aliquots (50 µl) were removed from the tubes every 5 min, over a 120 min period, and fixed with glutaraldehyde (0.5% v/v final conc.). For each of the 3 replicas, P/C was determined for 10 cells (see 2.2.3).

Each concentration was tested twice (n = 6) and each replica generated a graph of P/C verses time, from which linear regression analysis allowed the identification of, (i) ingestion rate (IR)(prey/cell/min), from the gradient of the fitted line and, (ii) feeding lag time (min), from where the fitted line crossed the X-axis, where P/C = 0. The average ± SEM of IR and feeding lag was then determined.

2.5. Effect of blocking *T. pyriformis* receptors on its feeding behaviour

2.5.1. Preliminary toxicity experiments

The working concentrations of the blockers were determined from the literature and are summarised in Appendix 2. However, prior to carrying out blocking experiments, the proposed working concentration was tested against a suspension of *T. pyriformis* for 120 min (30 min for sugars) to confirm no negative effect on cell concentration. Controls received an equivalent volume of solvent. Experiments were repeated twice (n = 6).

2.5.2. Blocking receptors (other than CLRs and SRs)

Concentrated ciliate and prey suspensions were prepared (see 2.1.1., 2.1.3.– 2.1.5.) and concentrations determined (see 2.2.1. and 2.2.2.). Half of the *T. pyriformis* suspension was pre-incubated, at room temperature, with the receptor blocker ('Blocked') at its working concentration for the required duration (see 2.3.3). The other half (Control) received the same volume of solvent. Each was then divided into 6 aliquots and CBD was added to three (at 4 µM, '+CBD') while the remaining three received an equivalent volume of ethanol ('-CBD'). This yielded four experimental systems (each in triplicate): Control (no

blocker and no CBD), CBD alone, blocker alone and CBD with blocker. After 5 min, live *Synechococcus* was added to all 6 tubes to give a starting concentration of 2 x 10^7 cells/ml. The ciliate was left to feed on the prey for 20 minutes before being fixed with glutaraldehyde (0.5% v/v final conc.). For each of the 3 replicas, P/C and V/C was determined for 10 cells (see 2.2.3). This experiment was repeated three times (n = 9) and each replica generated a value for P/C and V/C after 20 mins feeding. The average ± SEM was then determined.

2.5.3 Blocking C-type lectin receptors (CLR) and Scavenger Receptors (SRs)

2.5.3.1 Experiments devoid of CBD – CLRs and SRs

For CLR blocking, a *T. pyriformis* suspension was divided into four aliquots and pre-incubated at room temperature, for 30 min, with either mannose, GlcNac, GalNac (at 100 mM, 'Blocked'), or left untreated (Control). Each of these four systems was then divided into 9 aliquots and prey was added at a concentration of 2 x 10^7 cells/ml. For each 'Blocked' and 'Control' system, live *Synechococcus* was added to three tubes, dead *Synechococcus* was added to three tubes and finally, beads were added to three tubes. The ciliate was left to feed on the prey for 5 min before being fixed with glutaraldehyde (0.5% v/v final conc.). For each of the 3 replicas, P/C and V/C was determined for 10 cells (see 2.2.3). This experiment was repeated three times (n = 9) and each replica generated a value for P/C and V/C after 5 mins feeding. The average ± SEM was then determined.

The experiment for SR blocking followed that described above but the ciliate was pre-incubated with DS, CS (both at 400 µg/ml, 'Blocked') or left untreated (Control).

2.5.3.2. Experiments involving CBD – CLRs only

A *T. pyriformis* suspension was divided into four aliquots and pre-incubated at room temperature, for 30 min, with either mannose, GlcNac, GalNac (at 100 mM, 'Blocked'), or left untreated (Control). Each of these four systems was then divided into 18 aliquots and CBD was added to nine (at 4 µM, '+CBD') while the remaining nine received the same volume of ethanol ('-CBD'). After 5 min, prey was added at a concentration of 2 x 10^7 cells/ml. For each 'Blocked' and 'Control' system, live *Synechococcus* was added to three '+CBD' tubes and three '-CBD' tubes, dead *Synechococcus* was added to three '+CBD' tubes and three '-CBD' tubes and finally, beads were added to three '+CBD' tubes and three '-CBD' tubes (this was time zero). Aliquots (50 µl) were removed from the tubes every 5 min, over a 120 min period, and fixed with glutaraldehyde (0.5% v/v final conc.). For each of the 3 replicas, P/C was determined for 10 cells (see 2.2.3). This experiment was repeated twice (n = 6) and each replica generated a value for lag and IR from which the average ± SEM was determined.

2.6. Statistical analysis

Data comprising two variables (3.3 – 3.5, 3.6.2) were subject to an independent student T-test with a confidence limit of 95% ($P \leq 0.05$). Data comprising >2 variables (3.1, 3.2, 3.6.1) were subject to a one-way ANOVA and a post-hoc Tukey test, also with confidence limit of 95% ($P \leq 0.05$).

Chapter 3. Results

3.1. The effect of CBD concentration on *T. pyriformis* feeding

T. pyriformis was subjected to a range of CBD concentrations and the feeding lag period (min) and ingestion rate (prey/cell/min), with Live *Synechococcus*, were determined at each concentration (Fig. 3.1).

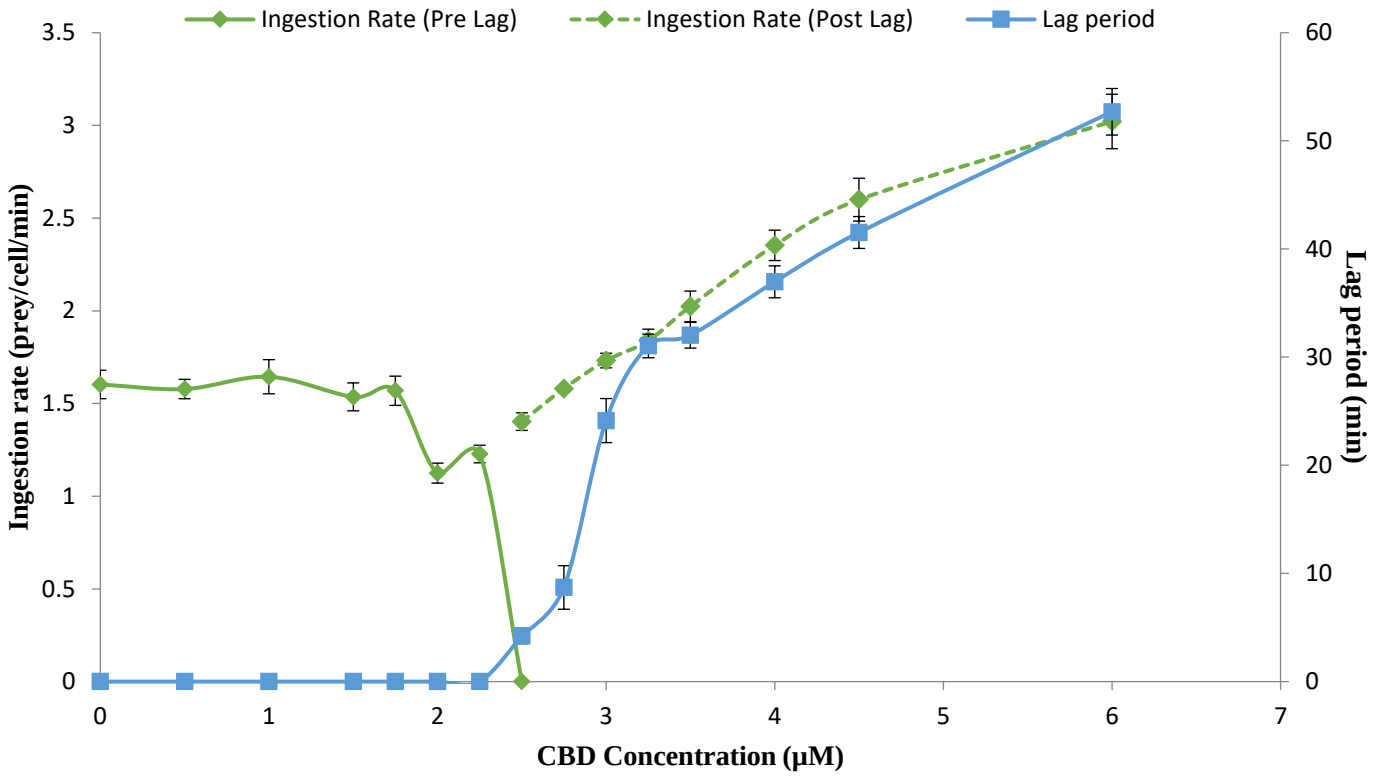

Figure 3.1. *The effect of CBD concentration (µM) on the feeding lag (min) and ingestion rate (IR, prey/cell/min) of T. pyriformis, feeding on live Synechococcus at 1 x 10^7 cells/ml. Continuous green line denoted IR before the onset of a lag, while dotted green line denotes IR after the feeding lag. Data points are an average 6 replicas (± SEM).*

CBD concentrations of 0.25-1.75 µM had no significant effect on *T. pyriformis* feeding, i.e., no feeding lag was induced and instantaneous IR was equivalent to the Control ($P>0.01$) (Fig. 3.1., continuous green line). At 2 µM, IR significantly reduced ($P<0.01$) until it was zero at 2.5 µM; suggesting an MIC of >1.75≤2 µM (Fig. 3.1, continuous green line). This cessation of feeding at 2.5 µM led to a feeding lag of 5 min (Fig. 3.1., blue line) and when feeding resumed, IR was 1.4 prey/cell/min (Fig. 3.1. dotted green line). This IR was not significantly different to the Control, as was the IRs up to 3.25 µM ($P>0.01$), but the length of the lag phase increased sharply (Fig. 3.1). From 3.5 µM, IRs were significantly higher than

the Control (P<0.01) ('hyperphagia') and continued to increase, with increasing CBD concentration, alongside a less rapid rise in lag phase (Fig. 3.1).

There was a significant correlation (R^2 0.888) between lag period duration and subsequent IR (Fig. 3.2). This suggests that the primary target of CBD is to stop feeding completely and induce a lag (which is dose-dependent), and then, possibly after the CBD wears off or is degraded, the subsequent IR is directly proportional to the length of that lag. So, it appears that a lag period of *ca.* 32 mins is required to induce hyperphagia in this ciliate, i.e., a significantly higher IR than the Control (Fig. 3.1).

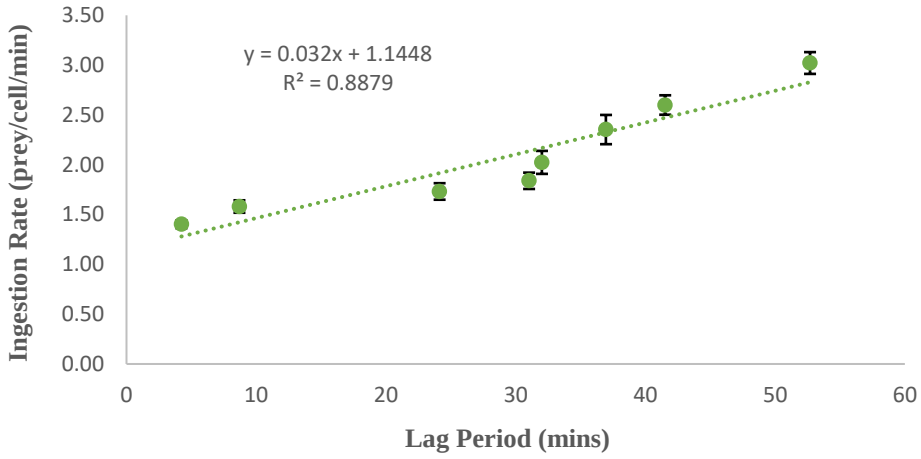

Figure 3.2. *Relationship between the length of the CBD-induced lag period (min) and the subsequent ingestion rate (prey/cell/min). Equation of the line is displayed on the graph and data were acquired from Figure 3.1.*

3.2. Toxic effects of antagonists/blockers on *T. pyriformis*

Working antagonist concentrations were screened for cytotoxic effects prior to using in feeding experiments. All sugars (at 100 mM, Fig 3.3A), PTX (at 100 ng/ml) and all other receptor antagonists except Melittin (at 10 µM, Fig 3.3B) proved to be non-toxic to the ciliate – as determined by no significant change in cell concentration over 120 min in their presence (P>0.05) (Fig. 3.3). All antagonists against components of the MAPK pathway (at 10 µM, Fig 3.3C) also proved non-toxic.

Due to the detected melittin toxicity, additional melittin concentrations were tested and a working concentration of 0.3 µM was accepted as being non-toxic to the ciliate (P>0.05) (Fig. 3.4). This was used as the new working concentration.

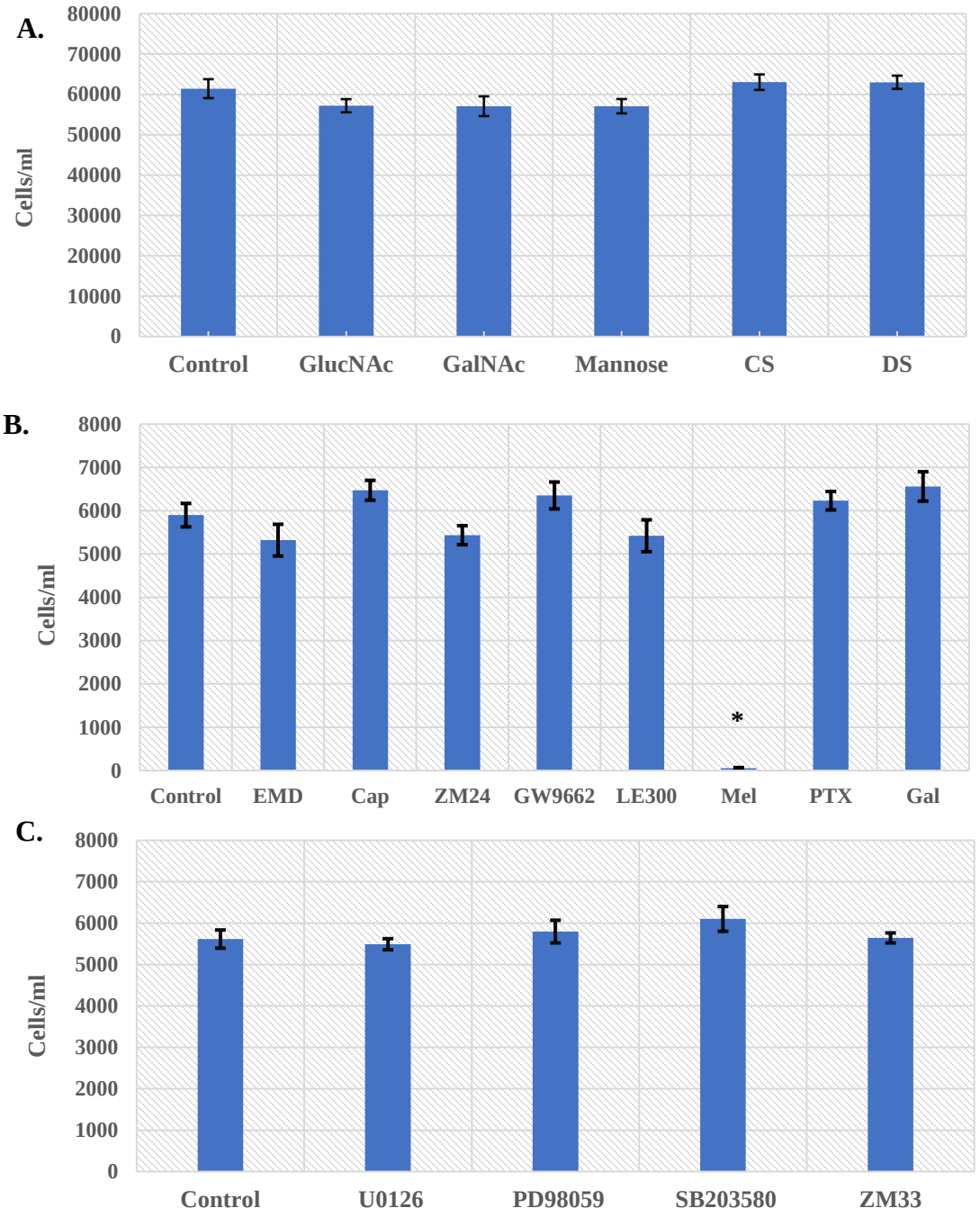

Figure 3.3. *Concentration of T. pyriformis cells (cells/ml) after incubation with* ***A)*** *100 mM Mannose, N-Acetyl-α-D-glucosamine (GlcNAc), N-Acetyl-D-galactosamine (GalNAc) and 400 µg/ml of Dextran Sulphate (DS) and Chondroitin Sulphate (CS) for 30 min.* ***B)*** *10 µM of EMD281014, Capsazepine, ZM241385, GW9662, LE300, Melittin, and Gallein, and 100ng/ml of PTX for 120 min.* ***C)*** *10 µM of U0126, PD98059, SB203580, ZM336273 for 120 min. Data are averages (± SEM) of 3 experiments (n = 9). * = significantly different to control (P<0.01).*

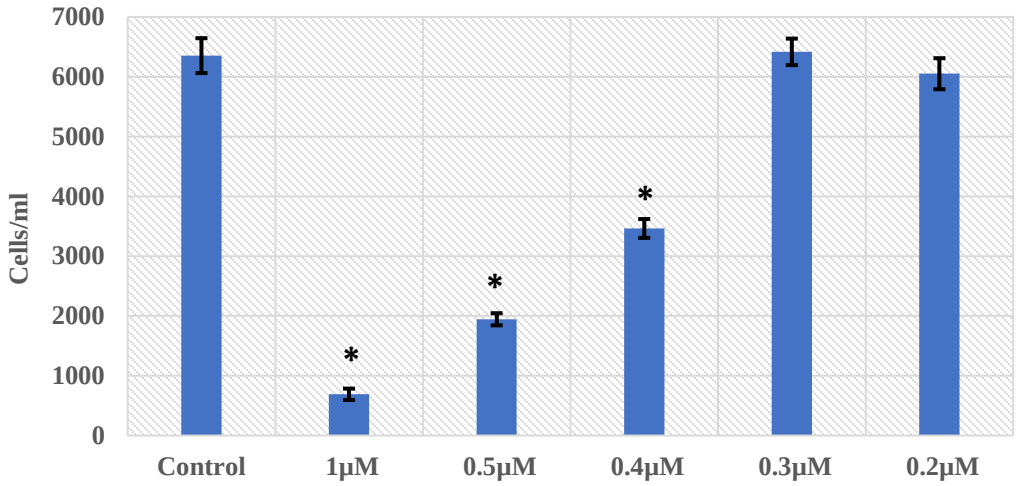

Figure 3.4. *Concentration of T. pyriformis cells (cells/ml) after a 120-min incubation with varying Melittin concentrations. Data are averages (± SEM) of 3 experiments (n = 9). * = significantly different to control (P<0.01).*

3.3. The effect of blocking receptors and components of the MAPK pathway

Tables 3.1-3.3 show that the presence of CBD significantly reduced P/C compared to the Control (P<0.01), but none of the antagonists tested alleviated this negative response. In addition, none of the antagonists affected the P/C in the **absence** of CBD (Tables 3.1-3.3), suggesting that none are even involved in the normal feeding behaviour of *T. pyriformis*.

Table 3.1. *Number of prey/cell in T. pyriformis cells feeding on live Synechococcus after pre-incubation with* ***GPCR antagonists*** *Gallein (βγ complex), PTX (Gi/o and Gt), and Melittin (G_s) followed by CBD addition. Results are averages (± SEM) of 2 experiments (n = 6). * = significant difference between with and without CBD (P<0.01).*

Antagonist	**Prey/cell**	
	Without CBD (± SEM)	**With CBD (± SEM)**
Control	24.70 (±1.45)	0.67 (±0.19)*
+ Gallein	23.18 (±1.11)	0.73 (±0.17)*
+ Pertussis Toxin (PTX)	25.08 (±1.37)	1.23 (±0.33)*
+ Melittin	24.17 (±1.18)	0.30 (±0.09)*

Table 3.2. *Number of prey/cell in T. pyriformis cells feeding on live Synechococcus after preincubation with* ***non-GPCR antagonists*** *Capsazepine (TRVP), EMD281014 (5-HT_{2A}), GW9662 (all PPARs), ZM241385 (Adenosine A2), LE300 (Dopamine D1), followed by CBD addition. Results are averages (± SEM) of 2 experiments (n = 6). * = significant difference between with and without CBD (P<0.01).*

Antagonist	**Prey/cell**	
	Without CBD (± SEM)	**With CBD (± SEM)**
Control	26.68 (±1.41)	0.45 (± 0.12)*
+ Capsazepine	24.43 (±1.63)	0.53 (±0.18)*
+ EMD281014	25.77 (±1.69)	0.17 (±0.10)*
+ GW9662	25.40 (±2.12)	1.17 (±0.36)*
+ ZM241385	26.18 (±1.83)	0.25 (±0.10)*
+ LE300	26.35 (± 1.78)	1.14 (±0.36)*

Table 3.3. *Number of prey/cell in T. pyriformis cells feeding on live Synechococcus after preincubation with* ***MAPK pathway component antagonists*** *U0126 (MEK1/2), PD98059 (MEK), SB203580 (P38 MAPK), and ZM336372 (c-Raf), followed by CBD addition. Results are averages (± SEM) of 2 experiments (n = 6). * = significant difference between with and without CBD (P<0.01).*

Antagonist	**Prey/cell**	
	Without CBD (± SEM)	**With CBD (± SEM)**
Control	21.19 (±1.25)	0.28 (±0.14)*
+ U0126	23.63 (±1.65)	0.23 (±0.11)*
+ PD98059	24.50 (±1.67)	0.12 (±0.08)*
+ SB203580	23.45 (±1.66)	0.32 (±0.16)*
+ ZM336372	23.00 (±1.93)	0.28 (±0.15)*

3.4. The effect of blocking C-type lectin receptors (CLRs) and scavenger receptors (SRs)

3.4.1. Effect on *T. pyriformis* feeding in the absence of CBD

T. pyriformis cells were subject to a 30-minute pre-incubation period with one of 5 sugars (Mannose, GlcNac, GalNac, DS or CS) in order to block their corresponding receptor. Cells were then fed with 3

types of prey: live *Synechococcus*, dead *Synechococcus* and inert beads, for 5 minutes, before fixing in glutaraldehyde (0.5% v/v final conc). Average Prey/cell (P/C) and Vacuoles/cell (V/C) were recorded.

3.4.1.1 Effect of prey type

Comparison of the uptake of the three prey types after 5 min in the Control *T. pyriformis* cells only (Fig. 3.5), shows a striking pattern, in that live *Synechococcus* cells are ingested significantly more than dead *Synechococcus* cells or beads ($P<0.01$), which were themselves equivalent ($P = 0.9$) (Fig. 3.5, A, C, E, Fig. 3.6 A). Live *Synechococcus* cells also induced in the formation of significantly more food vacuoles than dead *Synechococcus* cells and beads ($P<0.01$), which were themselves equivalent ($P=0.75$) (Fig. 3.5, B, D, F, Fig. 3.6 B).

3.4.1.2. Blocking CLRS

The pre-blocking of CLRs (with Mannose, GalNAc or GlcNAc), prior to adding prey, also showed a striking pattern (Fig. 3.5.). Firstly, no matter what receptor was blocked, the uptake of, and food vacuole formation in the presence of, beads was not significantly affected (P/C: $P=0.116$, V/C: $P=0.157$). At the other extreme, the uptake of prey (P/C) and vacuole formation (V/C) with live *Synechococcus* cells was significantly reduced in the presence of all three sugars. Blocking with mannose decreased uptake of live cells by 36.9% ($P<0.01$), compared to the un-blocked Control, and the formation of food vacuoles was reduced by 27% ($P<0.01$). Blocking with GlcNAc reduced prey uptake and food vacuole formation by 40.52% and 33.7%, respectively ($P<0.01$) while blocking with GalNAc reduced prey uptake and food vacuole formation by 47.9% and 40.48% ($P<0.01$), respectively.

The effect of receptor blocking on dead *Synechococcus* cells differed in that, blocking CLRs with mannose or GlcNAc caused no significant reduction in P/C or V/C (Mannose P/C: $P=0.65$, V/C: $P=0.089$; GlcNAc P/C: $P= 0.18$, V/C: $P= 0.11$) (Fig 3.5, A-D). However, blocking with GalNAc did reduced dead prey uptake by 32% ($P<0.01$) and lowered food vacuole formation by 25% ($P<0.01$) (Fig 3.5, E, F).

These data suggest that the uptake of live *Synechococcus* cells involves all three CLRs, the uptake of dead *Synechococcus* only involves a GalNAc receptor, whilst no CLRs are involved in the uptake of beads.

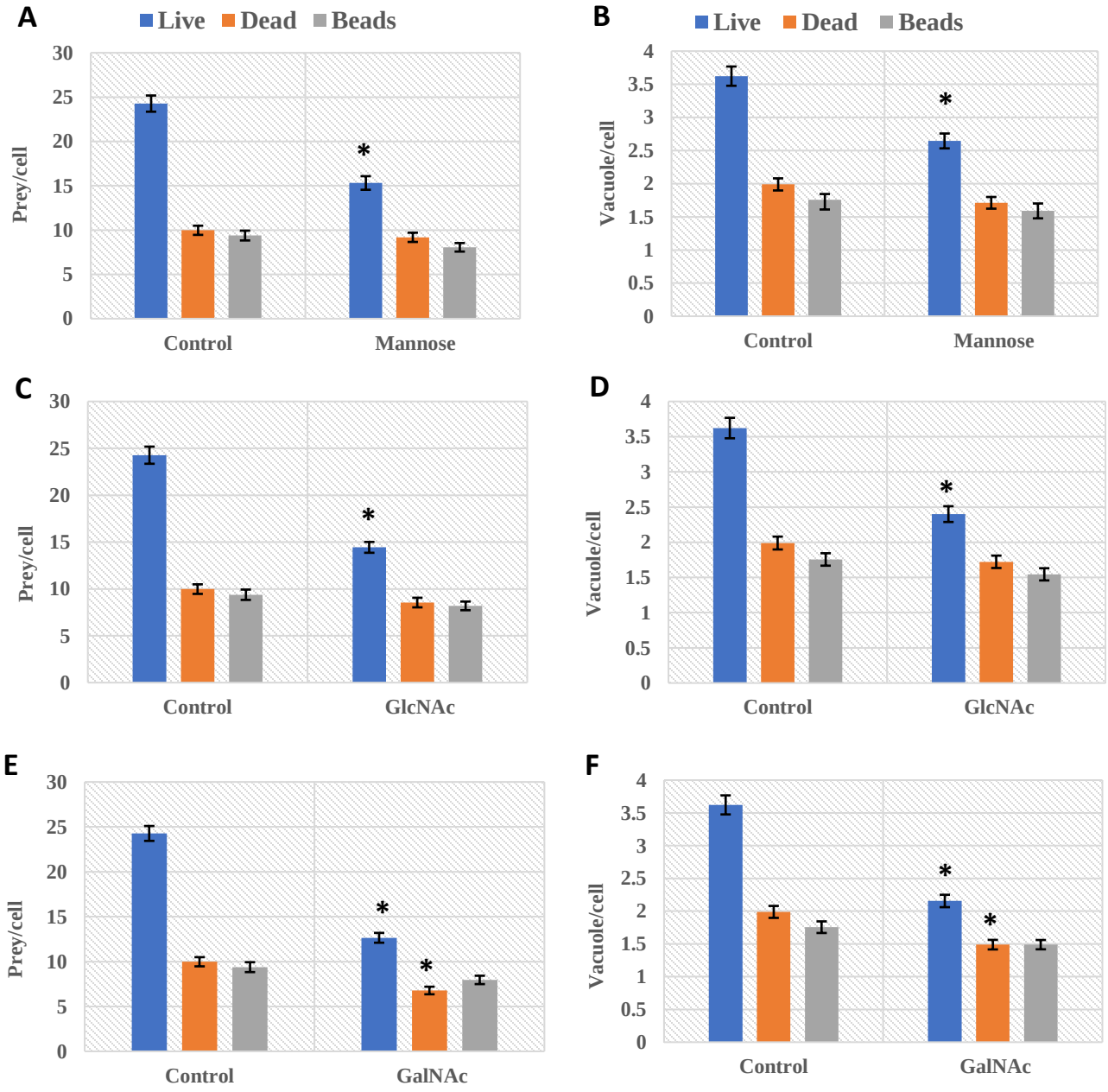

Figure 3.5. *Number of Prey/cell and Vacuoles/cell in T. pyriformis cells after pre-incubation with* ***A, B:*** *D (+) Mannose;* ***C, D****: N-Acetyl-α-D-glucosamine (GlcNAc);* ***E, F****: N-Acetyl-D-galactosamine (GalNAc) at 100 mM for 30 min, and then feeding with Synechococcus sp. (live or dead) or beads (at 2 x 10^7 particles/ml) for 5 minutes. Data are averages (± SEM) of 3 experiments (n = 9) * = significantly different to Control (P<0.01).*

3.4.1.3. Blocking SRs

Pre-incubating *T. pyriformis* with dextran sulphate (DS) (and chondroitin sulphate [CS] as an additional Control) revealed no significant effect on the uptake of, or vacuole formation in the presence of, dead

Synechococcus and beads (Dead: P/C P=0.90, V/C P=0.71; Beads: P/C P=0.90, V/C P=0.90) (Fig 3.6.). It also did not affect vacuole formation in the presence of live *Synechococcus* cells (P = 0.76) (Fig 3.6. B), however, P/C with these live cells significantly reduced by 12.9% (P<0.01) (Figure 3.6. A). This suggests a possible involvement of SRs in the uptake of live cells only.

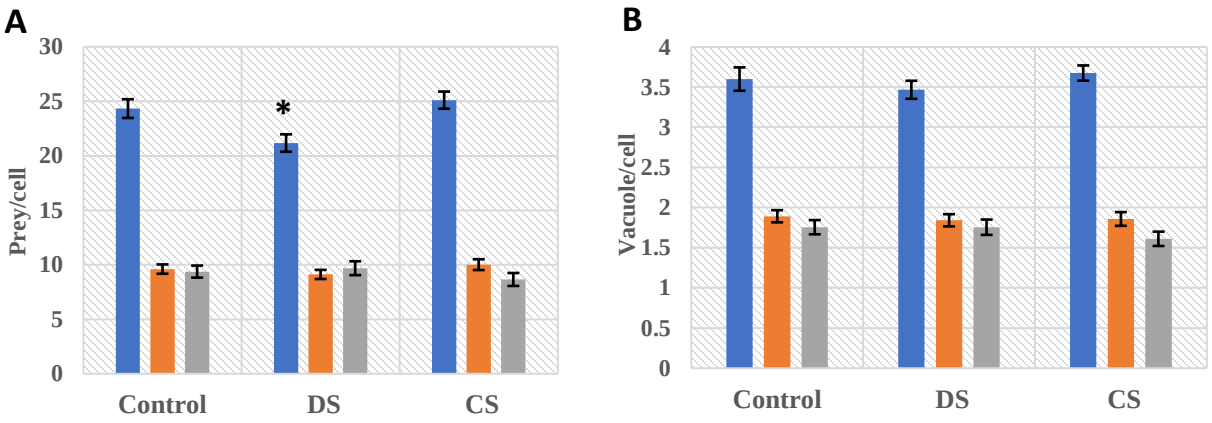

Figure 3.6. *Number of Prey/cell (**A**) and Vacuoles/cell (**B**) in T. pyriformis cells after pre-incubation with Dextran sulphate (DS) and Chondroitin Sulphate (CS) at 400 µg/ml for 30 min, and then feeding with Synechococcus sp. (live or dead) or beads (at 2 x 10^7 particles/ml) for 5 minutes. Data are averages (± SEM) of 3 experiments (n = 9) * = significantly different to Control (P<0.01).*

3.4.2. Effect on *T. pyriformis* feeding in the presence of CBD

Following clear evidence for the involvement of Mannose, GalNAc, and GlucNAc CLRs in the uptake of live *Synechococcus* cells by *T. pyriformis*, feeding experiments were performed to test whether CLRs interacted with CBD. CLRs were pre-blocked with the sugar and ciliate feeding was monitored in the presence/absence of a subsequent dose of CBD (4 µM).

Figure 3.7 shows the feeding response of *T. pyriformis* over time and clearly shows a reduced IR in the presence of sugar blocking (as seen in the 5 min experiments in 3.4.1) however, these data do now confirm that it is not due to presence of a lag period but it a true reduction in IR. This reduction was significant in all cases (P<0.01) with Mannose, GalNAc and GlcNAc reducing IR by 59.4%, 43.1%, and 54.5% respectively (Table 3.4).

In the absence of a sugar (Control), with CBD, a significant feeding lag, followed by hyperphagia was recorded (Fig. 3.7, Table 3.4). In these experiments, the lag period averaged 59.35 min (Table 3.4), which is longer than previously recorded, and after this the IR was higher than that of the Control (Table 3.4).

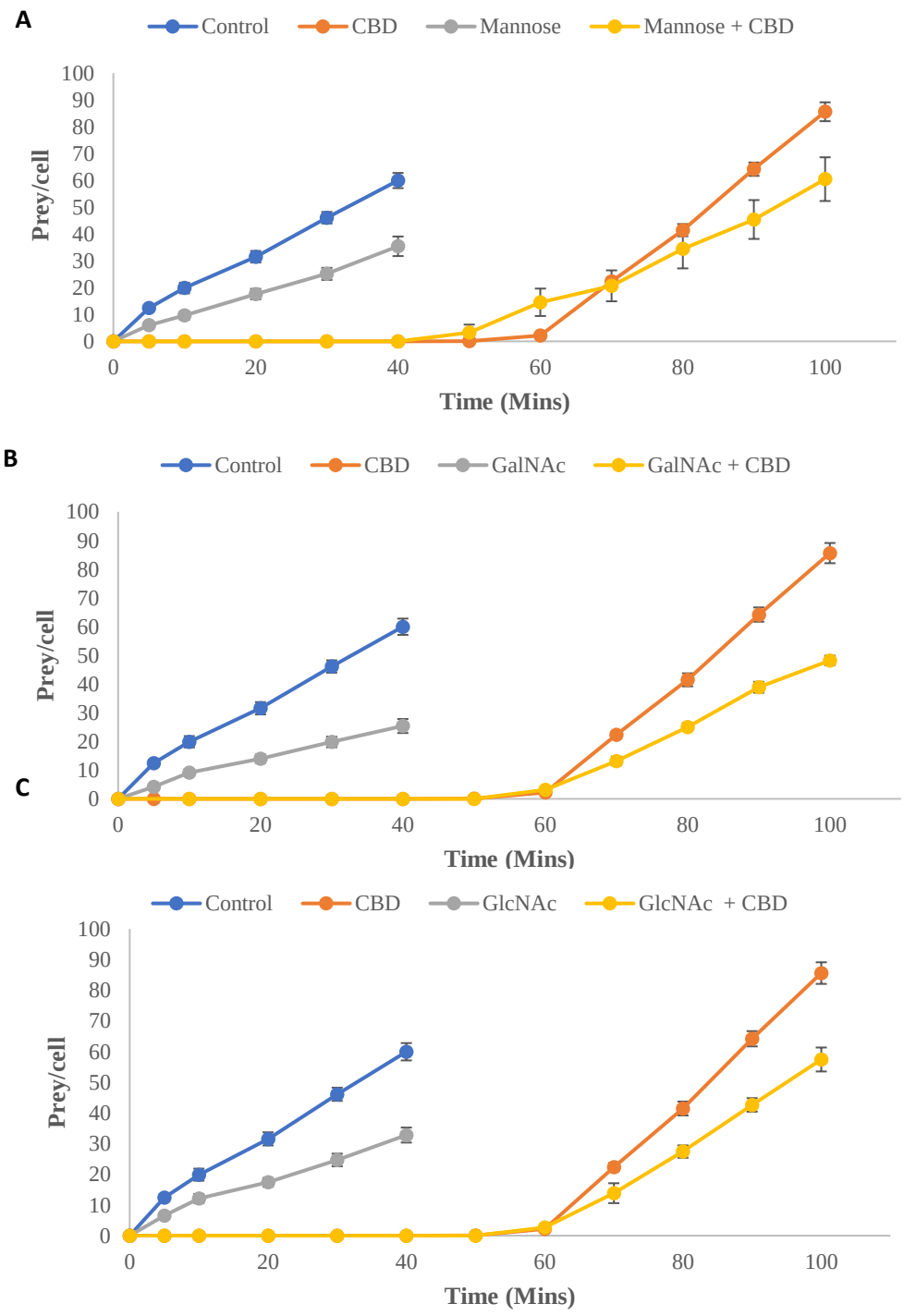

Figure 3.7. *Feeding of T. pyriformis cells on live Synechococcus after pre-incubation with Mannose (A), GalNAc (B) or GlcNAc (C) at 100mM. Feeding was then performed in the absence/presence of 4µM CBD. Data are averages (± SEM) of two experiments (n=6).*

Table 3.4. *Feeding lag (mins) and subsequent ingestion rate (IR) in T. pyriformis cells feeding on live Synechococcus at 1 x 10^7 cells/ml. Cells were preincubated, for 30 minutes with one of three sugars: Mannose, GalNAc or GlcNAc (at 100 mM) and feeding in the presence/absence of 4 µM of CBD was recorded. Data are averages (± SEM) of 2 experiments (n=6). Significant difference (P<0.01) to:* **^** *= Respective sugar with no CBD,* **“** *= Control with no CBD and no sugar,* ***** *= Control with CBD.*

Sugar Condition	Without CBD	With CBD
Control		
Feeding Lag (min)	0	59.35 (± 0.320) **“**
Ingestion Rate (prey/cell/min)	1.43 (± 0.065)	2.09 (± 0.074) **“**
Mannose		
Feeding Lag (min)	0	54.41 (± 3.40) **^ “**
Ingestion Rate (prey/cell/min)	0.85 (± 0.079) **“**	1.31 (± 0.087) **^ ***
GalNAc		
Feeding Lag (min)	0	57.70 (± 1.57) **^ “**
Ingestion Rate (prey/cell/min)	0.62 (± 0.063) **“**	1.13 (± 0.071) **^ “ ***
GlcNAc		
Feeding Lag (min)	0	58.38 (± 1.40) **^ “**
Ingestion Rate (prey/cell/min)	0.78 (± 0.058) **“**	1.31 (± 0.057) **^ ***

Pre-incubating cells with sugars, prior to the addition of CBD, did not affect the duration of the CBD-induced lag (Fig. 3.7, Table 3.4), even though Mannose does appear to allow a slight earlier onset of feeding compared to GalNAc and GlcNAc (Fig. 3.7 A). However, all sugars significantly reduced (but did not abolish) the extent of the CBD-induced hyperphagia (Mannose and GlcNAc by 37% and GalNAc by 46% (P<0.01) (Table 3.4.).

Chapter 4. Discussion

4.1. Summary of results

The main aim of this study was to investigate the potential molecular targets that are responsible for mediating CBD-induced changes in the feeding behaviour of *T. pyriformis.* These changes were first evaluated at different concentrations of CBD and it appeared that the primary response of the ciliate to CBD was a reduction in ingestion rate (IR) (at >1.75≤2 μM CBD). IR was then zero (at ≥2.5 μM CBD) and this gave rise to a feeding lag. The lag was however temporary, with its duration being positively correlated to CBD concentration. Following the lag's cessation, the ciliate began to feed again and the resulting IR correlated positively with the duration of the lag. A lag duration of 32 min led to IRs that were significantly higher than those in the untreated controls; the ciliate exhibited hyperphagia.

In light of a dose-response effect a dozen putative CBD molecular targets were screened for any potential involvement in the mediation of CBD-induced feeding changes. These targets were either known cannabinoid interacting-receptors or were common MAPKs which are widely known to be involved in eukaryotic cellular reception of external stimuli. Unfortunately, none of the tested antagonists were able to alleviate the CBD-induced lag phase, nor did they affect feeding behaviour in non-treated cells which suggests that these targets are not involved in normal *T. pyriformis* feeding either.

As an extension of the prior experiments, this study also investigated the involvement of CLRs and SRs in normal *T. pyriformis* feeding via receptor blockage with their respective sugars (mannose, GalNAc and GlcNAc). Feeding on 3 prey types was monitored: (i) live *Synechococcus* (ii) heat-killed (dead) *Synechococcus* and, (iii) inert latex beads. None of the CLRs or SRs were involved in the processing of the beads. All 3 CLRs were implicated in the uptake of, and vacuole formation with, live *Synechococcus* whereas SRs were only implicated in the ingestion of live *Synechococcus* (but not vacuole formation in its presence). Only GalNAc was implicated in the uptake of, and vacuole formation with, dead *Synechococcus* suggesting the heat treatment had destroyed the Mannose and GlcNAc receptor ligands on the live *Synechococcus* cells.

CLRs were also tested as candidates for CBD affect mediators. CLR blockage, with their respective sugar, was not able to alleviate the CBD-induced lag phase. However, all 3 sugars reduced the subsequent hyperphagic feeding associated after the lag period.

4.2. *T. pyriformis* feeding in the absence of CBD

4.2.1 Receptors involved in the uptake of live, dead and inert prey by *T. pyriformis*

The feeding of *T. pyriformis* on three prey types was investigated; live *Synechococcus*, heat-killed-DTAF-stained *Synechococcus* (Dead) and fluorescent microspheres (beads). A striking pattern was recorded, in that, live *Synechococcus* cells were ingested significantly more than dead *Synechococcus* or beads, which were themselves equivalent. Live *Synechococcus* also resulted in the formation of significantly more food vacuoles than dead *Synechococcus* and beads, which were themselves equivalent.

Pre-blocking *T. pyriformis* cells with mannose, GalNAc, GlcNAc or dextran sulphate showed that ingestion/food vacuole formation with live *Synechococcus* involved all three C-type lectin receptors (CLRs) and, for ingestion only, Scavenger Receptors (SRs). The involvement of all three CLRs has previously been reported for live *Synechococcus* ingestion by the amoeba *V. vermiformis* (Al-hammadi, 2020) and for live *Salmonella enterica* ingestion by *T. pyriformis* (Boboc, 2020). Potential SR involvement has also very recently been observed in the ingestion of live *Synechococcus* by *T. pyriformis* (Parsons, 2021).

The ingestion/food vacuole formation with beads did not involve any of these receptors, as has been reported previously, albeit only for the mannose receptor (Allen and Dawidowicz, 1990; Boboc, 2020) and SRs (Parsons, 2021). Only the GalNAc receptor was involved with ingestion/food vacuole formation with dead *Synechococcus* suggesting that the mannose and GlcNAc receptors are more heat labile than the GalNAc receptor. Considering that ingestion/food vacuole formation with beads (no receptors) and dead *Synechococcus* (GalNAc receptor) were equivalent, it either suggests that GalNAc is less important than mannose/GlcNAc receptors in *T. pyriformis* feeding (but this was not evident with live cells, where the blocking GalNAc produced the greatest reductions in P/C and V/C of all 3 CLRs) or, that beads enter the cell via a different route to bacterial prey and their ingestion cannot be directly compared to that of dead cells.

Vogel et al. (1980) was the first to postulate that different prey types enter a protist cell via two functionally distinct routes: a non-specific receptor-based route (primary governed by hydrophobicity), and a receptor route (based on the recognition of prey by a lectin receptor). Since inert particles have no surface ligands which are recognizable by CLRs or SRs, they are thought to enter via the first route. It has also been postulated that this unselective phagocytosis of inert particles is attributed to a ‘mechanical’ action only, where particle ingestion and vacuole formation is induced by the physical action of a particle entering the cytostome; and circumventing the need for any receptor-ligand interactions (Allen and Fokt,

2000; Grønlien et al., 2002). This would give rise to a basal (low) ingestion/vacuole formation rate which, based on the current study, would be 9 beads/cell in 5 min and 1.8 vacuoles/cell in 5 min (at 2 x 10^7 beads/ml). In contrast, live prey uptake is attributed to a combination of mechanical **and** biochemical mechanisms (Montagnes et al., 2008), creating a cumulative ingestion/vacuole formation rate, hence the consistently greater ingestion of live cells over beads as seen in this and other studies (Elliott and Clemmons, 1966; Sherr and Sherr, 1987; Nygaard et al., 1988; Boenigk et al., 2001a; Parry et al., 2001; Grønlien et al., 2002; Boenigk and Novarino, 2004).

4.2.2. Interaction between *Synechococcus* and the receptors

4.2.2.1. Mannose and the mannose receptor

Polysaccharides are common in bacterial cells and mannose residues can be found in a range bacterial structures such as the core oligosaccharides and O-antigens of the LPS layer, or in the glycoproteins comprising the S layer (Sahly et al., 2002; Golowczyc et al., 2009; Man-Kupisinska et al., 2018). However, the composition of the *Synechococcus* LPS layer appears to have a low proportion of mannose residues compared to other oligosaccharides (Snyder et al., 2009). Even so, mannose has been found in the O-antigens of *S. elongatus* suggesting a wider distribution of this sugar (Katz et al., 1977; Fujii et al., 2012). *Synechococcus* cells do possess an S-layer which is comprised mainly of the glycoprotein SwmA (McCarren and Brahamsha, 2009; Strom et al., 2017). However, it seems to possess little to no mannose residues, as it exhibits no interaction with the mannose binding lectin Concanavalin A (Con A) (Strom et al., 2017). This might explain why pre-blocking *T. pyriformis* with mannose in the current study resulted in the smallest (though still significant) reduction in P/C and V/C, compared to blocking with GlcNAc and GalNAc.

It was noticeable that upon heat-treatment of *Synechococcus*, the mannose receptor was unable to interact with these dead cells, suggesting that the mannose residues were heat-labile. This contrasts with the cells of *Salmonella enterica*, where the mannose receptor is involved in the uptake up, and food vacuole formation with, dead cells, suggesting this species possessed more heat-stable mannose residues (Boboc, 2020). *Synechococcus* on the whole does seem to be very sensitive to heat treatment. Boboc (2020) showed that heat-killing *Synechococcus* resulted in an ingestion rate similar to that seen by beads. This was an identical response to that observed in the current study, and is presumably solely due to the damage or complete loss of surface ligands.

4.2.2.2 GalNac and the GalNAc receptor

The pre-blocking of *T. pyriformis* with GalNAc resulted in the most significant reduction in P/C and V/C with live *Synechococcus*, suggesting that GalNAc residues are abundant in/on its cells. However, GalNAc residues are not considered to comprise a significant part of the LPS of *Synechococcus* (Snyder et al., 2009) and no further information about its presence in other cell structures could be found by the author. In other bacteria, GalNAc is present in many structures, including lipooligosaccharide, capsules, cell wall teichoic acids and O-antigens (Michael et al., 2002; Freymond et al., 2006; Liu et al., 2014a).

Protistan GalNAc receptors are known to bind galactose in addition to GalNAc (Venkataraman et al., 1997; Padilla-Vaca et al., 1999) and galactose is a significant component in the LPS layers of several species of *Synechococcus* (Snyder et al., 2009). Therefore, the blocking of the GalNAc receptor by GalNAc might have been preventing an interaction between the receptor and galactose (not GalNAc) moieties in/on *Synechococcus* cells.

The GalNac receptor was the only receptor involved in the ingestion of heat-killed *Synechococcus* showing that the ligands are somewhat heat-stable. The decrease in prey uptake and vacuole formation caused by GalNAc blockage when fed with dead *Synechococcus* (32% and 25%, respectively) was smaller than the decrease seen when fed with live *Synechococcus* (48% and 41%, respectively) which suggests a partial loss of residues. In mammalian cells, receptors for GlcNAc and mannose possess the same tripeptide carbohydrate recognition domain (EPN motif) whereas receptors for GalNAc possess a QPD motif (Dambuza and Brown, 2015; Brown et al., 2018). If this pattern is conserved in protists, it seems likely that ligand that bind to the EPN motif are lost/more severely damaged during heat treatment, whereas the QPD ligand is at least partially retained. GalNAc ligands seem to be more conserved across species as *S. enterica* also seemed to possess a partially heat-stable GalNAc ligand which was utilised in its uptake by *T. pyriformis*.

4.2.2.3. GlcNAc and the GlcNAc receptor

GlcNAc residues are found at a relatively low proportion in the LPS of *Synechococcus,* even when compared to mannose (Snyder et al., 2009). However, this is likely because GlcNAc is typically localised to the peptidoglycan (within the cell wall) where it forms one of the two primary components (repeating units of GlcNAc and N-acetylmuramic acid [MurNAc)]) (Dörr et al., 2019). Knowing that cyanobacteria possess a cell wall that is significantly thicker than normally seen in Gram-negative bacteria (~10 nm in most *Synechococcus*) (Hoiczyk and Hansel, 2000) it is now clear as to why blocking GlcNAc receptors had such a significant effect on live *Synechococcus* uptake; this thicker cell wall would be a major ligand

for the *T. pyriformis* GlcNAc receptor. Little information could be found on other cellular locations of GlcNAc in *Synechococcus* but beyond *Synechococcus*, several other bacterial species interact with the PRR Dendritic cell-specific intercellular adhesion molecule-3-grabbing non-integrin (DC-SIGN) through GlcNAc interactions (Maeda et al., 2003; Klena et al., 2005; Zhang et al., 2006).

As with mannose, GlcNAc receptors played no role in the uptake of dead cells, suggesting complete loss of GlcNAc residues in/on the *Synechococcus* cells. Peptidoglycan is not heat liable at 40-50ºC (but is at >50ºC) although true gram-positive cell walls (i.e. ~40nm seen in gram positive species (Hoiczyk and Hansel, 2000)) are more resilient than thinner gram-negative walls (Russell, 2003). It is likely that the 60ºC temperature used in the heat treatment here was sufficient to completely destroy the 10nm layer peptidoglycan in *Synechococcus.* As previously stated, mannose and GlcNAc residues share an EPN carbohydrate recognition motif, and so can often share ligands (Zhang et al., 2006; Dambuza and Brown, 2015). It is likely that there was overlap in the ligands used to bind to the mannose- and GlcNAc receptors of *T. pyriformis* which could explain why blockage of either of them had no effect on the uptake of heat-killed *Synechococcus* cells. It seems that ligands recognised by EPN on *Synechococcus* are very heat liable. This does not seem to carry over to *S. enterica*, which, at 100mM of GlcNAc, saw a significant decrease in dead cell uptake suggesting the *S. enterica* GlcNAc residue remained and are heat stable (Boboc, 2020) suggesting a different ligand.

4.2.4.4. Interactions with scavenger receptors

Scavenger receptors class A and B are the primary and best understood of the SR classes able to act as PRRs (Zani et al., 2015). Their activation allows for the non-opsonic phagocytosis of microbes and are common in mammalian phagocytes (Plüddemann et al., 2006; Plüddemann et al., 2011; Canton et al., 2013). Class A (SR-A) is the primary macrophage SR class mediating non-opsonic phagocytosis (Zani et al., 2015). The main ligands of SR-A are LPS (specifically lipid A in LPS) from Gram-negative species (Hampton et al., 1991), lipoteichoic acid (LTA) from Gram-positive species (Dunne et al., 1994), and CpG bacterial DNA motifs (common bacterial immunostimulatory motifs) (Zhu et al., 2001). SR-A also binds various bacterial surface proteins, although these are more limited and less common targets (Peiser et al., 2002; Peiser et al., 2006). Although less is known about them, Class B (SR-B) ligands seem to be similar to SR-A, being primarily LTA (Hoebe et al., 2005; Stuart et al., 2005) and LPS (particularly rough LPS, i.e, lacking O-antigen) (Stuart et al., 2005; Biedroń et al., 2016; Olonisakin et al., 2016). Some specific SR-Bs can also bind peptidoglycan (Tan et al., 2019) making Gram-positive bacteria particular targets.

SR-B members have been identified in the slime mold *Dictyostelium discoideum* (Lmp A and B, homologues of Limp-2 and CD36 respectively) (Sattler et al., 2018) and a Lmp B homologue is present in *Tetrahymena* (www.ciliate.org); although no published literature has made mention of it yet. Being a Gram-negative bacterium, *Synechococcus* possesses a simple, fairly well elucidated LPS layer which could indeed act as an SR-A/B ligand (Snyder et al., 2009). Their Gram-negative classification means *Synechococcus* does not possess traditional LTA, however, an unpublished PhD thesis did suggest it possesses a teichoic acid-like polysaccharide with a similar structure to the teichoic acids of Gram-positive bacteria (Arnosti, 1993). Whether this could substitute as an LTA ligand is unknown. The thick peptidoglycan layer characteristic of *Synechococcus* (Hoiczyk and Hansel, 2000) is also a potential target for SR-Bs, although not as thick as in a traditional Gram-positive bacteria, it does provide other potential epitope.

The data suggested SRs played a role in the uptake of live *Synechococcus*, however, this was lost upon heat-treatment, suggesting the SR ligand was heat liable. This provides evidence against the idea that LPS might be the primary SR ligand, as SR blockage when feeding on dead *S. enterica* has no effect on prey uptake or vacuole formation (Boboc, 2020), and *S. enterica* is a true Gram negative cell. This suggests either a secondary, yet unidentified, *Synechococcus* SR ligand (not found in *S. enterica*) is present or that the 'semi-Gram-positive characteristics' of *Synechococcus* (thick wall, teichoic acid like peptidoglycan) are the SR ligand(s). To confirm this SR, experiments should be repeated using a true Gram-positive species with well-defined SR ligand structures.

4.3. The effect of CBD on *T. pyriformis* feeding

T. pyriformis, feeding on live *Synechococcus* sp., was subjected to a dose response feeding experiment with CBD concentrations from 0-6 μM. The MIC for a reduced ingestion rate (IR) was $>1.75 \leq 2$ μM and then, at $>2.25 \leq 2.5$ μM, feeding stopped completely. This cessation in feeding was temporary and a positive correlation in its duration with CBD concentration was recorded. When the lag ended, feeding resumed and the IR was positively correlated to the duration of the feeding lag. A feeding lag of 32 min, induced hyperphagia in *T. pyriformis*.

This suggests that one of the primary targets of CBD is to stop feeding completely and induce a lag, and then, possibly after the CBD is inactivated or degraded (mechanism still unknown), the subsequent IR is directly proportional to the length of that lag. The latter suggests that the post-lag feeding is directly related to the satiation level of the ciliate, as the cell would continue to defecate FVs during the lag period, so the length of the lag would determine the satiation level of the ciliate.

4.3.1. The CBD-induced feeding lag

4.3.1.1. MIC and duration

The MIC for a reduced IR was >1.75≤2 μM which is very close to the >1.50≤1.75 μM recorded by Jaisswar (2020) using the same *T. pyriformis* and *Synechococcus* strains. The cessation of feeding also occurred at a very similar CBD concentration (>2.25≤2.5 μM, current study; >2.20≤2.25 μM, Jaisswar, 2020). The only discrepancy was that at 4 μM CBD the average lag duration in the current study was *ca*. 40 min whereas Jaisswar (2020) recorded a duration of *ca*. 60 min. These slight discrepancies might be attributed to CBD age/potency, with an older stock being used for the earlier current experiments until a new stock was used for CBD + C-type lectin receptor experiments (Fig 3.7); where the lag duration was *ca*. 60 min.

The MIC for the CBD-induced lag in *T. pyriformis* is higher than the >0.1≤1.0 μM recorded for the amoeba *V. vermiformis* (Al-hammadi, 2020). Also, this amoeba only required 2 μM CBD to induce a 37 min lag (duration was >100 min at 5 μM), showing that it is more sensitive to CBD than *T. pyriformis*.

4.3.1.2. CBD targets for induction of feeding lag

CBD is known to interact with at least 65 different molecular targets within the human body, with 10 of these targets being characterised receptors (Bih et al., 2015) *T. pyriformis* was therefore subjected to experiments whereby these receptors were blocked, prior to CBD treatment, then feeding on live *Synechococcus* sp. was determined after 5 min and compared to an untreated Control (with vehicle only).

None of the blockers tested alleviated the CBD-induced lag period, and none (in the absence of CBD) affected IR which suggested they play no role in the *T. pyriformis* feeding mechanism. The GPCRs tested included those coupled to Gi/o or Gt (CB1, CB2, Dopamine D2, Adenosine A1, Serotonin 5-HT1A and Opioid [all forms]), and those coupled to Gs (GPR55, GPR119 and the two GPCRs in *T. pyriformis* [6 and 31]). The non-GPCRs receptors included TRVP, 5-HT2_A, all PPAR isoforms, Adenosine A2 and Dopamine D1.

Results indicating the lack of involvement of CB1, CB2, TRVP, GPR55 and GPR119 in feeding (and then interacting with CBD) were to be expected as a *de novo* phylogenetic analysis strongly suggested that *Tetrahymena* does not possess them (McPartland et al., 2006). In addition, an Adenosine receptor has yet to been found in *Tetrahymena* even though adenosine is known to be used for metabolism of its phosphate linked derivatives (Voichick et al., 1973). Of the remining receptors, there is evidence of either their existence in *Tetrahymena*, or the existence of their agonists.

Tetrahymena has been reported to possess a dopamine D1-like receptor - but the authors also alluded to the possibility of a D2 like receptor (Ud-Daula et al., 2012). Dopamine is synthesised, stored and secreted by *Tetrahymena* although no effect on phagocytosis has been recorded to date (Csaba, 2015). Therefore, its lack of involvement in *T. pyriformis* phagocytosis in the current study might not be so surprising.

Tetrahymena possesses an opioid receptor homologue which appears to be most similar to the μ (MOR) class of opioid receptors (Chiesa et al., 1993). Opioids, both exogenous and endogenous, can inhibit phagocytosis in *Tetrahymena* through a receptor mediated mechanism (Salaman et al., 1990; Renaud et al., 1995; Rodriguez et al., 2004), presumed to be via the identified opioid receptor (Chiesa et al., 1993). Even though CBD exhibits allosteric modulation of MOR in other cells (Vaysse et al., 1987; Kathmann et al., 2006), it did not appear to interact this receptor to cause the inhibited phagocytosis in *T. pyriformis*.

Tetrahymena possesses two annotated GPCRs, 6 and 37, which are involved in chemo-attraction and chemo-repulsion, respectively (Lampert et al., 2011; Zou and Hennessey, 2017). Indeed, GPCRs have been previously shown to be involved in prey detection and taxis in the ciliates *Paramecium* and *Stentor* (Marino et al., 2001; Ondarza et al., 2003), so the lack of their involvement in the phagocytic process might not be surprising. Additionally, even though Lampert et al. are still annotating 7 remining putative GPCRs in *T. thermophila*, based on the current experiment's blocking experiments (e.g. using Gallein, a blocker for all GPCRs), it is likely that these will also not be involved in phagocytosis.

Tetrahymena is known to synthesize and respond to its own serotonin (Csaba, 2015) which increases phagocytosis (Quiñones-Maldonado and Renaud, 1987), and some evidence exists for the direct interactions of the cannabinoids with serotonin receptor subtypes (Russo et al., 2005; Gonca and Darıcı, 2015; De Gregorio et al., 2019). However, a receptor has yet to be characterized in *T. pyriformis*, but if it is related to classical 5-HT receptors, results from the current study suggest that it is not involved in ciliate phagocytosis and does not interact with CBD. This contrasts with the study of Al-hammadi (2020) who found that the CBD-induced feeding lag in the amoeba *Naegleria gruberi* was abolished in the presence of (S)-WAY 100135 dihydrochloride which is a potent and selective 5-$HT1_A$ antagonist. This response appeared specific to *N. gruberi* as all the other amoeba genera tested did not respond to this blocker.

Peroxisome proliferator activated receptors (PPARs) are not currently acknowledged to exist in *Tetrahymena*, via genome annotation, although their cells do contain peroxisomes (De Duve and Baudhuin, 1966; Fok and Allen, 1975). However, the existence of a single, promiscuous PPAR-like molecule (which can bind all isoform agonists) has been proposed to exist in both *T. pyriformis* (Wanlahbeh, 2020) and *V. vermiformis* (Al-hammadi 2020). Moreover, pre-blocking *V. vermiformis* with

a PPAR α antagonist eliminated the CBD-induced reduction in population growth (Al-hammadi, 2020), and the same PPAR α pre-blocking of *T. pyriformis* eliminated CBD-induced population death (blocking of all PPAR isoforms blocked AEA-induced population death) (Wanlahbeh, 2020). However, another study suggested that PPARs play no role in *T. pyriformis* feeding and the CBD-induced lag period could not be eliminated with the PPAR α blocker; which agrees with the current study. It therefore seems that CBD-induced effects on feeding and death in *T. pyriformis* are separate and PPARs are only involved in cell death.

Two other receptors, with known CBD interaction, remain untested. Nicotinic acetylcholine receptor (nAchR) and Glycine receptors (GlyR) are both ligand gated ion channels exhibiting CBD interactions at physiologically relevant concentrations (Bih et al., 2015). No evidence for either receptor is present in protists, nor is there any suggestion that their natural ligands (glycine and choline/acetylcholine) affect ciliate phagocytosis in any way. Furthermore, members of the 4 primary families of PRRs (Toll-like receptors, CLRs, Nod-like receptors, and RIG-like receptors) are almost all metabotropic receptors (Jang et al., 2015). This makes it unlikely that the ionotropic nAchR and GlyR receptors, even if present, would be involved in ciliate feeding. It is difficult to advocate testing their involvement in the CBD-induced effect on *T. pyriformis* in the future, although they could be examined to make certain they are not involved (like all the other receptors tested).

4.3.1.3. Ending the feeding lag

A key feature of the lag period was that it was temporary, at the concentrations tested, suggesting that either the CBD naturally 'wears off' or is degraded within the cell. No study to date has evaluated the ability of *T. pyriformis* to metabolise CBD, which is unlike the situation for AEA, whereby two homologues of FAAH in *T. pyriformis* are known to hydrolyse this endocannabinoid (Karava et al., 2001; Karava et al., 2005).

Mammalian studies indicate that the vast majority of CBD is excreted as mono/dihydroxylated derivatives or as glucuronide conjugates, with the enzymes responsible being CYP450 oxidases, glucuronyl transferases, or sulfotransferases (Ujváry and Hanuš, 2016). The author could find no evidence for *Tetrahymena* possessing glucuronyl transferases or sulfotransferases but analysis of available databases has suggested 102 CYP gene homologues are present in the *T. thermophila* genome. Three of these have been named as putative cytochrome CYP450s and all belong to the CYP13 family: CYP13A1, CYP13B1 and CYP13A3 (www.ciliate.org).

Cytochrome P450s are membrane bound, haem-containing, monooxygenases which are well-known for their role in the metabolism of both xenobiotics and endogenous compounds (Zendulka et al., 2016;

Manikandan and Nagini, 2018). At least 57 human CYP genes have been discovered, with 18 different families and 44 distinct subfamilies (Manikandan and Nagini, 2018). Despite this, the majority of hepatic xenobiotic metabolism is attributed to 6 members of families 1-3 (CYP1A2, 2C9, 2C19, 2D6, 2E1 and 3A4) (Manikandan and Nagini, 2018). CYP-mediated CBD metabolism is mainly performed by CYP2C19 and CYP3A4 (Zendulka et al., 2016) although it is known that at least 7 CYPs (CYP1A1, 1A2, 2C9, 2C19, 2D6, 3A4, 3A5) are capable of CBD metabolism (Jiang et al., 2011).

Considering the CYP13 family is a member of the CYP3 clade (Yan and Cai, 2010), it is conceivable that the *Tetrahymena* CYPs (tCYP) might be responsible for CBD metabolism which leads to the end of the lag period. Further evidence comes from examining amoeba gene databases, and knowing that lag period duration is longer in *V. vermiformis* (Al-hammadi, 2020). Although data are not yet available for *V. vermiformis*, it appears that *Acanthamoeba castellanii* only has one putative CYP homologue, whilst *Entamoeba* spp. and *Naegleria fowleri* possess no CYP homologues at all; possibly suggesting that amoebae have less capacity to degrade CBD than *T. pyriformis*, hence the longer lags (www.amoebadb.org).

A direct approach must be taken to compare the ability of amoeba and ciliates to metabolise CBD. Using labelled CBD and measuring rate of clearance from *Tetrahymena* sp. vs *Entamoeba* spp. or *Naegleria fowleri* (both of which have no CYP homologues) could indeed show whether possessing CYP homologues was correlated with a faster clearance rate. Radiolabeling of cannabinoids has long been used to test their interactions within the human body (Huestis, 2007) and could provide a way to quantify CBD concentrations (and thus clearance over time) between the two species. Alternatively, treating *T. pyriformis* with CYP inhibitors and observing the changes to the lag period afforded by CBD could confirm the role of CYPs in the metabolism of CBD in ciliates. If the lag were extended to become similar in length to that seen in amoeba sp. it would explain the species differences seen in lag phase length.

4.3.2 *T. pyriformis* feeding post the CBD-induced lag period

As stated previously, the post-lag IR is directly proportional to the duration of the lag period, suggesting that IR is directly related to the 'fullness/emptiness' of the ciliate; because cells would continue to defecate FVs during the lag period. Indeed, it is accepted that 'starved' protistan cells have higher IRs than their satiated counterparts (Boenigk et al., 2001b), which is corroborated by the post starvation hyperphagia seen in this study. These experiments employed *T. pyriformis* cultures that were 3 days old and as such, cells would be in stationary phase; they would be near starvation and **not** contain the maximum number of pre-existing FV at the start of the feeding experiment, i.e., maximum is 8 FVs/cell at

1 x 10^7 *Synechococcus* cells/ml (Jaisswar, 2020). Considering Jaisswar (2020) estimated that it takes *T. pyriformis* 12 mins to defecate a single *Synechococcus*-containing-FV at its cytoproct, a period of 32 minutes would equate to the defecation of *ca*. 3 FVs, which seems to be the trigger for the cells 'feeling starved'. Visual examination of the number of pre-formed FVs at the start of experiments (via DAPI staining) would have been useful to confirm this hypothesis. It is suggested they are performed in future experiments.

The CBD dose-response experiments involved *T. pyriformis* feeding on live *Synechococcus*, which is now known to involve all three CLRs (for P/C and V/C) and SRs (for P/C only), so the potential interaction of these receptors with CBD was investigated. Pre-blocking *T. pyriformis* cells with mannose, GalNAc, GlcNAc or dextran sulphate did not themselves induce a feeding lag and their presence did not affect a CBD-induced lag period; so, the main CBD target remains at large (see 4.4). However, their presence did significantly reduce the CBD-induced hyperphagia but inspection of the data suggests that this is a 'mechanical' response to the presence of the sugars, rather than being a specific interaction with CBD. For example, both mannose and GlcNAc reduced hyperphagic IR by 37% and GalNAc reduced it by 46%. This reflects their natural blocking ability in the **absence** of CBD whereby mannose/GlcNAc reduced IR by 40-45% and GalNAc reduces it by 57%. So, the only reason why IR in cells treated with sugar + CBD are significantly higher than with sugar alone (Table 3.4), is that the former cells were 'emptier' than the latter because the cells had experienced a feeding lag (with associated FV defecation).

A previous study on the amoeba *V. vermiformis* feeding on live *Synechococcus*, also found that CBD did not directly interact with CLRs (Al-hammadi, 2020) and this was further confirmed in a feeding experiment using inert beads (that do not interact with CLRs), which showed an equivalent CBD-induced feeding lag duration to that recorded with live *Synechococcus* (Al-hammadi, 2020). She also suggested, as does the current study, that CBD bound to a yet unidentified target to induce the feeding lag and narrowed it down to possibly being an (unidentified) component within the signal cascade required for the activation of actin polymerisation for the formation of the phagocytic cup (see 4.4). In contrast, the CBD response in *V. vermiformis* was more complicated than that seen in *T. pyriformis* in that, after the CBD-induced lag period, IRs in the amoebae were unexplainably lower than the Controls (compared to the relatively easy-to-explain hyperphagia seen in *T. pyriformis*) (Al-hammadi, 2020). This might be due to a reduced ability of amoeba to metabolise CBD, compared to ciliates, so as the CBD is slowly metabolized, the concentration falls below that which is able to induce a lag but remains at a concentration able to still reduce the IR (via phagocytic cup formation). Another possibility is that CBD has an alternative target in *V. vermiformis* and this might indeed be the case, as the CBD-induced lag period was completely

abolished in the presence of a PPARα antagonist whereas no effect of PPAR blocking was recorded in *T. pyriformis*.

4.4 Potential cellular targets of CBD in *T. pyriformis*

4.4.1 Targets involved in *T. pyriformis* feeding

Based on the current study, it appears that the target for CBD in *T. pyriformis* is **not** involved with receptor-based prey capture (Fig. 4.1. stage 1), and based on Jaisswar (2020), it is also **not** involved in vacuole trafficking (Fig. 4.1. stages 3-5) and defecation (Fig. 4.1. stage 6). This leaves phagosome/food vacuole formation as the prime physiological target.

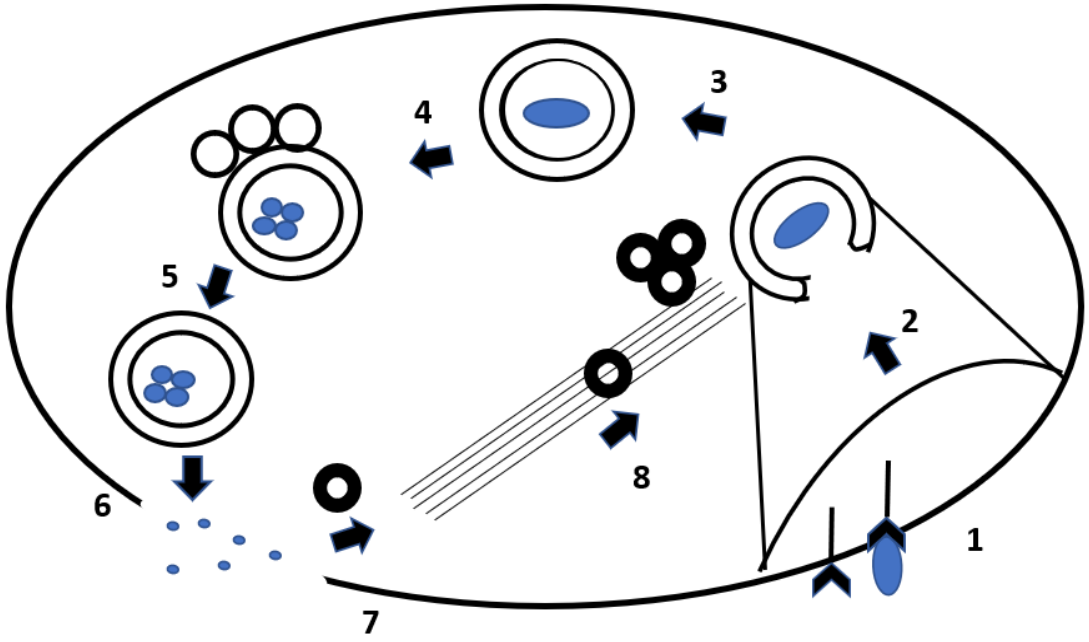

Figure 4.1. *Simplified diagram representing the overall process of the ciliate phagocytic cycle. 1. Receptors available at the oral cavity (precise receptor location unknown) bind available prey filtered into the oral apparatus via ciliary beating. 2. Prey is swept down the cytopharynx into the cytostome where recycled membrane is used to form a food vacuole (FV) around the prey via the polymerisation of F-actin. 3. Myosin activation and actin depolymerisation begins FV closure and dynactin activation facilitates scission of the FV from the cytostome. The Nascent FV then travels into the cytoplasm. 4. Nascent FV binds endosomes and lysosomes for FV maturation and digestion of prey 5. Mature FV is transported to cytoproct. 6. Indigestible particles are exocytosed via binding of FV membrane with membrane of cytoproct. 7. FV membrane is endocytosed from the cytoproct membrane and forms small disc-shaped vesicles. 8. Discoid vesicles are transported back to oral cytostome via a microtubule network and recycled for use in additional nascent FV synthesis. (Figure adapted from Al-Hammadi, 2020).*

Formation of a new FVs at the cytostome requires recycled FV membrane from the cytoproct (Fig. 4.1 stages 7 and 8) and then the formation of a phagocytic cup, which then closes before the FV is released into the cytoplasm (Fig. 4.1., stage 2). Jaisswar (2020) considered it unlikely that FV closure and

detachment were the targets for CBD because if they were, an unclosed vacuole would still be present at the base of the cytostome which could be filled with *Synechococcus* cells; and she never observed any accumulation of cells at the very base of the oral apparatus. However, the assumption that the vacuole could be filled with prey might be wrong, as CBD is thought to negatively affect cilia function (see 4.4.2) and this might have prevented the physical movement of prey down the oral cavity and into the awaiting FV (whether FV closure and detachment were affected by CBD or not).

It is also considered that any downstream signaling cascades initiated by receptor-prey binding are not viable CBD targets, as blocking CLRs with their respective sugars would have halted these downstream signaling events and yet CBD still induced a feeding lag. In addition, because a CBD-induced feeding lag was obtained when *T. pyriformis* fed on inert beads, and these are considered to enter FVs via a non-specific receptor-based route (Vogel et al., 1980) which is attributed to a 'mechanical' action of a cilia-generated vortex only (Allen and Fokt, 2000; Grønlien et al., 2002), potential CBD targets associated with only the basal vacuole formation rate are sought. Future experiments might now be better placed in using beads as opposed to live *Synechococcus*, to identify the CBD target as this would provide less cellular 'complications'.

Unfortunately for this study, there is very little in the literature on FV formation and membrane recycling in ciliates. However, ciliate cells have long been known to have a limited volume of membrane available for FV formation and hence the requirement for it to be recycled (Allen, 1974; Allen and Fok, 1980). Jaisswar (2020) estimated that 48-56 μm^3 of membrane was available for FV manufacture *T. pyriformis* (total membrane volume unknown); no data on other species can be found by the author. It is suggested that a future experiment should employ confocal microscopy to assess whether FV recycling is affected by CBD. Confocal microscopy could also allow for live cell imaging, allowing visualisation of recycling in real time (Jensen, 2013). If recycling is halted, a collection of discoidal vesicles should be evident at the cytoproct. If these are absent, then it strongly suggests that they have been effectively transported to the cytostome and FV membrane recycling is not the target of CBD action.

The recycling process begins with the fusion of the membrane from a 'spent' FVs with the plasma membrane at the cytoproct, then it is removed and deposited in the cytoplasm as small disk-shaped fractions which become flattened into discoidal vesicles (Allen and Fok, 1980). Within 3 minutes, these vesicles are coated with F-actin (Sugita et al., 2009) and become aligned to a bundle of microtubule ribbons, where they are then transported from the cytoproct to the cytostome in *ca*. 4 minutes (Allen and Fok, 1980). This is an example of 'direct recycling', i.e., no involvement of the lysosomal or Golgi systems on the vesicle's journey back to the cytostome and has been shown to occur in *Tetrahymena, Paramecium* and *Ophrydium* (Allen and Fok, 1980; Goff and Stein, 1981; Grønlien et al., 2002).

Studies on ciliates have confirmed that actin plays a role in the formation of the phagocytic cup, migration of newly formed phagosomes into the cell, trafficking of phagosomes within the cell, and their fusion with lysosomes (Tiggemann and Plattner, 1981; Tiggemann et al., 1981; Allen and Fok, 1983; Méténier, 1984). More recently, it has been shown to be involved in the first stage of FV membrane recycling, i.e., the retrieval of spent FV membrane from the plasma membrane, and in the coating of discoidal vesicles (Sugita et al., 2009). Considering actin is involved in the trafficking of food vacuoles, and this was a process not affected by CBD, it might suggest that this part of the membrane recycling process, and phagocytic cup formation, are not the targets for CBD in *T. pyriformis*.

However, studies suggest that ciliates, including *Tetrahymena*, possess a repertoire of actin molecules and actin-related proteins (ARPs), each with different functions (Sehring et al., 2007a). Indeed, it is known that the actin isoforms on FVs change throughout their trafficking through the cytoplasm in *Paramecium* suggesting each has a specific role rather than having a general role (Sehring et al., 2007b). These isoforms also have varying sensitivities to antagonistic or agonistic drugs (Sehring et al., 2007a) which might possibly suggest that an actin isoform/ARP involved in one process (e.g. phagosome cup formation/closure/detachment) might interact with CBD, whilst another isoform involved with another process (e.g. FV trafficking) might not. However, the identity of the specific isoforms involved in phagocytic cup formation/closure/detachment, and the transport of discoidal vesicles along the microtubule network to the cytostome, is alluding the author due to the generic terms used in publications. For example, F-actin is considered to be involved in 'vacuole synthesis' in *Paramecium* and *Tetrahymena* (Cohen et al., 1984; Kersken et al., 1986) and, in *Tetrahymena*, genetic silencing of the *ACT1* gene (which encodes the single essential gene for actin) 'inhibits vacuole formation' (Williams et al., 2006).

Very recently, co-administration of Cannabichromene (CBC) with THC or CBD has been shown to cause disintegration of F-actin filaments inside urothelial carcinoma cells (Anis et al., 2021). Whether this was due to the CBC, or activation of CB1/2 activation is unknown, although use of a CB1/2 inverse agonist reduced the overall cytotoxic effects of the cannabinoids suggesting the latter played some role (Anis et al., 2021). No information could be found on the sole interaction of CBD with F-actin, making it hard to deduce whether it could act upon the actin in *T. pyriformis*.

Microtubules play an important auxiliary role to actin in ciliate FV membrane recycling and 'vacuole formation' together with acting as a guide to maturing phagosome by facilitating their contact with incoming endosomes and lysosomes (Harrison and Grinstein, 2002). Microtubule ribbons are also present around the oral cavity and are responsible for the selective transport of endosomes, such as acidosomes, to newly formed food vacuoles (Schroeder et al., 1990). *Tetrahymena* possess 2 isotypes of β-tubulin and 1

isotype of α-tubulin but assembles 17 distinct types via distinct post translational modifications (PTMs) (Gaertig, 2000). Specific sub-populations are assigned to specific cellular locations depending on these defining PTMs (Wloga et al., 2008). For example, glutamylation of α-tubulin dictates localisation to cilia or the basal bodies, and are indirectly required for prey capture due to the requirement of the cilia in the filter feeding mechanism (Wloga et al., 2008). No information on the specific PTMs required for FV transport or recycling could be found. Microtubules and microfilaments in mammalian cells have been shown to be disrupted in a dose-dependent manner following treatment with CBD, THC and CBN (Tahir et al., 1992).

In addition, the motor protein dynein, is also present in *Tetrahymena*, with at least 25 DHY genes being expressed (Wilkes et al., 2008). However, even though dyneins drive retrograde microtubule transport, they are more renowned for driving the beating of the cilia (see 4.4.2.1). Primary defects in dynein structure in the sensory and motile cilia in humans results in multiple ciliopathies, which share clinical features, such as mental retardation, cystic kidney, retinal defects and polydactyly (Lee and Gleeson, 2011).

4.4.2 Other cellular targets of CBD

4.4.2.1. Cilia – movement and feeding

Ciliate cilia are structurally and molecularly conserved within higher eukaryotes (Carvalho-Santos et al., 2011). On their cell surface, the cilia are arranged in an array and they beat in a biphasic whip-like motion (Wood et al., 2007; Funfak et al., 2015). Motile cilia have a 9 + 2 microtubule pair ultrastructure, with inner and outer dynein arms (Fawcett and Porter, 1954; Lee and Gleeson, 2011). Dynein is essentially the microtubule molecular motor, which makes cilia move, and was first identified in the 1960's (Gibbons, 1963). It is unknown whether dynein is affected by CBD, but it is known that microtubules are (Tahir et al., 1992). In addition, Ca/CaM signalling is involved in controlling the stroke motion of ciliary beating in ciliates and cellular influx is controlled by voltage-gated calcium channels (VGCCs) (Tanida et al., 1986; Gonda et al., 2000; Lodh et al., 2016). CBD is known to inhibit human T-type VGCCs along with the non-selective cation channels TRPs, also known to regulate intracellular Ca^{2+} (Bih et al., 2015). Should CBD also target ciliary VGCCs in *T. pyriformis*, it could disrupt regular ciliary motility. Indeed, the very first report on ciliate interactions with cannabinoids did mention that, in addition to THC-induced delays in cell division, the treated *T. pyriformis* cells moved in a sluggish and irregular manner (McClean and Zimmerman, 1976). Such sluggish movement of *T. pyriformis* cells has also been observed in the presence of CBD (Parry, personal communication).

T. pyriformis is a classic filter feeder and as such, uses its cilia to direct prey into its oral cavity as it swims (Verni and Gualtieri, 1997; Caron et al., 2012; Geisen et al., 2018; Diaz and Laybourn-Parry, 2019), thus a slower rate of swimming would mean fewer prey reaching the oral cavity. In addition, the oral cavity itself comprises an undulating membrane (UM) which is a line of kinetosomes (ciliary basal bodies), and 3 oral membranelles (short/stiffer cilia) (Smith, 1982). It is the beating of these membranelles, plus the cilia on the UM, that creates the mechanical currents that bring prey into the cavity from the external medium (Rasmussen, 1976; Smith, 1982). If these were also targeted by CBD then it is likely that no prey whatsoever would make it into, and through, the oral cavity to an awaiting FV. This might explain why, under CBD treatment, Jaisswar (2020) and the current author have never seen an accumulation of *Synechococcus* in the oral cavity during the CBD-induced lag phase. And it is interesting to note that when *Tetrahymena* was treated with an F-actin inhibitor (Cytochalasin B) it arrested food vacuole formation **but** the author did observe an accumulation of prey (carmine particles) in the oral cavity (Nilsson, 1977). Further work on cilia, particularly in the oral cavity, requires further investigation.

4.4.2.2. Cell death and MAPK

CBD appears to act more specifically on cancer cells than normal cells, by inducing apoptosis, and has thus been extensively investigated as a potential anti-cancer agent (Choipark et al., 2008; Shrivastava et al., 2011). Even so, CBD can also inhibit cell migration and proliferation in healthy cells (Pagano et al., 2020). McClean and Zimmerman (1976) were the first to show that a ciliate (*T. pyriformis*) responded to a cannabinoid, i.e. THC, but cell death was not reported to have occurred. Instead, there was a delay in cell division (McClean and Zimmerman, 1976) which was predominantly in the G2 phase of the cell cycle (Zimmerman et al., 1981). More recently, Jones (2017) recorded *T. pyriformis* cell death in the presence of CBD (MIC 3.16 µM, IC50 4.38 µM) and Wanlahbeh (2020) showed that the population was able to recover from this death in ~90 minutes.

Considering many of the current study's experiments employed a standard CBD concentration of 4 µM, cells would have been dying during the experiment and feeding would have only been monitored in those surviving cells. It therefore begs the question as to whether the CBD-induced feeding response reported here is a side-effect of cell death. It is thought not. Firstly, Jones (2017) established the MIC for cell death as being 3.16µM yet, in the current study, a significant reduction in IR was observed at $>1.75 \leq 2$ µM and the feeding lag began at 2.5 µM. These concentrations are below the MIC for cell death which shows that the action of CBD (at these concentrations) was independent of cell death. Secondly, Wanlahbeh (2020) reported that the blocking of PPAR α in *T. pyriformis* abolished CBD-induced cell death, yet Jaisswar

(2020) found that blocking this receptor had no effect on the CBD-induced feeding lag. Indeed, by blocking all PPAR isoforms with GW9662 in the current study, it was confirmed that PPARs play no role in CBD's action on *T. pyriformis* feeding. It therefore seems that the CBD-induced effect on feeding and death in *T. pyriformis* are two separate processes and that PPAR is only involved in cell death.

This demonstrates that the action of CBD on *T. pyriformis* might be more complicated than first thought and demonstrates the promiscuous behaviour it is renowned for. It is already known to be acting on two cellular processes in *T. pyriformis* (feeding and cell death), and possibly on cilia, but there may be others also. What was very interesting though, was the lack of involvement of a mitogen-activated protein kinase (MAPK) signaling pathway when CBD was applied to the cells.

MAPK signalling cascades are a diverse set of signal transduction pathways that regulate various cellular functions including apoptosis, translation/transduction, proliferation and differentiation (Plotnikov et al., 2011). At present, 4 MAPK pathways have been characterised in humans and named after the key MAPK in the pathway: Extracellular signal regulated kinase 1/2 (ERK 1/2), p38, cc-Jun N-terminal kinase (JNK) and ERK5 (Plotnikov et al., 2011). The former two pathways (ERK1/2 and p38) have been identified in *Tetrahymena*, and although not as well characterized as human MAPKs, the cells seem to utilise these signaling cascades in response to environmental stressors (Arslanyolu, 2006; 2007; Li et al., 2009; Arslanyolu and Yıldız, 2014).

Annotation of the *T. thermophila* genome identified 11 MAPKs (TtMPK) of which 8 belonged to the ERK1/2, which are involved in abiotic stress responses (TtMPK 1-3 and 5-9) (Yıldız and Arslanyolu, 2014). Only TtMPK 2 received further characterisation, displaying the closest sequence similarity with human ERK5, followed by the stress activated p38 MAPK (Arslanyolu and Yıldız, 2014). The p38 MAPK pathway has been termed the 'stress activated protein kinases' (Nakashima et al., 1999) and responses to osmotic stress and decreases in temperature. In *Tetrahymena*, this response appear to be mediated by a MAPK-like protein sharing close sequence similarity to the mammalian p38 MAPK (Nakashima et al., 1999). Treatment of *Tetrahymena* with hydrogen peroxide has been found to induce an oxidative stress response (which arrests mitotic division) which can be abolished using the antagonists SB203580 (for p38) and PD98059 (for MEK) (Li et al., 2009). It is therefore surprising that *T. pyriformis* did not perceive the presence of CBD as an external stress in the current study, and that the CBD-induced lag was not alleviated with SB203580 (for p38) and PD98059 (for MEK); or indeed the other MAPK blockers. And, given the large range of CBD-interacting receptors in humans, a range of MAPKs will inevitably be responsible for transducing CBD signals in mammals (Hwang et al., 2017; Gugliandolo et al., 2020), and this ubiquity and diversity of function probably evolved to meet the complexity that

coincides with multicellularity. However, this is clearly not mimicked in *Tetrahymena*, as blocking these known CBD-interacting receptors, in the current study, also did not alleviate the CBD-induced feeding lag.

On the one hand this could be viewed as the MAPK cascades of multicellular organisms being linked to CBD-interacting receptors (amongst many others) while the *Tetrahymena* MAPK system is likely to be much more limited in its coupled receptors and activating ligands. On the other hand, even though a CBD-induced feeding lag was not considered a stress response, the other CBD-induced mechanism of cell death might be, particularly since MAPK signalling cascades regulate various cellular functions including apoptosis (Plotnikov et al., 2011). Therefore, *T. pyriformis* survival experiments should be performed with all antagonists tested in the current study, to see if CBD-interacting receptors and MAPK pathways are involved, or whether CBD is simply not perceived as an external stress by *T. pyriformis*.

Chapter 5. Conclusion

This study investigated the effects and molecular targets for CBD in *T. pyriformis*, which is known to possess a basic endocannabinoid system as well as the ability to react to exogenous phytocannabinoids. Results showed that CBD affected ciliate feeding on live *Synechococcus* cells in a dose dependent manner. The primary effect was a reduction in ingestion rate (IR) which ultimately led to a temporary cessation in feeding (the 'feeding lag'); the duration of which was positively correlated to CBD concentration. Post-lag, the ciliate resumed feeding and IR was directly correlated to the duration of the lag period. This suggested that IR is related to the 'fullness/emptiness' of the ciliate at the end of the lag; because cells would continue to defecate FVs during the lag period (as food vacuole trafficking and defecation are unaffected by CBD). A lag period of 32 min (and defecation of *ca*. 3 food vacuoles) appeared to induce 'starvation' in *T. pyriformis* and this resulted in a significant increase in IR compared the un-treated Control (hyperphagia).

The molecular target(s) mediating this CBD effect were deemed likely to be involved in *T. pyriformis* prey capture and/or vacuole recycling/food vacuole formation. With regards to prey capture, this study showed that live *Synechococcus* cells were ingested at higher rates than heat-killed cells and beads (which were equivalent), due to the fact that at least three CLRs (for mannose, GalNac and GlcNac ligands) and SRs were involved in their uptake. Heat-treatment appeared to destroy the mannose, GlcNAc and SR ligands on *Synechococcus* cells, leaving only GalNAc residues to facilitate the uptake of dead cells. None of the receptors tested were involved in the uptake of beads. The blocking of these receptors, with their corresponding sugar, prior to the addition of CBD did not abolish the CBD-induced feeding lag. However, post-lag IRs were not hyperphagic, but equivalent to what would be expected when blocking these receptors in the absence of CBD. This suggests that these receptors have no direct interaction with CBD. In addition to these receptors, further receptors (GPCRs and non-GPCRs) which are known to interact with CBD in other eukaryotic cells, were also blocked but none of them abolished the CBD-induced feeding lag, suggesting that *T. pyriformis* has few, if any, CBD-interacting receptors.

It may therefore be the case that the molecular target is indeed involved in vacuole formation/membrane recycling rather than prey capture. Such processes involve microtubules, which may be structurally disrupted by CBD, resulting in fewer viable filaments (Tahir et al., 1992). They also involve actin and dynein but it is currently unknown whether any of their isoforms can react to CBD. However, cilia also contain microtubules and dynein and in the presence of CBD *T. pyriformis* cells move in a sluggish manner. If cilia themselves are directly affected by CBD then 'prey capture' would be back in the frame as a CBD target because numerous cilia exist in the oral cavity of the ciliate, and the beating of these cilia

creates currents in the extracellular fluid which bring prey into the cavity. Without these currents, no prey would enter the oral cavity and be subsequently pushed down the ciliated cytopharynx and packaged into a food vacuoles.

So, in this simple ciliate, CBD has already been shown to affect feeding and swimming, but there is another effect also (not studied here) whereby CBD can induce cell death in *T. pyriformis* and this involves PPARα (which is not involved in CBD-induced feeding lags). Whether any of the other CBD-interacting receptors are involved in cell death remains to be seem, as it did seem strange that *T. pyriformis* did not consider CBD as an external stress and activate the MAPK pathway; as is seen in other eukaryotic cells.

The fact that three responses to CBD (reduced feeding and swimming, and cell death) have been demonstrated in this simple ciliate suggests that the action of CBD on *T. pyriformis* is more complicated than first thought and demonstrates the promiscuous behaviour that CBD is renowned for in mammalian systems. However, whereas these latter cells contain a wealth of molecular targets for CBD, this study has shown that there does not appear to be too many in *T. pyriformis*, so elucidating which targets are the most important, and evolutionary conserved, might be achievable. Such information would help in the understanding as to why CBD is so promiscuous in multicellular organisms and by doing so, it is hoped that the knowledge gleaned will aid in the future implementation of CBD as an effective therapeutic agent for a number of conditions.

Acknowledgments.

The author would like to express his sincere gratitude to his primary supervisor Dr Jackie Parry for her constant guidance, patience, thoughts, and discussion that helped drive and make this thesis possible. I would also like to thank the technical team in BLS, particularly Janice Drinkall for her constant technical expertise and encouragement in the lab.

Further thanks goes to my family, friends and my girlfriend, Sarah Case, for the constant moral support and advice throughout the entire project.

Appendix.

Appendix 1.

Chalkley's medium.

Stock Solution in 100mL of distilled water:
NaCl – 2g
KCl – 0.08g
$CaCl_2$ – 0.12g

Add 5mL of stock solution to 995mL of distilled water. Resulting solution is to be autoclaved at 121ºC for 20 minutes.

Lysogeny broth (LB) agar.

NaCl – 10g
Tryptone – 10g
Yeast Extract – 5g
Agar No.2 – 15g

Add to 1L of distilled water. Resulting solution is to be autoclaved at 121ºC for 20 minutes. Once cool enough to handle the agar was poured into petri dishes under aseptic techniques. Once set, plates were stored at 4ºC.

Blue green 11 (BG 11) broth.

Stock solutions A-H in 500mL of distilled water:

Stock A: Sodium Nitrate ($NaNO_3$) – 75 g

Stock B: Dipotassium phosphate (K_2HPO_4) – 2g

Stock C: Magnesium Sulphate Heptahydrate ($MgSO_47H_2O$) – 3.75g

Stock D: Calcium Chloride Dihydrate ($CaCl_2.2H_2O$) – 1.8g

Stock E: Citric acid – 0.3g

Stock F: Ammonium ferric citrate green – 0.3g

Stock G: EDTANa2 – 0.05g

Stock H: Sodium Carbonate (Na_2CO_3) – 1g

Stock solution I of trace metals in 1L of distilled water:

Stock I:

Boric Acid (H_3BO_3) – 2.86g

Manganese Chloride Tetrahydrate ($MnCl_2.4H_2O$) – 1.81g

Zinc Sulphate heptahydrate ($ZnSO_4.7H_2O$) – 0.22g

Sodium Molybdate dihydrate ($Na_2MoO_4.2H_2O$) – 0.39g

Copper Sulphate Pentahydrate ($CuSO_4.5H_2O$) – 0.08g

Cobalt Nitrate Hexahydrate ($CO(NO_3)_2.6H_2O$) – 0.05g

Combine 10mL of stock solutions A-H and 1mL of stock solution I and make up to 1L using distilled water. Adjust pH to 7.1 using 1M Sodium hydroxide (NaOH) or Hydrochloric acid (HCl) and autoclave at 121ºC for 20 minutes.

5-(4,6-Dichlorotriazin-2-yl) aminofluorescein (DATF) staining solutions.

Solution 1.

Na_2HPO_4 – 0.71g
NaCl – 0.85g

Add to 100 mL of distilled water and autoclave at 121ºC for 20 minutes.

Solution 2.

Tetrasodium pyrophosphate ($Na_4P_2O_7$) – 0.89g
NaCl – 0.85 g

Add to 100 mL of distilled water and autoclave at 121ºC for 20 minutes.

Appendix 2.

Evidence for Chosen Working Concentrations:

Antagonist	Working Concentration	Reference
GPCR Antagonists		
Gallein	10µM	(Casey et al., 2010; Ukhanov et al., 2011)
Pertussis toxin (PTX)	100ng/ml	(Ondarza et al., 2003; Lampert et al., 2011)
Melittin	0.3µM	(Sommer et al., 2012)
Non-GPCR Antagonists		
Capsazepine	10µM	(Yamamura et al., 2004; Yang et al., 2019)
GW9662	10µM	(Shen et al., 2007; Wanlahbeh, 2020; Jaisswar, 2020)
ZM241385	10µM	(Poucher et al., 1995)
LE300	10µM	(Kawamoto et al., 2012; Li et al., 2019)
MAPK signalling components		
U0126	10µM	(Ong et al., 2015; Wang et al., 2018)
PD98059	10µM	(Kojima et al., 2007; Wang et al., 2017)
SB203580	10µM	(Li et al., 2009; Liu et al., 2014b)
ZM336372	10µM	(Deming et al., 2008)

Bibliography:

Aizpurua-Olaizola, O., Elezgarai, I., Rico-Barrio, I., Zarandona, I., Etxebarria, N. & Usobiaga, A. 2017. Targeting the Endocannabinoid System: Future Therapeutic Strategies. *Drug Discovery Today,* 22(1)**,** 105-110.

Al-Hammadi, I. 2020. Actions of Cannabinoids on Amoebae. Phd Thesis. Lancaster University.

Alger, B. E. 2013. Getting High on the Endocannabinoid System. *Cerebrum: the dana forum on brain science,* V.2013(6)**,** 14.

Allen, R. D. 1974. Food Vacuole Membrane Growth with Microtubule-Associated Membrane Transport in *Paramecium*. *The Journal of Cell Biology,* 63(3)**,** 904-922.

Allen, R. D. & Fok, A. K. 1980. Membrane Recycling and Endocytosis in *Paramecium* Confirmed by Horseradish Peroxidase Pulse-Chase Studies. *Journal of Cell Science,* 45(1)**,** 131-145.

Allen, R. D. & Fokt, A. K. 2000. Membrane Trafficking and Processing in *Paramecium*. *International Review of Cytology.* Academic Press.

Allen, R. D., Ma, L. & Fok, A. K. 1993. Acidosomes: Recipients of Multiple Sources of Membrane and Cargo During Development and Maturation. *Journal of Cell Science,* 106(1)**,** 411 - 422.

Anagnostopoulos, D., Rakiec, C., Wood, J., Pandarinathan, L., Zvonok, N., Makriyannis, A. & Siafaka-Kapadai, A. 2010. Identification of Endocannabinoids and Related N-Acylethanolamines in *Tetrahymena*. A New Class of Compounds for *Tetrahymena*. *Protist,* 161(3)**,** 452-465.

Anis, O., Vinayaka, A. C., Shalev, N., Namdar, D., Nadarajan, S., Anil, S. M., Cohen, O., Belausov, E., Ramon, J., Mayzlish Gati, E. & Koltai, H. 2021. Cannabis-Derived Compounds Cannabichromene and Δ9-Tetrahydrocannabinol Interact and Exhibit Cytotoxic Activity against Urothelial Cell Carcinoma Correlated with Inhibition of Cell Migration and Cytoskeleton Organization. *Molecules,* 26(2)**,** 465.

Arnosti, C. 1993. Structural Characterization and Bacterial Degradation of Marine Carbohydrates. phd Thesis. Massachusetts Institute of Technology.

Arslanyolu, M. & Yıldız, M. T. 2014. Cloning, Expression and Characterization of a Gene Encoding Mitogen Activated Protein Kinase 2 (Mpk2) from *Tetrahymena thermophila*. *Gene,* 546(1)**,** 40-9.

Ashton, J. & Glass, M. 2007. The Cannabinoid Cb2 Receptor as a Target for Inflammation-Dependent Neurodegeneration. *Current Neuropharmacology,* 5(2)**,** 73-80.

Azam, F., Fenchel, T., Field, J., Gray, J. S., Meyer, L. & Thingstad, T. F. 1983. The Ecological Role of Water-Column Microbes in the Sea. *Marine Ecology Progress Series,* 10**,** 257-263.

Babuta, M., Mansuri, M. S., Bhattacharya, S. & Bhattacharya, A. 2015. The *Entamoeba histolytica*, Arp2/3 Complex Is Recruited to Phagocytic Cups through an Atypical Kinase Ehak1. *PLOS Pathogens,* 11(12)**,** e1005310.

Beltramo, M., De Fonseca, F. R. G., Navarro, M., Calignano, A., Gorriti, M. A., Grammatikopoulos, G., Sadile, A. G., Giuffrida, A. & Piomelli, D. 2000. Reversal of Dopamine D2 Receptor Responses by an Anandamide Transport Inhibitor. *The Journal of Neuroscience,* 20(9)**,** 3401-3407.

Benarroch, E. E. 2012. Endogenous Opioid Systems. *Neurology,* 79(8)**,** 807.

Benito, C., Tolón, R. M., Pazos, M. R., Núñez, E., Castillo, A. I. & Romero, J. 2008. Cannabinoid Cb2receptors in Human Brain Inflammation. *British Journal of Pharmacology,* 153(2)**,** 277-285.

Biedroń, R., Peruń, A. & Józefowski, S. 2016. Cd36 Differently Regulates Macrophage Responses to Smooth and Rough Lipopolysaccharide. *PLOS ONE,* 11(4)**,** e0153558.

Bih, C., Chen, T., Nunn, A. V., Bazelot, M., Dallas, M. & Whalley, B. J. 2015. Molecular Targets of Cannabidiol in Neurological Disorders. *Neurotherapeutics,* 12(4)**,** 699-730.

Bisogno, T., Hanuš, L., De Petrocellis, L., Tchilibon, S., Ponde, D. E., Brandi, I., Moriello, A. S., Davis, J. B., Mechoulam, R. & Di Marzo, V. 2001. Molecular Targets for Cannabidiol and Its Synthetic Analogues: Effect on Vanilloid Vr1 Receptors and on the Cellular Uptake and Enzymatic Hydrolysis of Anandamide. *British Journal of Pharmacology,* 134(4)**,** 845-852.

Blankman, J. L., Simon, G. M. & Cravatt, B. F. 2007. A Comprehensive Profile of Brain Enzymes That Hydrolyze the Endocannabinoid 2-Arachidonoylglycerol. *Chemistry & Biology,* 14(12)**,** 1347-1356.

Blum, J. J. & Greenside, H. 1976. Particle Ejection from the Cytoproct of *Tetrahymena*. *The Journal of Protozoology,* 23(4)**,** 500-502.

Boboc, A. 2020. Evaluation of Bacterial Ligands Involved in Receptor Mediated Phagocytosis in *Tetrahymena pyriformis*. Mres Thesis. Lancaster University.

Bockaert, J., Claeysen, S., Dumuis, A. & Marin, P. 2010. Classification and Signaling Characteristics of 5-Ht Receptors. *Handbook of Behavioural Neuroscience,* 21(3)**,** 103-121.

Boenigk, J., Matz, C., Jurgens, K. & Arndt, H. 2001a. Confusing Selective Feeding with Differential Digestion in Bacterivorous Nanoflagellates. *Journal of Eukaryotic Microbiology,* 48(4)**,** 425-432.

Boenigk, J., Matz, C., Jürgens, K. & Arndt, H. 2001b. The Influence of Preculture Conditions and Food Quality on the Ingestion and Digestion Process of Three Species of Heterotrophic Nanoflagellates. *Microbial Ecology,* 42(2)**,** 168-176.

Boenigk, J. & Novarino, G. 2004. Effect of Suspended Clay on the Feeding and Growth of Bacterivorous Flagellates and Ciliates. *Aquatic Microbial Ecology,* 34**,** 181-192.

Bright, L. J., Kambesis, N., Nelson, S. B., Jeong, B. & Turkewitz, A. P. 2010. Comprehensive Analysis Reveals Dynamic and Evolutionary Plasticity of Rab Gtpases and Membrane Traffic in *Tetrahymena thermophila*. *PLoS Genetics,* 6(10)**,** e1001155.

Brown, G. D., Willment, J. A. & Whitehead, L. 2018. C-Type Lectins in Immunity and Homeostasis. *Nature Reviews Immunology,* 18(6)**,** 374-389.

Brown, M. S. & Goldstein, J. L. 1979. Receptor-Mediated Endocytosis: Insights from the Lipoprotein Receptor System. *Proceedings of the National Academy of Sciences,* 76(7)**,** 3330-3337.

Cadas, H., Gaillet, S., Beltramo, M., Venance, L. & Piomelli, D. 1996. Biosynthesis of an Endogenous Cannabinoid Precursor in Neurons and Its Control by Calcium and Camp. *The Journal of Neuroscience,* 16(12)**,** 3934-3942.

Canton, J., Neculai, D. & Grinstein, S. 2013. Scavenger Receptors in Homeostasis and Immunity. *Nature Reviews Immunology,* 13(9)**,** 621-634.

Caron, D. A., Countway, P. D., Jones, A. C., Kim, D. Y. & Schnetzer, A. 2012. Marine Protistan Diversity. *Annual Review of Marine Science,* 4(1)**,** 467-493.

Caron, D. A., Goldman, J. C. & Dennett, M. R. 1988. Experimental Demonstration of the Roles of Bacteria and Bacterivorous Protozoa in Plankton Nutrient Cycles. *Hydrobiologia,* 159(1)**,** 27-40.

Carvalho-Santos, Z., Azimzadeh, J., Pereira-Leal, J. B. & Bettencourt-Dias, M. 2011. Tracing the Origins of Centrioles, Cilia, and Flagella. *Journal of Cell Biology,* 194(2)**,** 165-175.

Casey, L. M., Pistner, A. R., Belmonte, S. L., Migdalovich, D., Stolpnik, O., Nwakanma, F. E., Vorobiof, G., Dunaevsky, O., Matavel, A., Lopes, C. M. B., Smrcka, A. V. & Blaxall, B. C. 2010. Small Molecule Disruption of Gβγ Signaling Inhibits the Progression of Heart Failure. *Circulation Research,* 107(4)**,** 532-539.

Castillo, A., Tolón, M. R., Fernández-Ruiz, J., Romero, J. & Martinez-Orgado, J. 2010. The Neuroprotective Effect of Cannabidiol in an in Vitro Model of Newborn Hypoxic–Ischemic Brain Damage in Mice Is Mediated by Cb2 and Adenosine Receptors. *Neurobiology of Disease,* 37(2)**,** 434-440.

Caterina, M. J. 2014. Trp Channel Cannabinoid Receptors in Skin Sensation, Homeostasis, and Inflammation. *ACS Chemical Neuroscience,* 5(11)**,** 1107-1116.

Chiesa, R., Silva, W. I. & Renaud, F. L. 1993. Pharmacological Characterization of an Opioid Receptor in the Ciliate *Tetrahymena*. *Journal of Eukaryotic Microbiology,* 40(6)**,** 800-4.

Choipark, W.-H.-D., Baek, S.-H., Chu, J.-P., Kang, M.-H. & Mi, Y.-J. 2008. Cannabidiol Induces Cytotoxicity and Cell Death Via Apoptotic Pathway in Cancer Cell Lines. *Biomolecules and Therapeutics,* 16(2)**,** 87-94.

Chye, Y., Christensen, E., Solowij, N. & Yücel, M. 2019. The Endocannabinoid System and Cannabidiol's Promise for the Treatment of Substance Use Disorder. *Frontiers in Psychiatry,* 10(2)**,** 63.

Cinar, R. & Szücs, M. 2009. Cb1 Receptor-Independent Actions of Sr141716 on G-Protein Signaling: Coapplication with the Mu-Opioid Agonist Tyr-D-Ala-Gly-(Nme)Phe-Gly-Ol Unmasks Novel, Pertussis Toxin-Insensitive Opioid Signaling in Mu-Opioid Receptor-Chinese Hamster Ovary Cells. *Journal of Pharmacology and Experimental Therapeutics,* 330(2)**,** 567-74.

Cohen, J., Garreau De Loubresse, N. & Beisson, J. 1984. Actin Microfilaments in *Paramecium*: Localization and Role in Intracellular Movements. *Cell Motility,* 4(6)**,** 443-68.

Corliss, J. O. 2002. Biodiversity and Biocomplexity of the Protists and an Overview of Their Significant Roles in Maintenance of Our Biosphere. *Acta Protozoologica,* 41(3)**,** 199-219.

Cravatt, B. F., Demarest, K., Patricelli, M. P., Bracey, M. H., Giang, D. K., Martin, B. R. & Lichtman, A. H. 2001. Supersensitivity to Anandamide and Enhanced Endogenous Cannabinoid Signaling in Mice Lacking Fatty Acid Amide Hydrolase. *Proceedings of the National Academy of Sciences of the United States of America,* 98(16)**,** 9371-6.

Csaba, G. 2012. The Hormonal System of the Unicellulartetrahymena:A Review with Evolutionary Aspects. *Acta Microbiologica et Immunologica Hungarica,* 59(2)**,** 131-156.

Csaba, G. 2015. Biogenic Amines at a Low Level of Evolution: Production, Functions and Regulation in the Unicellular *Tetrahymena*. *Acta Microbiologica et Immunologica Hungarica,* 62(2)**,** 93-108.

Csaba, G. 2017. Is There a Hormonal Regulation of Phagocytosis at Unicellular and Multicellular Levels? A Critical Review. *Acta Microbiologica et Immunologica Hungarica,* 64(4)**,** 357-372.

Cummings, R. & Mcever, R. 2009. C-Type Lectins. *In:* VARKI A, C. R., ESKO JD, (ed.) *Essentials of Glycobiology.* 2nd ed. Cold Spring Harbor (NY): Cold Spring Harbor Laboratory Press.

Da Silva, V. K., De Freitas, B. S., Da Silva Dornelles, A., Nery, L. R., Falavigna, L., Ferreira, R. D. P., Bogo, M. R., Hallak, J. E. C., Zuardi, A. W., Crippa, J. A. S. & Schröder, N. 2014. Cannabidiol Normalizes Caspase 3, Synaptophysin, and Mitochondrial Fission Protein Dnm1l Expression Levels in Rats with Brain Iron Overload: Implications for Neuroprotection. *Molecular Neurobiology,* 49(1)**,** 222-233.

Dambuza, I. M. & Brown, G. D. 2015. C-Type Lectins in Immunity: Recent Developments. *Current Opinion in Immunology,* 32(1)**,** 21-27.

Dart, A. E., Tollis, S., Bright, M. D., Frankel, G. & Endres, R. G. 2012. The Motor Protein Myosin 1g Functions in Fc r-Mediated Phagocytosis. *Journal of Cell Science,* 125(24)**,** 6020-6029.

De Duve, C. & Baudhuin, P. 1966. Peroxisomes (Microbodies and Related Particles). *Physiological Reviews,* 46(2)**,** 323-357.

De Filippis, D., Iuvone, T., D'amico, A., Esposito, G., Steardo, L., Herman, A. G., Pelckmans, P. A., De Winter, B. Y. & De Man, J. G. 2008. Effect of Cannabidiol on Sepsis-Induced Motility Disturbances in Mice: Involvement of Cb 1 Receptors and Fatty Acid Amide Hydrolase. *Neurogastroenterology and Motility,* 20(8)**,** 919-927.

De Gregorio, D., Mclaughlin, R. J., Posa, L., Ochoa-Sanchez, R., Enns, J., Lopez-Canul, M., Aboud, M., Maione, S., Comai, S. & Gobbi, G. 2019. Cannabidiol Modulates Serotonergic Transmission and Reverses Both Allodynia and Anxiety-Like Behavior in a Model of Neuropathic Pain. *Pain,* 160(1)**,** 136-150.

Deming, D., Geiger, P., Chen, H., Vaccaro, A., Kunnimalaiyaan, M. & Holen, K. 2008. Zm336372, a Raf-1 Activator, Causes Suppression of Proliferation in a Human Hepatocellular Carcinoma Cell Line. *Journal of Gastrointestinal Surgery,* 12(5)**,** 852-857.

Deutsch, D. G. & Chin, S. A. 1993. Enzymatic Synthesis and Degradation of Anandamide, a Cannabinoid Receptor Agonist. *Biochemical pharmacology,* 46(5)**,** 791-6.

Devane, W., Hanus, L., Breuer, A., Pertwee, R., Stevenson, L., Griffin, G., Gibson, D., Mandelbaum, A., Etinger, A. & Mechoulam, R. 1992. Isolation and Structure of a Brain Constituent That Binds to the Cannabinoid Receptor. *Science,* 258(5090)**,** 1946-1949.

Devinsky, O., Cilio, M. R., Cross, H., Fernandez-Ruiz, J., French, J., Hill, C., Katz, R., Di Marzo, V., Jutras-Aswad, D., Notcutt, W. G., Martinez-Orgado, J., Robson, P. J., Rohrback, B. G., Thiele, E., Whalley, B. & Friedman, D. 2014. Cannabidiol: Pharmacology and Potential Therapeutic Role in Epilepsy and Other Neuropsychiatric Disorders. *Epilepsia,* 55(6)**,** 791-802.

Di Marzo, V. & Piscitelli, F. 2015. The Endocannabinoid System and Its Modulation by Phytocannabinoids. *Neurotherapeutics,* 12(4)**,** 692-698.

Diaz, J. & Laybourn-Parry, J. 2019. *Protozoan* [Online]. Encyclopædia Britannica: Encyclopædia Britannica, inc. Available: https://www.britannica.com/science/protozoan.

Dinh, T. P., Freund, T. F. & Piomelli, D. 2002. A Role for Monoglyceride Lipase in 2-Arachidonoylglycerol Inactivation. *Chemistry and Physics of Lipids.,* 121(1-2)**,** 149-58.

Dolan, J. R. 1997. Phosphorus and Ammonia Excretion by Planktonic Protists. *Marine Geology,* 139(1-4)**,** 109-122.

Dunne, D. W., Resnick, D., Greenberg, J., Krieger, M. & Joiner, K. A. 1994. The Type I Macrophage Scavenger Receptor Binds to Gram-Positive Bacteria and Recognizes Lipoteichoic Acid. *Proceedings of the National Academy of Sciences,* 91(5)**,** 1863-1867.

Dörr, T., Moynihan, P. J. & Mayer, C. 2019. Editorial: Bacterial Cell Wall Structure and Dynamics. *Frontiers in Microbiology,* 10**,** 2051.

Dürichen, H., Siegmund, L., Burmester, A., Fischer, M. S. & Wöstemeyer, J. 2016. Ingestion and Digestion Studies in *Tetrahymena pyriformis* Based on Chemically Modified Microparticles. *European Journal of Protistology,* 52(1)**,** 45-57.

Elde, N. C., Morgan, G., Winey, M., Sperling, L. & Turkewitz, A. P. 2005. Elucidation of Clathrin-Mediated Endocytosis in *Tetrahymena* Reveals an Evolutionarily Convergent Recruitment of Dynamin. *PLoS Genetics,* 1(5)**,** e52.

Elliott, A. M. & Clemmons, G. L. 1966. An Ultrastructural Study of Ingestion and Digestion in *Tetrahymena pyriformis*. *The Journal of Protozoology,* 13(2)**,** 311-323.

Elsohly, M. A., Radwan, M. M., Gul, W., Chandra, S. & Galal, A. 2017. Phytochemistry of Cannabis Sativa L. *Progress in the Chemistry of Organic Natural Products,* 103(1)**,** 1-36.

Evagorou, A., Anagnostopoulos, D., Farmaki, E. & Siafaka-Kapadai, A. 2010. Hydrolysis of 2-Arachidonoylglycerol in *Tetrahymena thermophila*. Identification and Partial Characterization of a Monoacylglycerol Lipase-Like Enzyme. *European Journal of Protistology,* 46(4)**,** 289-97.

Fawcett, D. W. & Porter, K. R. 1954. A Study of the Fine Structure of Ciliated Epithelia. *Journal of Morphology,* 94(2)**,** 221-281.

Fenchel, T. 1982. Ecology of Heterotrophic Microflagellates. Iv Quantitative Occurrence and Importance as Bacterial Consumers. *Marine Ecology Progress Series,* 9(3)**,** 35-42.

Fenchel, T. & Finlay, B. J. 2004. The Ubiquity of Small Species: Patterns of Local and Global Diversity. *BioScience,* 54(8)**,** 777-784.

Fernández-Ruiz, J., Berrendero, F., Hernández, M. L. & Ramos, J. A. 2000. The Endogenous Cannabinoid System and Brain Development. *Trends in Neurosciences,* 23(1)**,** 14-20.

Finlay, B. J. & Esteban, G. F. 1998. Freshwater Protozoa: Biodiversity and Ecological Function. *Biodiversity & Conservation,* 7(9)**,** 1163-1186.

Finlay, B. J. & Fenchel, T. 2004. Cosmopolitan Metapopulations of Free-Living Microbial Eukaryotes. *Protist,* 155(2)**,** 237-44.

Fogaça, M. V., Reis, F. M., Campos, A. C. & Guimarães, F. S. 2014. Effects of Intra-Prelimbic Prefrontal Cortex Injection of Cannabidiol on Anxiety-Like Behavior: Involvement of 5ht1a Receptors and Previous Stressful Experience. *European Neuropsychopharmacology,* 24(3)**,** 410-9.

Foissner, W. 2008. Protist Diversity and Distribution: Some Basic Considerations. *Biodiversity and Conservation,* 17(2)**,** 235-242.

Fok, A. K. & Allen, R. D. 1975. Cytochemical Localization of Peroxisomes in *Tetrahymena pyriformis*. *Journal of Histochemistry & Cytochemistry,* 23(8)**,** 599-606.

Fok, A. K., Lee, Y. & Allen, R. D. 1982. The Correlation of Digestive Vacuole Ph and Size with the Digestive Cycle in *Paramecium caudatum*. *The Journal of Protozoology,* 29(3)**,** 409-414.

Fonseca, B. M., Costa, M. A., Almada, M., Correia-Da-Silva, G. & Teixeira, N. A. 2013. Endogenous Cannabinoids Revisited: A Biochemistry Perspective. *Prostaglandins & Other Lipid Mediators* 102-103(2013)**,** 13-30.

Fredriksson, R., Höglund, P. J., Gloriam, D. E. I., Lagerström, M. C. & Schiöth, H. B. 2003. Seven Evolutionarily Conserved Human Rhodopsin G Protein-Coupled Receptors Lacking Close Relatives. *FEBS Letters,* 554(3)**,** 381-388.

Freire-Garabal, M., Núñez, M. J., Balboa, J., López-Delgado, P., Gallego, R., García-Caballero, T., Fernández-Roel, M. D., Brenlla, J. & Rey-Méndez, M. 2003. Serotonin Upregulates the Activity of Phagocytosis through 5-Ht 1a Receptors. *The British Journal of Pharmacology,* 139(2)**,** 457-463.

Freymond, P.-P., Lazarevic, V., Soldo, B. & Karamata, D. 2006. Poly(Glucosyl-N-Acetylgalactosamine 1-Phosphate), a Wall Teichoic Acid of *Bacillus subtilis* 168: Its Biosynthetic Pathway and Mode of Attachment to Peptidoglycan. *Microbiology,* 152(6)**,** 1709-1718.

Fu, J., Gaetani, S., Oveisi, F., Lo Verme, J., Serrano, A., Rodríguez De Fonseca, F., Rosengarth, A., Luecke, H., Di Giacomo, B., Tarzia, G. & Piomelli, D. 2003. Oleylethanolamide Regulates

Feeding and Body Weight through Activation of the Nuclear Receptor Ppar-A. *Nature,* 425(6953)**,** 90-93.

Fujii, M., Sato, Y., Ito, H., Masago, Y. & Omura, T. 2012. Monosaccharide Composition of the Outer Membrane Lipopolysaccharide and O-Chain from the Freshwater Cyanobacterium *Microcystis aeruginosa* Nies-87. *Journal of Applied Microbiology,* 113(4)**,** 896-903.

Funfak, A., Fisch, C., Abdel Motaal, H. T., Diener, J., Combettes, L., Baroud, C. N. & Dupuis-Williams, P. 2015. *Paramecium* Swimming and Ciliary Beating Patterns: A Study on Four Rna Interference Mutations. *Integrative Biology,* 7(1)**,** 90-100.

Gantz, I., Muraoka, A., Yang, Y.-K., Samuelson, L. C., Zimmerman, E. M., Cook, H. & Yamada, T. 1997. Cloning and Chromosomal Localization of a Gene (Gpr18) Encoding a Novel Seven Transmembrane Receptor Highly Expressed in Spleen and Testis. *Genomics,* 42(3)**,** 462-466.

Gaoni, Y. & Mechoulam, R. 1964. Isolation, Structure, and Partial Synthesis of an Active Constituent of Hashish. *Journal of the American Chemical Society,* 86(8)**,** 1646-1647.

Geisen, S., Mitchell, E. A. D., Adl, S., Bonkowski, M., Dunthorn, M., Ekelund, F., Fernández, L. D., Jousset, A., Krashevska, V., Singer, D., Spiegel, F. W., Walochnik, J. & Lara, E. 2018. Soil Protists: A Fertile Frontier in Soil Biology Research. *FEMS Microbiology Reviews,* 42(3)**,** 293-323.

Gerdeman, G. L., Ronesi, J. & Lovinger, D. M. 2002. Postsynaptic Endocannabinoid Release Is Critical to Long-Term Depression in the Striatum. *Nature Neuroscience,* 5(5)**,** 446-451.

Giang, D. K. & Cravatt, B. F. 1997. Molecular Characterization of Human and Mouse Fatty Acid Amide Hydrolases. *Proceedings of the National Academy of Sciences of the United States of America,* 94(6)**,** 2238-2242.

Gibbons, I. R. 1963. Studies on the Protein Components of Cilia from *Tetrahymena pyriformis*. *Proceedings of the National Academy of Sciences of the United States of America,* 50(5)**,** 1002-1010.

Goff, L. J. & Stein, J. R. 1981. Digestion in the Peritrich Ciliateophrydium Versatile. *Protoplasma,* 107(3-4)**,** 235-254.

Goldman, M. E., Gundersen, R. E., Erickson, C. K. & Thompson, G. A., Jr. 1981. High Performance Liquid Chromatographic Analysis of Catecholamines in Growing and Non-Growing *Tetrahymena pyriformis*. *Biochim Biophys Acta,* 676(2)**,** 221-5.

Golowczyc, M. A., Mobili, P., Garrote, G. L., De Los Angeles Serradell, M., Abraham, A. G. & De Antoni, G. L. 2009. Interaction between *Lactobacillus kefir* and *Saccharomyces lipolytica* Isolated from Kefir Grains: Evidence for Lectin-Like Activity of Bacterial Surface Proteins. *Journal of Diary Research,* 76(1)**,** 111-6.

Gonca, E. & Darıcı, F. 2015. The Effect of Cannabidiol on Ischemia/Reperfusion-Induced Ventricular Arrhythmias. *Journal of Cardiovascular Pharmacology and Therapeutics,* 20(1)**,** 76-83.

Gonda, K., Komatsu, M. & Numata, O. 2000. Calmodulin and Ca2+/Calmodulin-Binding Proteins Are Involved in *Tetrahymena thermophila* Phagocytosis. *Cell Structure and Function,* 25(4)**,** 243-251.

Gong, J.-P., Onaivi, E. S., Ishiguro, H., Liu, Q.-R., Tagliaferro, P. A., Brusco, A. & Uhl, G. R. 2006. Cannabinoid Cb2 Receptors: Immunohistochemical Localization in Rat Brain. *Brain Research,* 1071(1)**,** 10-23.

Goparaju, S. K., Ueda, N., Yamaguchi, H. & Yamamoto, S. 1998. Anandamide Amidohydrolase Reacting with 2-Arachidonoylglycerol, Another Cannabinoid Receptor Ligand. *FEBS Letters,* 422(1)**,** 69-73.

Graham, E. S., Angel, C. E., Schwarcz, L. E., Dunbar, P. R. & Glass, M. 2010. Detailed Characterisation of Cb2 Receptor Protein Expression in Peripheral Blood Immune Cells from Healthy Human Volunteers Using Flow Cytometry. *International Journal of Immunopathology and Pharmacology,* 23(1)**,** 25-34.

Grønlien, H. K., Berg, T. & Løvlie, A. M. 2002. In the Polymorphic Ciliate *Tetrahymena vorax*, the Non-Selective Phagocytosis Seen in Microstomes Changes to a Highly Selective Process in Macrostomes. *Journal of Experimental Biology,* 205(14)**,** 2089.

Guerrier, S., Plattner, H., Richardson, E., Dacks, J. B. & Turkewitz, A. P. 2017. An Evolutionary Balance: Conservation Vs Innovation in Ciliate Membrane Trafficking. *Traffic,* 18(1)**,** 18-28.

Gugliandolo, A., Pollastro, F., Bramanti, P. & Mazzon, E. 2020. Cannabidiol Exerts Protective Effects in an in Vitro Model of Parkinson's Disease Activating Akt/Mtor Pathway. *Fitoterapia,* 143**,** 104553.

Gundersen, R. E. & Thompson, G. A., Jr. 1985. Further Studies of Dopamine Metabolism and Function in *Tetrahymena*. *The Journal of Protozoology,* 32(1)**,** 25-31.

Guzmán, M., Lo Verme, J., Fu, J., Oveisi, F., Blázquez, C. & Piomelli, D. 2004. Oleoylethanolamide Stimulates Lipolysis by Activating the Nuclear Receptor Peroxisome Proliferator-Activated Receptor A (Ppar-A). *Journal of Biological Chemistry,* 279(27)**,** 27849-27854.

Gérard, C. M., Mollereau, C., Vassart, G. & Parmentier, M. 1991. Molecular Cloning of a Human Cannabinoid Receptor Which Is Also Expressed in Testis. *Biochemical Journal,* 279(1)**,** 129-134.

Gómez-Ruiz, M., Hernández, M., De Miguel, R. & Ramos, J. A. 2007. An Overview on the Biochemistry of the Cannabinoid System. *Molecular Neurobiology,* 36(1)**,** 3-14.

Hampton, R. Y., Golenbock, D. T., Penman, M., Krieger, M. & Raetz, C. R. H. 1991. Recognition and Plasma Clearance of Endotoxin by Scavenger Receptors. *Nature,* 352(6333)**,** 342-344.

Haskó, G., Pacher, P., Deitch, E. A. & Vizi, E. S. 2007. Shaping of Monocyte and Macrophage Function by Adenosine Receptors. *Pharmacology & Therapeutics,* 113(2)**,** 264-275.

Herkenham, M., Lynn, A. B., Little, M. D., Johnson, M. R., Melvin, L. S., De Costa, B. R. & Rice, K. C. 1990. Cannabinoid Receptor Localization in Brain. *Proceedings of the National Academy of Sciences,* 87(5)**,** 1932-1936.

Hillard, C. J., Wilkison, D. M., Edgemond, W. S. & Campbell, W. B. 1995. Characterization of the Kinetics and Distribution of N-Arachidonylethanolamine (Anandamide) Hydrolysis by Rat Brain. *Biochimica et Biophysica Acta (BBA) - Lipids and Lipid Metabolism,* 1257(3)**,** 249-256.

Hoebe, K., Georgel, P., Rutschmann, S., Du, X., Mudd, S., Crozat, K., Sovath, S., Shamel, L., Hartung, T., Zähringer, U. & Beutler, B. 2005. Cd36 Is a Sensor of Diacylglycerides. *Nature,* 433(7025)**,** 523-527.

Hoiczyk, E. & Hansel, A. 2000. Cyanobacterial Cell Walls: News from an Unusual Prokaryotic Envelope. *Journal of Bacteriology,* 182(5)**,** 1191-1199.

Hosein, R. E., Williams, S. A. & Gavin, R. H. 2005. Directed Motility of Phagosomes in *Tetrahymena thermophila* Requires Actin and Myo1p, a Novel Unconventional Myosin. *Cell Motility and the Cytoskeleton,* 61(1)**,** 49-60.

Howlett, A. C., Blume, L. C. & Dalton, G. D. 2010. Cb(1) Cannabinoid Receptors and Their Associated Proteins. *Current Medicinal Chemistry,* 17(14)**,** 1382-93.

Howlett, A. C., Johnson, M. R., Melvin, L. S. & Milne, G. M. 1988. Nonclassical Cannabinoid Analgetics Inhibit Adenylate Cyclase: Development of a Cannabinoid Receptor Model. *Molecular Pharmacology,* 33(3)**,** 297-302.

Howlett, A. C., Qualy, J. M. & Khachatrian, L. L. 1986. Involvement of Gi in the Inhibition of Adenylate Cyclase by Cannabimimetic Drugs. *Molecular Pharmacology* 29(3)**,** 307-13.

Huestis, M. A. 2007. Human Cannabinoid Pharmacokinetics. *Chemistry & Biodiversity,* 4(8)**,** 1770-1804.

Hwang, Y. S., Kim, Y. J., Kim, M. O., Kang, M., Oh, S. W., Nho, Y. H., Park, S. H. & Lee, J. 2017. Cannabidiol Upregulates Melanogenesis through Cb1 Dependent Pathway by Activating P38 Mapk and P42/44 Mapk. *Chemico-Biological Interactions,* 273**,** 107-114.

Iannotti, F. A., Di Marzo, V. & Petrosino, S. 2016. Endocannabinoids and Endocannabinoid-Related Mediators: Targets, Metabolism and Role in Neurological Disorders. *Progress in Lipid Research,* 62**,** 107-128.

Iffland, K. & Grotenhermen, F. 2017. An Update on Safety and Side Effects of Cannabidiol: A Review of Clinical Data and Relevant Animal Studies. *Cannabis and Cannabinoid Research,* 2(1)**,** 139-154.

Issemann, I. & Green, S. 1990. Activation of a Member of the Steroid Hormone Receptor Superfamily by Peroxisome Proliferators. *Nature,* 347(6294)**,** 645-650.

Jacobs, M. E., Desouza, L. V., Samaranayake, H., Pearlman, R. E., Siu, K. W. M. & Klobutcher, L. A. 2006. The *Tetrahymena thermophila* Phagosome Proteome. *Eukaryotic Cell,* 5(12)**,** 1990-2000.

Jaisswar, C. 2020. Study of the Effects of the Cannabinoids Anandamide and Cannabidiol on the Feeding Processes of *Tetrahymena pyriformis.* Mres Thesis. Lancaster University.

Jang, J.-H., Shin, H. W., Lee, J. M., Lee, H.-W., Kim, E.-C. & Park, S. H. 2015. An Overview of Pathogen Recognition Receptors for Innate Immunity in Dental Pulp. *Mediators of inflammation,* 2015**,** 794143-794143.

Jensen, E. C. 2013. Overview of Live-Cell Imaging: Requirements and Methods Used. *The Anatomical Record: Advances in Integrative Anatomy and Evolutionary Biology,* 296(1)**,** 1-8.

Jiang, R., Yamaori, S., Takeda, S., Yamamoto, I. & Watanabe, K. 2011. Identification of Cytochrome P450 Enzymes Responsible for Metabolism of Cannabidiol by Human Liver Microsomes. *Life Sciences,* 89(5-6)**,** 165-170.

Kano, M. 2014. Control of Synaptic Function by Endocannabinoid-Mediated Retrograde Signaling. *Proceedings of the Japan Academy, Series B,* 90(7)**,** 235-250.

Karava, V., Fasia, L. & Siafaka-Kapadai, A. 2001. Anandamide Amidohydrolase Activity, Released in the Medium by *Tetrahymena pyriformis*. Identification and Partial Characterization. *FEBS Letters,* 508(3)**,** 327-31.

Karava, V., Zafiriou, P. M., Fasia, L., Anagnostopoulos, D., Boutou, E., Vorgias, C. E., Maccarrone, M. & Siafaka-Kapadai, A. 2005. Anandamide Metabolism by *Tetrahymena pyriformis* in Vitro. Characterization and Identification of a 66 Kda Fatty Acid Amidohydrolase. *Biochimie,* 87(11)**,** 967-74.

Kathmann, M., Flau, K., Redmer, A., Tränkle, C. & Schlicker, E. 2006. Cannabidiol Is an Allosteric Modulator at Mu- and Delta-Opioid Receptors. *Naunyn-Schmiedeberg's Archives of Pharmacology,* 372(5)**,** 354-361.

Katz, A., Weckesser, J., Drews, G. & Mayer, H. 1977. Chemical and Biological Studies on the Lipopolysaccharide (O-Antigen) of *Anacystis Nidulans*. *Archives of Microbiology,* 113(3)**,** 247-256.

Kawamoto, K., Otsuguro, K., Ishizuka, M. & Ito, S. 2012. Inhibitory Effects of Dopamine on Spinal Synaptic Transmission Via Dopamine D1-Like Receptors in Neonatal Rats. *British Journal of Pharmacology,* 166(2)**,** 788-800.

Kersken, H., Momayezi, M., Braun, C. & Plattner, H. 1986. Filamentous Actin in *Paramecium* Cells: Functional and Structural Changes Correlated with Phalloidin Affinity Labeling in Vivo. *Journal of Histochemistry and Cytochemistry,* 34(4)**,** 455-65.

Kirchman, D. L. 1994. The Uptake of Inorganic Nutrients by Heterotrophic Bacteria. *Microbial Ecology,* 28(2)**,** 255-271.

Kleberg, K., Hassing, H. A. & Hansen, H. S. 2014. Classical Endocannabinoid-Like Compounds and Their Regulation by Nutrients. *BioFactors,* 40(4)**,** 363-372.

Klena, J., Zhang, P., Schwartz, O., Hull, S. & Chen, T. 2005. The Core Lipopolysaccharide of *Escherichia coli* Is a Ligand for the Dendritic-Cell-Specific Intercellular Adhesion Molecule Nonintegrin Cd209 Receptor. *Journal of Bacteriology,* 187(5)**,** 1710-1715.

Kliewer, S. A., Forman, B. M., Blumberg, B., Ong, E. S., Borgmeyer, U., Mangelsdorf, D. J., Umesono, K. & Evans, R. M. 1994. Differential Expression and Activation of a Family of Murine Peroxisome Proliferator-Activated Receptors. *Proceedings of the National Academy of Sciences,* 91(15)**,** 7355-7359.

Kohno, M., Hasegawa, H., Inoue, A., Muraoka, M., Miyazaki, T., Oka, K. & Yasukawa, M. 2006. Identification of N-Arachidonylglycine as the Endogenous Ligand for Orphan G-Protein-Coupled Receptor Gpr18. *Biochemical and Biophysical Research Communications,* 347(3)**,** 827-832.

Kojima, K., Konopleva, M., Samudio, I. J., Ruvolo, V. & Andreeff, M. 2007. Mitogen-Activated Protein Kinase Kinase Inhibition Enhances Nuclear Proapoptotic Function of P53 in Acute Myelogenous Leukemia Cells. *Cancer Research,* 67(7)**,** 3210-3219.

Kozak, K. R., Crews, B. C., Morrow, J. D., Wang, L.-H., Ma, Y. H., Weinander, R., Jakobsson, P.-J. & Marnett, L. J. 2002. Metabolism of the Endocannabinoids, 2-Arachidonylglycerol and Anandamide, into Prostaglandin, Thromboxane, and Prostacyclin Glycerol Esters and Ethanolamides. *Journal of Biological Chemistry,* 277(47)**,** 44877-44885.

Kozak, K. R., Rowlinson, S. W. & Marnett, L. J. 2000. Oxygenation of the Endocannabinoid, 2-Arachidonylglycerol, to Glyceryl Prostaglandins by Cyclooxygenase-2. *Journal of Biological Chemistry,* 275(43)**,** 33744-33749.

Kreitzer, A. C. & Regehr, W. G. 2001. Retrograde Inhibition of Presynaptic Calcium Influx by Endogenous Cannabinoids at Excitatory Synapses onto Purkinje Cells. *Neuron,* 29(3)**,** 717-727.

Kuribara, S., Kato, M., Kato-Minoura, T. & Numata, O. 2006. Identification of a Novel Actin-Related Protein In *Tetrahymena* Cilia. *Cell Motility and the Cytoskeleton,* 63(7)**,** 437-446.

Lampert, T. J., Coleman, K. D. & Hennessey, T. M. 2011. A Knockout Mutation of a Constitutive Gpcr in *Tetrahymena* Decreases Both G-Protein Activity and Chemoattraction. *PLoS ONE,* 6(11)**,** e28022.

Lane, J. R., Beukers, M. W., Mulder-Krieger, T. & Ijzerman, A. P. 2010. The Endocannabinoid 2-Arachidonylglycerol Is a Negative Allosteric Modulator of the Human A3 Adenosine Receptor. *Biochemical Pharmacology,* 79(1)**,** 48-56.

Laprairie, R. B., Bagher, A. M., Kelly, M. E. M. & Denovan-Wright, E. M. 2015. Cannabidiol Is a Negative Allosteric Modulator of the Cannabinoid Cb1 Receptor. *British Journal of Pharmacology,* 172(20)**,** 4790-4805.

Lastres-Becker, I., Molina-Holgado, F., Ramos, J. A., Mechoulam, R. & Fernández-Ruiz, J. 2005. Cannabinoids Provide Neuroprotection against 6-Hydroxydopamine Toxicity in Vivo and in Vitro: Relevance to Parkinson's Disease. *Neurobiology of Disease,* 19(1)**,** 96-107.

Lauckner, J. E., Jensen, J. B., Chen, H. Y., Lu, H. C., Hille, B. & Mackie, K. 2008. Gpr55 Is a Cannabinoid Receptor That Increases Intracellular Calcium and Inhibits M Current. *Proceedings of the National Academy of Sciences,* 105(7)**,** 2699-2704.

Laun, A. S., Shrader, S. H., Brown, K. J. & Song, Z.-H. 2019. Gpr3, Gpr6, and Gpr12 as Novel Molecular Targets: Their Biological Functions and Interaction with Cannabidiol. *Acta Pharmacologica Sinica,* 40(3)**,** 300-308.

Lee, H.-J., Woo, Y., Hahn, T.-W., Jung, Y. M. & Jung, Y.-J. 2020. Formation and Maturation of the Phagosome: A Key Mechanism in Innate Immunity against Intracellular Bacterial Infection. *Microorganisms,* 8(9)**,** 1298.

Lee, J. E. & Gleeson, J. G. 2011. A Systems-Biology Approach to Understanding the Ciliopathy Disorders. *Genome Medicine,* 3(9)**,** 59.

Levin, R., Grinstein, S. & Canton, J. 2016. The Life Cycle of Phagosomes: Formation, Maturation, and Resolution. *Immunological Reviews,* 273(1)**,** 156-179.

Li, S., Song, J.-H., Kim, T. I., Yoo, W. G., Won, M.-H., Dai, F. & Hong, S.-J. 2019. Chemotactic Migration of Newly Excysted Juvenile Clonorchis Sinensis Is Suppressed by Neuro-Antagonists. *PLOS Neglected Tropical Diseases,* 13(8)**,** e0007573.

Li, W., Zhang, S., Numata, O., Nozawa, Y. & Wang, S. 2009. Tpmrk Regulates Cell Division of *Tetrahymena* in Response to Oxidative Stress. *Cell Biochemistry and Function,* 27(6)**,** 364-9.

Liu, B., Knirel, Y. A., Feng, L., Perepelov, A. V., Senchenkova, S. Y. N., Reeves, P. R. & Wang, L. 2014a. Structural Diversity in *Salmonella* O Antigens and Its Genetic Basis. *FEMS Microbiology Reviews,* 38(1)**,** 56-89.

Liu, J., Wang, L., Harvey-White, J., Osei-Hyiaman, D., Razdan, R., Gong, Q., Chan, A. C., Zhou, Z., Huang, B. X., Kim, H. Y. & Kunos, G. 2006. A Biosynthetic Pathway for Anandamide. *Proceedings of the National Academy of Sciences of the United States of America,* 103(36)**,** 13345-50.

Liu, X.-W., Ji, E.-F., He, P., Xing, R.-X., Tian, B.-X. & Li, X.-D. 2014b. Protective Effects of the P38 Mapk Inhibitor Sb203580 on Nmda-Induced Injury in Primary Cerebral Cortical Neurons. *Molecular Medicine Reports,* 10(4)**,** 1942-1948.

Lodh, S., Yano, J., Valentine, M. S. & Van Houten, J. L. 2016. Voltage-Gated Calcium Channels of *Paramecium* Cilia. *Journal of Experimental Biology,* 219(19)**,** 3028-3038.

Lu, H. C. & Mackie, K. 2016. An Introduction to the Endogenous Cannabinoid System. *Biological Psychiatry,* 79(7)**,** 516-25.

Lutz, B. 2004. On-Demand Activation of the Endocannabinoid System in the Control of Neuronal Excitability and Epileptiform Seizures. *Biochemical pharmacology,* 68(1)**,** 1691-8.

Ma, L., Rohatgi, R. & Kirschner, M. W. 1998. The Arp2/3 Complex Mediates Actin Polymerization Induced by the Small Gtp-Binding Protein Cdc42. *Proceedings of the National Academy of Sciences,* 95(26)**,** 15362-15367.

Maccarrone, M., Bab, I., Bíró, T., Cabral, G. A., Dey, S. K., Di Marzo, V., Konje, J. C., Kunos, G., Mechoulam, R., Pacher, P., Sharkey, K. A. & Zimmer, A. 2015. Endocannabinoid Signaling at the Periphery: 50 Years after Thc. *Trends in Pharmacological Sciences,* 36(5)**,** 277-296.

Macek, M., Carlos, G., Memije, P. & Ramírez, P. 1997. Ciliate-*Vibrio cholerae* Interactions within a Microbial Loop: An Experimental Study. *Aquatic Microbial Ecology,* 13(2)**,** 257-266.

Maeda, N., Nigou, J., Herrmann, J.-L., Jackson, M., Amara, A., Lagrange, P. H., Puzo, G., Gicquel, B. & Neyrolles, O. 2003. The Cell Surface Receptor Dc-Sign Discriminates between *Mycobacterium* Species through Selective Recognition of the Mannose Caps on Lipoarabinomannan. *Journal of Biological Chemistry,* 278(8)**,** 5513-5516.

Man-Kupisinska, A., Swierzko, A. S., Maciejewska, A., Hoc, M., Rozalski, A., Siwinska, M., Lugowski, C., Cedzynski, M. & Lukasiewicz, J. 2018. Interaction of Mannose-Binding Lectin with Lipopolysaccharide Outer Core Region and Its Biological Consequences. *Frontiers in Immunology,* 9.

Manikandan, P. & Nagini, S. 2018. Cytochrome P450 Structure, Function and Clinical Significance: A Review. *Current Drug Targets,* 19(1)**,** 38-54.

Marie-Anaïs, F., Mazzolini, J., Herit, F. & Niedergang, F. 2016. Dynamin-Actin Cross Talk Contributes to Phagosome Formation and Closure. *Traffic,* 17(5)**,** 487-499.

Marino, M. J., Sherman, T. G. & Wood, D. C. 2001. Partial Cloning of Putative G-Proteins Modulating Mechanotransduction in the Ciliate Stentor. *The Journal of Eukaryotic Microbiology,* 48(5)**,** 527-536.

Masson, J., Emerit, M. B., Hamon, M. & Darmon, M. 2012. Serotonergic Signaling: Multiple Effectors and Pleiotropic Effects. *Wiley Interdisciplinary Reviews: Membrane Transport and Signaling,* 1(6)**,** 685-713.

Matias, I., Bisogno, T., Melck, D., Vandenbulcke, F., Verger-Bocquet, M., De Petrocellis, L., Sergheraert, C., Breton, C., Di Marzo, V. & Salzet, M. 2001. Evidence for an Endocannabinoid System in the Central Nervous System of the Leech *Hirudo Medicinalis*. *Molecular Brain Research,* 87(2)**,** 145-159.

Mccarren, J. & Brahamsha, B. 2009. Swimming Motility Mutants of Marine *Synechococcus* Affected in Production and Localization of the S-Layer Protein Swma. *Journal of Bacteriology,* 191(3)**,** 1111-1114.

Mcclean, D. K. & Zimmerman, A. M. 1976. Action of Delta 9-Tetrahydrocannabinol on Cell Division and Macromolecular Synthesis in Division-Synchronized Protozoa. *Pharmacology,* 14(4)**,** 307-21.

Mchugh, D., Hu, S. S., Rimmerman, N., Juknat, A., Vogel, Z., Walker, J. M. & Bradshaw, H. B. 2010. N-Arachidonoyl Glycine, an Abundant Endogenous Lipid, Potently Drives Directed Cellular Migration through Gpr18, the Putative Abnormal Cannabidiol Receptor. *BMC Neuroscience,* 11(1)**,** 44.

Mcpartland, J. M., Matias, I., Di Marzo, V. & Glass, M. 2006. Evolutionary Origins of the Endocannabinoid System. *Gene,* 370(1)**,** 64-74.

Mecha, M., Feliú, A., Iñigo, P. M., Mestre, L., Carrillo-Salinas, F. J. & Guaza, C. 2013. Cannabidiol Provides Long-Lasting Protection against the Deleterious Effects of Inflammation in a Viral Model of Multiple Sclerosis: A Role for A2a Receptors. *Neurobiology of Disease,* 59**,** 141-150.

Meyer, M., Mayer, T. & Tiedtke, A. 1998. Maturation of Phagosomes Is Accompanied by Specific Patterns of Small Gtpases. *Electrophoresis* 19(14)**,** 2528-2535.

Michael, F., Szymanski, C. M., Li, J., Chan, K. H., Khieu, N. H., Larocque, S., Wakarchuk, W. W., Brisson, J. R. & Monteiro, M. A. 2002. The Structures of the Lipooligosaccharide and Capsule

Polysaccharide of *Campylobacter jejuni* Genome Sequenced Strain Nctc 11168. *European Journal of Biochemistry,* 269(21)**,** 5119-36.

Minakami, R. & Sumimotoa, H. 2006. Phagocytosis-Coupled Activation of the Superoxide-Producing Phagocyte Oxidase, a Member of the Nadph Oxidase (Nox) Family. *International Journal of Hematology,* 84(3)**,** 193-198.

Mishra, A., Singh, S. & Shukla, S. 2018. Physiological and Functional Basis of Dopamine Receptors and Their Role in Neurogenesis: Possible Implication for Parkinson's Disease. *Journal of Experimental Neuroscience,* 12(1)**,** 117906951877982.

Miyamoto, A., Yamamoto, T., Ohno, M., Watanabe, S., Tanaka, H., Morimoto, S. & Shoyama, Y. 1996. Roles of Dopamine D1 Receptors Inδ9-Tetrahydrocannabinol-Induced Expression of Fos Protein in the Rat Brain. *Brain Research,* 710(1-2)**,** 234-240.

Montagnes, D., Barbosa, A., Boenigk, J., Davidson, K., Jürgens, K., Macek, M., Parry, J., Roberts, E. & Imek, K. 2008. Selective Feeding Behaviour of Key Free-Living Protists: Avenues for Continued Study. *Aquatic Microbial Ecology,* 53(1)**,** 83-98.

Morales, P., Isawi, I. & Reggio, P. H. 2018. Towards a Better Understanding of the Cannabinoid-Related Orphan Receptors Gpr3, Gpr6, and Gpr12. *Drug Metabolism Reviews,* 50(1)**,** 74-93.

Mouhamed, Y., Vishnyakov, A., Qorri, B., Sambi, M., Frank, S. S., Nowierski, C., Lamba, A., Bhatti, U. & Szewczuk, M. R. 2018. Therapeutic Potential of Medicinal Marijuana: An Educational Primer for Health Care Professionals. *Drug , Healthcare and Patient Safety,* 10(1)**,** 45-66.

Moya, C. E. & Jacobs, R. S. 2006. Pseudopterosin a Inhibits Phagocytosis and Alters Intracellular Calcium Turnover in a Pertussis Toxin Sensitive Site in *Tetrahymena thermophila*. *Comparative Biochemistry and Physiology Part C: Toxicology & Pharmacology,* 143(4)**,** 436-443.

Muccioli, G. G. 2010. Endocannabinoid Biosynthesis and Inactivation, from Simple to Complex. *Drug Discovery Today,* 15(11-12)**,** 474-483.

Muller, C., Morales, P. & Reggio, P. H. 2019. Cannabinoid Ligands Targeting Trp Channels. *Frontiers in Molecular Neuroscience,* 11**,** 487.

Munro, S., Thomas, K. L. & Abu-Shaar, M. 1993. Molecular Characterization of a Peripheral Receptor for Cannabinoids. *Nature,* 365(6441)**,** 61-65.

Méténier, G. 1984. Actin in *Tetrahymena paravorax*: Ultrastructural Localization of Hmm-Binding Filaments in Glycerinated Cells. *The Journal of Protozoology,* 31(2)**,** 205-215.

Nakashima, S., Wang, S., Hisamoto, N., Sakai, H., Andoh, M., Matsumoto, K. & Nozawa, Y. 1999. Molecular Cloning and Expression of a Stress-Responsive Mitogen-Activated Protein Kinase-Related Kinase from *Tetrahymena* Cells. *Journal of Biological Chemistry,* 274(15)**,** 9976-9983.

Nilsson, J. R. 1977. Fine Structure and Rna Synthesis of *Tetrahymena* During Cytochalasin B Inhibition of Phagocytosis. *Journal of Cell Science,* 27(1)**,** 115.

Nilsson, J. R., Ricketts, T. R. & Zeuthen, E. 1973. Effects of Cytochalasin B on Cell Division and Vacuole Formation in *Tetrahymena pyriformis* Gl. *Experimental Cell Research,* 79(2)**,** 456-459.

Nunes, P., Demaurex, N. & Dinauer, M. C. 2013. Regulation of the Nadph Oxidase and Associated Ion Fluxes During Phagocytosis. *Traffic,* 14(11)**,** 1118-1131.

Nygaard, K., Børsheim, K. Y. & Thingstad, T. F. 1988. Grazing Rates on Bacteria by Marine Heterotrophic Microflagellates Compared to Uptake Rates of Bacterial-Sized Monodisperse Fluorescent Latex Beads. *Marine Ecology Progress Series,* 44(2)**,** 159-165.

O'neill, J. B., Pert, C. B., Ruff, M. R., Smith, C. C., Higgins, W. J. & Zipser, B. 1988. Identification and Characterization of the Opiate Receptor in the Ciliated Protozoan, Tetrahymena. *Brain Research,* 450(1)**,** 303-315.

O'sullivan, S. E. 2016. An Update on PPAR Activation by Cannabinoids. *British Journal of Pharmacology,* 173(12)**,** 1899-1910.

O'sullivan, S. E. & Kendall, D. A. 2010. Cannabinoid Activation of Peroxisome Proliferator-Activated Receptors: Potential for Modulation of Inflammatory Disease. *Immunobiology,* 215(8)**,** 611-616.

O'sullivan, S. E., Sun, Y., Bennett, A. J., Randall, M. D. & Kendall, D. A. 2009. Time-Dependent Vascular Actions of Cannabidiol in the Rat Aorta. *European Journal of Pharmacology,* 612(1-3)**,** 61-68.

Oka, S., Nakajima, K., Yamashita, A., Kishimoto, S. & Sugiura, T. 2007. Identification of Gpr55 as a Lysophosphatidylinositol Receptor. *Biochemical and Biophysical Research Communications,* 362(4)**,** 928-934.

Olonisakin, T. F., Li, H., Xiong, Z., Kochman, E. J., Yu, M., Qu, Y., Hulver, M., Kolls, J. K., St Croix, C., Doi, Y., Nguyen, M. H., Shanks, R. M., Mallampalli, R. K., Kagan, V. E., Ray, A., Silverstein, R. L., Ray, P. & Lee, J. S. 2016. Cd36 Provides Host Protection against *Klebsiella pneumoniae* Intrapulmonary Infection by Enhancing Lipopolysaccharide Responsiveness and Macrophage Phagocytosis. *Journal of Infectious Diseases,* 214(12)**,** 1865-1875.

Ondarza, J., Symington, S. B., Houten, J. L. & Clark, J. M. 2003. G-Protein Modulators Alter the Swimming Behavior and Calcium Influx of *Paramecium tetraurelia*. *The Journal of Eukaryotic Microbiology,* 50(5)**,** 349-355.

Ong, Q., Guo, S., Zhang, K. & Cui, B. 2015. U0126 Protects Cells against Oxidative Stress Independent of Its Function as a Mek Inhibitor. *ACS Chemical Neuroscience,* 6(1)**,** 130-137.

Overton, H. A., Babbs, A. J., Doel, S. M., Fyfe, M. C. T., Gardner, L. S., Griffin, G., Jackson, H. C., Procter, M. J., Rasamison, C. M., Tang-Christensen, M., Widdowson, P. S., Williams, G. M. & Reynet, C. 2006. Deorphanization of a G Protein-Coupled Receptor for Oleoylethanolamide and Its Use in the Discovery of Small-Molecule Hypophagic Agents. *Cell Metabolism,* 3(3)**,** 167-175.

O'sullivan, S. E., Tarling, E. J., Bennett, A. J., Kendall, D. A. & Randall, M. D. 2005. Novel Time-Dependent Vascular Actions of Δ9-Tetrahydrocannabinol Mediated by Peroxisome Proliferator-Activated Receptor Gamma. *Biochemical and Biophysical Research Communications,* 337(3)**,** 824-831.

Pacher, P., Bátkai, S. & Kunos, G. 2006. The Endocannabinoid System as an Emerging Target of Pharmacotherapy. *Pharmacol Rev,* 58(3)**,** 389-462.

Pacher, P., Kogan, N. M. & Mechoulam, R. 2020. Beyond Thc and Endocannabinoids. *Annual Review of Pharmacology and Toxicology,* 60(1)**,** 637-659.

Pacher, P. & Kunos, G. 2013. Modulating the Endocannabinoid System in Human Health and Disease - Successes and Failures. *FEBS Journal,* 280(9)**,** 1918-1943.

Padilla-Vaca, F., Ankri, S., Bracha, R., Koole, L. A. & Mirelman, D. 1999. Down Regulation of *Entamoeba histolytica* Virulence by Monoxenic Cultivation with *Escherichia coli* O55 Is Related to a Decrease in Expression of the Light (35-Kilodalton) Subunit of the Gal/Galnac Lectin. *Infection and Immunity,* 67(5)**,** 2096-2102.

Pagano, S., Coniglio, M., Valenti, C., Federici, M. I., Lombardo, G., Cianetti, S. & Marinucci, L. 2020. Biological Effects of Cannabidiol on Normal Human Healthy Cell Populations: Systematic Review of the Literature. *Biomedicine & Pharmacotherapy,* 132**,** 110728.

Parry, J. D., Heaton, K., Drinkall, J. & Jones, H. L. 2001. Feasibility of Using Gfp-Expressing *Escherichia col*i, Coupled with Fluorimetry, to Determine Protozoan Ingestion Rates. *FEMS Microbiology Ecology,* 35(1)**,** 11-17.

Parsons, S. 2021. The Role of Scavenger Receptors In Ciliate Phagocytosis. Bsc Research Dissertation. Lancaster University.

Pauwels, A.-M., Trost, M., Beyaert, R. & Hoffmann, E. 2017. Patterns, Receptors, and Signals: Regulation of Phagosome Maturation. *Trends in Immunology,* 38(6)**,** 407-422.

Pazos, M. R., Mohammed, N., Lafuente, H., Santos, M., Martínez-Pinilla, E., Moreno, E., Valdizan, E., Romero, J., Pazos, A., Franco, R., Hillard, C. J., Alvarez, F. J. & Martínez-Orgado, J. 2013. Mechanisms of Cannabidiol Neuroprotection in Hypoxic–Ischemic Newborn Pigs: Role of 5ht1a and Cb2 Receptors. *Neuropharmacology,* 71(1)**,** 282-291.

Peiser, L., De Winther, M. P. J., Makepeace, K., Hollinshead, M., Coull, P., Plested, J., Kodama, T., Moxon, E. R. & Gordon, S. 2002. The Class a Macrophage Scavenger Receptor Is a Major Pattern Recognition Receptor for *Neisseria meningitidis* Which Is Independent of Lipopolysaccharide and Not Required for Secretory Responses. *Infection and Immunity,* 70(10)**,** 5346-5354.

Peiser, L., Makepeace, K., PlüDdemann, A., Savino, S., Wright, J. C., Pizza, M., Rappuoli, R., Moxon, E. R. & Gordon, S. 2006. Identification of Neisseria Meningitidis Nonlipopolysaccharide Ligands for Class a Macrophage Scavenger Receptor by Using a Novel Assay. *Infection and Immunity,* 74(9)**,** 5191-5199.

Pernthaler, J. 2005. Predation on Prokaryotes in the Water Column and Its Ecological Implications. *Nature Reviews Microbiology,* 3(7)**,** 537-546.

Pernthaler, J., Šimek, K., Sattler, B., Schwarzenbacher, A., Bobkova, J. & Psenner, R. 1996. Short-Term Changes of Protozoan Control on Autotrophic Picoplankton in an Oligo-Mesotrophic Lake. *Journal of Plankton Research,* 18(3)**,** 443-462.

Pertwee, R. G., Howlett, A. C., Abood, M. E., Alexander, S. P. H., Di Marzo, V., Elphick, M. R., Greasley, P. J., Hansen, H. S., Kunos, G., Mackie, K., Mechoulam, R. & Ross, R. A. 2010.

International Union of Basic and Clinical Pharmacology. Lxxix. Cannabinoid Receptors and Their Ligands: Beyond Cb1 and Cb2. *Pharmacological Reviews,* 62(4)**,** 588-631.

Petitet, F., Donlan, M. & Michel, A. 2006. Gpr55 as a New Cannabinoid Receptor: Still a Long Way to Prove It. *Chemical Biology and Drug Design,* 67(3)**,** 252-253.

Plotnikov, A., Zehorai, E., Procaccia, S. & Seger, R. 2011. The Mapk Cascades: Signaling Components, Nuclear Roles and Mechanisms of Nuclear Translocation. *Biochimica et Biophysica Acta (BBA) - Molecular Cell Research,* 1813(9)**,** 1619-1633.

Plüddemann, A., Mukhopadhyay, S. & Gordon, S. 2006. The Interaction of Macrophage Receptors with Bacterial Ligands. *Expert Reviews in Molecular Medicine,* 8(28)**,** 1-25.

Plüddemann, A., Mukhopadhyay, S. & Gordon, S. 2011. Innate Immunity to Intracellular Pathogens: Macrophage Receptors and Responses to Microbial Entry. *Immunological Reviews,* 240(1)**,** 11-24.

Poucher, S. M., Keddie, J. R., Singh, P., Stoggall, S. M., Caulkett, P. W. R., Jones, G. & Collis, M. G. 1995. The in Vitro Pharmacology of Zm 241385, a Potent, Non-Xanthine, A2a Selective Adenosine Receptor Antagonist. *British Journal of Pharmacology,* 115(6)**,** 1096-1102.

Quiñones-Maldonado, V. & Renaud, F. L. 1987. Effect of Biogenic Amines on Phagocytosis in *Tetrahymena thermophila*. *The Journal of Protozoology,* 34(4)**,** 435-438.

Rasmussen, L. 1976. Nutrient Uptake in *Tetrahymena pyriformis*. *Carlsberg Research Communications,* 41(3)**,** 143-167.

Renaud, F. L., Colon, I., Lebron, J., Ortiz, N., Rodriguez, F. & Cadilla, C. 1995. A Novel Opioid Mechanism Seems to Modulate Phagocytosis in *Tetrahymena*. *Journal of Eukaryotic Microbiology,* 42(3)**,** 205-7.

Ricketts, T. R. 1971. Endocytosis in *Tetrahymena pyriformis.* The Selectivity of Uptake of Particles and the Adaptive Increase in Cellular Acid Phosphatase Activity. *Experimental Cell Research,* 66(1)**,** 49-58.

Ricketts, T. R. & Rappitt, A. F. 1976. Endocytosis, Digestive Vacuolar Movement and Exocytosis on Refeeding Starved *Tetrahymena pyriformis* Gl-9. *Protoplasma,* 87(1-3)**,** 221-236.

Ritter, K., Buning, C., Halland, N., Pöverlein, C. & Schwink, L. 2016. G Protein-Coupled Receptor 119 (Gpr119) Agonists for the Treatment of Diabetes: Recent Progress and Prevailing Challenges. *Journal of Medicinal Chemistry,* 59(8)**,** 3579-3592.

Rock, E., Bolognini, D., Limebeer, C., Cascio, M., Anavi-Goffer, S., Fletcher, P., Mechoulam, R., Pertwee, R. & Parker, L. 2012. Cannabidiol, a Non-Psychotropic Component of Cannabis, Attenuates Vomiting and Nausea-Like Behaviour Via Indirect Agonism of 5-Ht1a Somatodendritic Autoreceptors in the Dorsal Raphe Nucleus. *British Journal of Pharmacology,* 165(8)**,** 2620-2634.

Rodriguez, E., Lazaro, M. I., Renaud, F. L. & Marino, M. 2004. Opioid Activity of Beta-Endorphin-Like Proteins from *Tetrahymena*. *The Journal of Eukaryotic Microbiology,* 51(1)**,** 60-65.

Rosales, C. & Uribe-Querol, E. 2017. Phagocytosis: A Fundamental Process in Immunity. *BioMed Research International,* Vol.2017**,** 1-18.

Rouzer, C. A. & Marnett, L. J. 2011. Endocannabinoid Oxygenation by Cyclooxygenases, Lipoxygenases, and Cytochromes P450: Cross-Talk between the Eicosanoid and Endocannabinoid Signaling Pathways. *Chemical Reviews,* 111(10)**,** 5899-5921.

Russell, A. D. 2003. Lethal Effects of Heat on Bacterial Physiology and Structure. *Science Progress,* 86(1-2)**,** 115-137.

Russo, E. B., Burnett, A., Hall, B. & Parker, K. K. 2005. Agonistic Properties of Cannabidiol at 5-Ht1a Receptors. *Neurochemical Research,* 30(8)**,** 1037-1043.

Ryberg, E., Larsson, N., Sjögren, S., Hjorth, S., Hermansson, N. O., Leonova, J., Elebring, T., Nilsson, K., Drmota, T. & Greasley, P. J. 2007. The Orphan Receptor Gpr55 Is a Novel Cannabinoid Receptor. *British Journal of Pharmacology,* 152(7)**,** 1092-1101.

Sahly, H., Ofek, I., Podschun, R., Brade, H., He, Y., Ullmann, U. & Crouch, E. 2002. Surfactant Protein D Binds Selectively to *Klebsiella pneumoniae* Lipopolysaccharides Containing Mannose-Rich O-Antigens. *The Journal of Immunology,* 169(6)**,** 3267-3274.

Salaman, A., Roman, M., Renaud, F. L. & Silva, W. I. 1990. Effect of Chronic Opioid Treatment on Phagocytosis in *Tetrahymena*. *Neuropeptides,* 16(3)**,** 115-120.

Sattler, N., Bosmani, C., Barisch, C., Guého, A., Gopaldass, N., Dias, M., Leuba, F., Bruckert, F., Cosson, P. & Soldati, T. 2018. Functions of The *Dictyostelium* Limp-2 and Cd36 Homologues in Bacteria Uptake, Phagolysosome Biogenesis and Host Cell Defence. *Journal of Cell Science,* 131(17)**,** jcs218040.

Sawzdargo, M., Nguyen, T., Lee, D. K., Lynch, K. R., Cheng, R., Heng, H. H. Q., George, S. R. & O'dowd, B. F. 1999. Identification and Cloning of Three Novel Human G Protein-Coupled Receptor Genes Gpr52, Ψgpr53 and Gpr55: Gpr55 Is Extensively Expressed in Human Brain. *Molecular Brain Research,* 64(2)**,** 193-198.

Schmid, P. C., Reddy, P. V., Natarajan, V. & Schmid, H. H. 1983. Metabolism of N-Acylethanolamine Phospholipids by a Mammalian Phosphodiesterase of the Phospholipase D Type. *Journal of Biological Chemistry,* 258(15)**,** 9302-6.

Seeman, P. 2016. Cannabidiol Is a Partial Agonist at Dopamine D2high Receptors, Predicting Its Antipsychotic Clinical Dose. *Translational Psychiatry,* 6(10)**,** e920-e920.

Sehring, I. M., Mansfeld, J., Reiner, C., Wagner, E., Plattner, H. & Kissmehl, R. 2007a. The Actin Multigene Family of *Paramecium tetraurelia. BMC Genomics,* 8(1)**,** 82.

Sehring, I. M., Reiner, C., Mansfeld, J., Plattner, H. & Kissmehl, R. 2007b. A Broad Spectrum of Actin Paralogs in *Paramecium tetraurelia* Cells Display Differential Localization and Function. *Journal of Cell Science,* 120(Pt 1)**,** 177-90.

Shen, D., Deng, C. & Zhang, M. 2007. Peroxisome Proliferator-Activated Receptor Agonists Inhibit the Proliferation and Invasion of Human Colon Cancer Cells. *Postgraduate Medical Journal,* 83(980)**,** 414-419.

Sherr, B. F., Sherr, E. B. & Berman, T. 1983. Grazing, Growth, and Ammonium Excretion Rates of a Heterotrophic Microflagellate Fed with Four Species of Bacteria. *Applied and Environmental Microbiology,* 45(4)**,** 1196-201.

Sherr, E. B. & Sherr, B. F. 1987. High Rates of Consumption of Bacteria by Pelagic Ciliates. *Nature,* 325(6106)**,** 710-711.

Sherr, E. B. & Sherr, B. F. 2007. Heterotrophic Dinoflagellates: A Significant Component of Microzooplankton Biomass and Major Grazers of Diatoms in the Sea. *Marine Ecology Progress Series,* 352(1)**,** 187-197.

Sheth, S., Brito, R., Mukherjea, D., Rybak, L. & Ramkumar, V. 2014. Adenosine Receptors: Expression, Function and Regulation. *International Journal of Molecular Sciences,* 15(2)**,** 2024-2052.

Shevyrin, V. A. & Morzherin, Y. Y. 2015. Cannabinoids: Structures, Effects, and Classification. *Russian Chemical Bulletin,* 64(6)**,** 1249-1266.

Shiozaki, N., Nakano, K., Kushida, Y., Noguchi, T. Q. P., Uyeda, T. Q. P., Wloga, D., Dave, D., Vasudevan, K. K., Gaertig, J. & Numata, O. 2013. Adf/Cofilin Is Not Essential but Is Critically Important for Actin Activities During Phagocytosis in *Tetrahymena thermophila*. *Eukaryotic Cell,* 12(8)**,** 1080-1086.

Shrivastava, A., Kuzontkoski, P. M., Groopman, J. E. & Prasad, A. 2011. Cannabidiol Induces Programmed Cell Death in Breast Cancer Cells by Coordinating the Cross-Talk between Apoptosis and Autophagy. *Molecular Cancer Therapeutics,* 10(7)**,** 1161-1172.

Simon, G. M. & Cravatt, B. F. 2006. Endocannabinoid Biosynthesis Proceeding through Glycerophospho-N-Acyl Ethanolamine and a Role for A/B-Hydrolase 4 in This Pathway. *Journal of Biological Chemistry,* 281(36)**,** 26465-26472.

Simon, G. M. & Cravatt, B. F. 2008. Anandamide Biosynthesis Catalyzed by the Phosphodiesterase Gde1 and Detection of Glycerophospho-N-Acyl Ethanolamine Precursors in Mouse Brain. *Journal of Biological Chemistry,* 283(14)**,** 9341-9349.

Smith, H. E. 1982. Oral Apparatus Structure in the Carnivorous Macrostomal Form of *Tetrahymena vorax*. *The Journal of Protozoology,* 29(4)**,** 616-627.

Smith, J. J. & Aitchison, J. D. 2013. Peroxisomes Take Shape. *Nature reviews. Molecular cell biology,* 14(12)**,** 803-817.

Snyder, D. S., Brahamsha, B., Azadi, P. & Palenik, B. 2009. Structure of Compositionally Simple Lipopolysaccharide from Marine *Synechococcus*. *Journal of Bacteriology,* 191(17)**,** 5499-5509.

Sommer, A., Fries, A., Cornelsen, I., Speck, N., Koch-Nolte, F., Gimpl, G., Andra, J., Bhakdi, S. & Reiss, K. 2012. Melittin Modulates Keratinocyte Function through P2 Receptor-Dependent Adam Activation. *The Journal of Biological Chemistry,* 287(28)**,** 23678-23689.

Sonego, A. B., Gomes, F. V., Del Bel, E. A. & Guimaraes, F. S. 2016. Cannabidiol Attenuates Haloperidol-Induced Catalepsy and C-Fos Protein Expression in the Dorsolateral Striatum Via 5-Ht1a Receptors in Mice. *Behavioural Brain Research,* 309(1)**,** 22-28.

Strom, S., Bright, K., Fredrickson, K. & Brahamsha, B. 2017. The Synechococcus Cell Surface Protein Swma Increases Vulnerability to Predation by Flagellates and Ciliates. *Limnology and Oceanography,* 62(2)**,** 784-794.

Stuart, L. M., Deng, J., Silver, J. M., Takahashi, K., Tseng, A. A., Hennessy, E. J., Ezekowitz, R. A. B. & Moore, K. J. 2005. Response to *Staphylococcus aureus* Requires Cd36-Mediated Phagocytosis Triggered by the Cooh-Terminal Cytoplasmic Domain. *Journal of Cell Biology,* 170(3)**,** 477-485.

Sugita, M., Nakano, K., Sato, M., Toyooka, K. & Numata, O. 2009. The Roles of Actin Cytoskeleton and Microtubules for Membrane Recycling of a Food Vacuole in *Tetrahymena thermophila*. *Cell Motility and the Cytoskeleton,* 66(7)**,** 371-377.

Sugiura, T., Kondo, S., Sukagawa, A., Nakane, S., Shinoda, A., Itoh, K., Yamashita, A. & Waku, K. 1995. 2-Arachidonoylglycerol: A Possible Endogenous Cannabinoid Receptor Ligand in Brain. *Biochemical and Biophysical Research Communications* 215(1)**,** 89-97.

Sun, Y. & Bennett, A. 2007. Cannabinoids: A New Group of Agonists of PPARs. *PPAR Research,* 2007(1)**,** 1-7.

Swanson, J. A., Johnson, M. T., Beningo, K., Post, P., Mooseker, M. & Araki, N. 1999. A Contractile Activity That Closes Phagosomes in Macrophages. *Journal of Cell Science,* 112 (Pt 3)**,** 307-16.

Tahir, S. K., Trogadis, J. E., Stevens, J. K. & Zimmerman, A. M. 1992. Cytoskeletal Organization Following Cannabinoid Treatment in Undifferentiated and Differentiated Pc12 Cells. *Biochemistry and Cell Biology,* 70(10-11)**,** 1159-73.

Takei, M., Watanabe, T. & Suga, T. 1982. Characterization of Peroxisomes in *Tetrahymena pyriformis*. *Biochimica et Biophysica Acta (BBA) - General Subjects,* 716(1)**,** 31-37.

Tan, F., Cao, M., Ge, X., Li, C., Tian, M., Zhang, L., Fu, Q., Song, L. & Yang, N. 2019. Identification and Initial Functional Characterization of Lysosomal Integral Membrane Protein Type 2 (Limp-2) in Turbot (*Scophthalmus maximus* L.). *Developmental and Comparative Immunology,* 99**,** 103412.

Tanida, S., Hasegawa, T. & Okazaki, H. 1986. Change in Swimming Behavior Of *Tetrahymena pyriformis* mediated by Calcium-Function Modulating Compounds. *Agricultural and Biological Chemistry,* 50(1)**,** 65-70.

Taylor, M. E. & Drickamer, K. 2019. Mammalian Sugar-Binding Receptors: Known Functions and Unexplored Roles. *The FEBS Journal,* 286(10)**,** 1800-1814.

Tham, M., Yilmaz, O., Alaverdashvili, M., Kelly, M. E. M., Denovan-Wright, E. M. & Laprairie, R. B. 2019. Allosteric and Orthosteric Pharmacology of Cannabidiol and Cannabidiol-Dimethylheptyl at the Type 1 and Type 2 Cannabinoid Receptors. *British Journal of Pharmacology,* 176(10)**,** 1455-1469.

Thurman, J., Drinkall, J. & Parry, J. 2010. Digestion of Bacteria by the Freshwater Ciliate *Tetrahymena pyriformis*. *Aquatic Microbial Ecology,* 60(2)**,** 163-174.

Tyagi, S., Gupta, P., Saini, A. S., Kaushal, C. & Sharma, S. 2011. The Peroxisome Proliferator-Activated Receptor: A Family of Nuclear Receptors Role in Various Diseases. *Journal of Advanced Pharmaceutical Technology and Research,* 2(4)**,** 236-40.

Ud-Daula, A., Pfister, G. & Schramm, K.-W. 2012. Identification of Dopamine Receptor in *Tetrahymena thermophila* by Fluorescent Ligands. *Pakistan Journal of Biological Sciences,* 15(23)**,** 1133-1138.

Ueda, N., Tsuboi, K., Uyama, T. & Ohnishi, T. 2011. Biosynthesis and Degradation of the Endocannabinoid 2-Arachidonoylglycerol. *BioFactors,* 37(1)**,** 1-7.

Uhlenbrock, K., Gassenhuber, H. & Kostenis, E. 2002. Sphingosine 1-Phosphate Is a Ligand of the Human Gpr3, Gpr6 and Gpr12 Family of Constitutively Active G Protein-Coupled Receptors. *Cellular Signalling,* 14(11)**,** 941-953.

Ujváry, I. & Hanuš, L. 2016. Human Metabolites of Cannabidiol: A Review on Their Formation, Biological Activity, and Relevance in Therapy. *Cannabis and Cannabinoid Research,* 1(1)**,** 90-101.

Ukhanov, K., Brunert, D., Corey, E. A. & Ache, B. W. 2011. Phosphoinositide 3-Kinase-Dependent Antagonism in Mammalian Olfactory Receptor Neurons. *Journal of Neuroscience,* 31(1)**,** 273-280.

Varga, T., Czimmerer, Z. & Nagy, L. 2011. Ppars Are a Unique Set of Fatty Acid Regulated Transcription Factors Controlling Both Lipid Metabolism and Inflammation. *Biochimica et Biophysica Acta (BBA) - Molecular Basis of Disease,* 1812(8)**,** 1007-1022.

Vaysse, P. J., Gardner, E. L. & Zukin, R. S. 1987. Modulation of Rat Brain Opioid Receptors by Cannabinoids. *Journal of Pharmacology and Experimental Therapeutics* 241(2)**,** 534-9.

Venkataraman, C., Haack, B. J., Bondada, S. & Kwaik, Y. A. 1997. Identification of a Gal/Galnac Lectin in the Protozoan *Hartmannella vermiformis* as a Potential Receptor for Attachment and Invasion by the Legionnaires' Disease Bacterium. *Journal of Experimental Medicine,* 186(4)**,** 537-547.

Verni, F. & Gualtieri, P. 1997. Feeding Behaviour in Ciliated Protists. *Micron,* 28(6)**,** 487-504.

Voichick, J., Elson, C., Granner, D. & Shrago, E. 1973. Relationship of Adenosine 3',5'-Monophosphate to Growth and Metabolism of *Tetrahymena pyriformis*. *Journal of bacteriology,* 115(1)**,** 68-72.

Wahli, W., Braissant, O. & Desvergne, B. 1995. Peroxisome Proliferator Activated Receptors: Transcriptional Regulators of Adipogenesis, Lipid Metabolism and More…. *Chemistry & Biology,* 2(5)**,** 261-266.

Wang, J.-Z., Long, C., Li, K.-Y., Xu, H.-T., Yuan, L.-L. & Wu, G.-Y. 2018. Potent Block of Potassium Channels by Mek Inhibitor U0126 in Primary Cultures and Brain Slices. *Scientific Reports,* 8(1).

Wang, K., Hou, Y., Gu, C., Zhao, D., Duan, Y., Ran, Z., Li, Q. & Li, X. 2017. Inhibitory Effect of the Mitogen Activated Protein Kinase Specific Inhibitor Pd98059 on Mtb-Ag-Activated Γδτ Cells. *International journal of clinical and experimental pathology,* 10(9)**,** 9644-9648.

Wanlahbeh, N. 2020. An Investigation into the Targets for Cannabinoid Action in the Ciliate *Tetrahymena pyriformis*. Mres Thesis. Lancaster University.

Wei, B. Q., Mikkelsen, T. S., Mckinney, M. K., Lander, E. S. & Cravatt, B. F. 2006. A Second Fatty Acid Amide Hydrolase with Variable Distribution among Placental Mammals. *Journal of Biological Chemistry,* 281(48)**,** 36569-36578.

Wilks, S. A. & Sleigh, M. A. 2004. Lectin Binding Sites on *Euplotes mutabilis* (Tuffrau, 1960) and the Implications for Food Particle Selection. *European Journal of Protisology,* 40(2)**,** 153-162.

Williams, N. E., Tsao, C.-C., Bowen, J., Hehman, G. L., Williams, R. J. & Frankel, J. 2006. The Actin Gene Act1 Is Required for Phagocytosis, Motility, and Cell Separation of *Tetrahymena thermophila*. *Eukaryotic Cell,* 5(3)**,** 555-567.

Wood, C. R., Hard, R. & Hennessey, T. M. 2007. Targeted Gene Disruption of Dynein Heavy Chain 7 of *Tetrahymena thermophila* Results in Altered Ciliary Waveform and Reduced Swim Speed. *Journal of Cell Science,* 120(17)**,** 3075-3085.

Yaeger, R. 1996. Protozoa: Structure, Classification, Growth, and Development. *In:* BARON, S. (ed.) *Medical Microbiology.* 4th ed.: Galveston, TX: University of Texas Medical Branch at Galveston, TX.

Yamamura, H., Ugawa, S., Ueda, T., Nagao, M. & Shimada, S. 2004. Capsazepine Is a Novel Activator of the Δ Subunit of the Human Epithelial Na+ Channel. *Journal of Biological Chemistry,* 279(43)**,** 44483-44489.

Yang, M., Jung, S., Sethi, G. & Ahn, K. 2019. Pleiotropic Pharmacological Actions of Capsazepine, a Synthetic Analogue of Capsaicin, against Various Cancers and Inflammatory Diseases. *Molecules,* 24(5)**,** 995.

Yates, R. M., Hermetter, A. & Russell, D. G. 2005. The Kinetics of Phagosome Maturation as a Function of Phagosome/Lysosome Fusion and Acquisition of Hydrolytic Activity. *Traffic,* 6(5)**,** 413-420.

Yıldız, M. T. & Arslanyolu, M. 2014. In Silico Identification and Characterization of the Mapk Family Members of Unicellular Model Eukaryote *Tetrahymena thermophila*. *European Journal of Protistology* 50(5)**,** 538-50.

Yin, H., Chu, A., Li, W., Wang, B., Shelton, F., Otero, F., Nguyen, D. G., Caldwell, J. S. & Chen, Y. A. 2009. Lipid G Protein-Coupled Receptor Ligand Identification Using B-Arrestin Pathhunter™ Assay. *Journal of Biological Chemistry,* 284(18)**,** 12328-12338.

Yoshino, H., Miyamae, T., Hansen, G., Zambrowicz, B., Flynn, M., Pedicord, D., Blat, Y., Westphal, R. S., Zaczek, R., Lewis, D. A. & Gonzalez-Burgos, G. 2011. Postsynaptic Diacylglycerol Lipase A Mediates Retrograde Endocannabinoid Suppression of Inhibition in Mouse Prefrontal Cortex. *The Journal of Physiology,* 589(20)**,** 4857-4884.

Zani, I., Stephen, S., Mughal, N., Russell, D., Homer-Vanniasinkam, S., Wheatcroft, S. & Ponnambalam, S. 2015. Scavenger Receptor Structure and Function in Health and Disease. *Cells,* 4(2)**,** 178-201.

Zelasko, S., Arnold, W. R. & Das, A. 2015. Endocannabinoid Metabolism by Cytochrome P450 Monooxygenases. *Prostaglandins & Other Lipid Mediators,* 116-117**,** 112-123.

Zendulka, O., Dovrtělová, G., Nosková, K., Turjap, M., Šulcová, A., Hanuš, L. & Juřica, J. 2016. Cannabinoids and Cytochrome P450 Interactions. *Current Drug Metabolism,* 17(3)**,** 206-26.

Zhang, P., Snyder, S., Feng, P., Azadi, P., Zhang, S., Bulgheresi, S., Sanderson, K. E., He, J., Klena, J. & Chen, T. 2006. Role of N-Acetylglucosamine within Core Lipopolysaccharide of Several Species of Gram-Negative Bacteria in Targeting the Dc-Sign (Cd209). *The Journal of Immunology,* 177(6)**,** 4002-4011.

Zhu, F.-G., Reich, C. F. & Pisetsky, D. S. 2001. The Role of the Macrophage Scavenger Receptor in Immune Stimulation by Bacterial Dna and Synthetic Oligonucleotides. *Immunology,* 103(2)**,** 226-234.

Zimmerman, S., Zimmerman, A. M. & Laurence, H. 1981. Effect of Delta 9-Tetrahydrocannabinol on Cyclic Nucleotides in Synchronously Dividing *Tetrahymena*. *Canadian Journal of Biochemistry and Physiology,* 59(7)**,** 489-93.

Zou, D. & Hennessey, T. M. 2017. Behavioral Effects of a Chemorepellent Receptor Knockout Mutation in *Tetrahymena thermophila*. *mSphere,* 2(4)**,** e00182-17.

Zou, S. & Kumar, U. 2018. Cannabinoid Receptors and the Endocannabinoid System: Signaling and Function in the Central Nervous System. *International Journal of Molecular Sciences,* 19(3)**,** 833.